NASA/TP—2004–213284

Toxic Gas Exposure Risks Associated With Potential Shuttle Catastrophic Failures

B. Jeffrey Anderson and Rebecca C. McCaleb
Marshall Space Flight Center, Marshall Space Flight Center, Alabama

June 2004

The NASA STI Program Office…in Profile

Since its founding, NASA has been dedicated to the advancement of aeronautics and space science. The NASA Scientific and Technical Information (STI) Program Office plays a key part in helping NASA maintain this important role.

The NASA STI Program Office is operated by Langley Research Center, the lead center for NASA's scientific and technical information. The NASA STI Program Office provides access to the NASA STI Database, the largest collection of aeronautical and space science STI in the world. The Program Office is also NASA's institutional mechanism for disseminating the results of its research and development activities. These results are published by NASA in the NASA STI Report Series, which includes the following report types:

- TECHNICAL PUBLICATION. Reports of completed research or a major significant phase of research that present the results of NASA programs and include extensive data or theoretical analysis. Includes compilations of significant scientific and technical data and information deemed to be of continuing reference value. NASA's counterpart of peer-reviewed formal professional papers but has less stringent limitations on manuscript length and extent of graphic presentations.

- TECHNICAL MEMORANDUM. Scientific and technical findings that are preliminary or of specialized interest, e.g., quick release reports, working papers, and bibliographies that contain minimal annotation. Does not contain extensive analysis.

- CONTRACTOR REPORT. Scientific and technical findings by NASA-sponsored contractors and grantees.

- CONFERENCE PUBLICATION. Collected papers from scientific and technical conferences, symposia, seminars, or other meetings sponsored or cosponsored by NASA.

- SPECIAL PUBLICATION. Scientific, technical, or historical information from NASA programs, projects, and mission, often concerned with subjects having substantial public interest.

- TECHNICAL TRANSLATION. English-language translations of foreign scientific and technical material pertinent to NASA's mission.

Specialized services that complement the STI Program Office's diverse offerings include creating custom thesauri, building customized databases, organizing and publishing research results…even providing videos.

For more information about the NASA STI Program Office, see the following:

- Access the NASA STI Program Home Page at ***http://www.sti.nasa.gov***

- E-mail your question via the Internet to help@sti.nasa.gov

- Fax your question to the NASA Access Help Desk at (301) 621–0134

- Telephone the NASA Access Help Desk at (301) 621–0390

- Write to:
  NASA Access Help Desk
  NASA Center for AeroSpace Information
  7121 Standard Drive
  Hanover, MD 21076–1320
  (301)621–0390

NASA/TP—2004–213284

Toxic Gas Exposure Risks Associated With Potential Shuttle Catastrophic Failures

B. Jeffrey Anderson and Rebecca C. McCaleb
Marshall Space Flight Center, Marshall Space Flight Center, Alabama

National Aeronautics and
Space Administration

Marshall Space Flight Center • MSFC, Alabama 35812

June 2004

Acknowledgments

The authors would like to acknowledge and express their gratitude to Mark Bennett, CH2M Hill, and Frank Leahy, Raytheon Corporation, for their valuable technical contributions to this work, portions of which are provided explicitly in appendices E and F. Likewise, the authors would like to thank Ralph Hayes, El Dorado Engineering, for his expert input on surfacing issues with modeling, general advice, and engineering insight relevant to solid rocket propellant characteristics; Scott Stevens, Intergraph Corporation, for his excellent graphics support, especially appendix D; and Belinda Hardin, Computer Sciences Corporation (CSC), for final preparation of this manuscript. Appreciation is also expressed to Jim Kennedy, Director, Kennedy Space Center (KSC) (formerly Deputy Director, Marshall Space Flight Center (MSFC)) for his support and encouragement to finish this effort in spite of the many difficulties and delays that slowed its completion.

The authors are appreciative of Jolene Martin, Deputy Manager, and Steve Glover, Environmental Lead Engineer, Propulsion Systems Engineering and Integration Office, Space Shuttle Propulsion Office, for their direction of an independent review of these results in an earlier form and the valuable contributions derived from that effort. Sharon Scroggins, an MSFC environmental engineer, provided expertise in augmenting mitigation alternatives. Greg Oliver, Manager, Range Safety Review Panel, Johnson Space Center (JSC), and Burt Summerfield, Chief, Safety, Occupational Health and Environmental Division, Spaceport Services Directorate, KSC, provided valuable information on procedures, advice, and response to questions as did the U.S. Air Force (USAF) 45th Space Wing (SW) and 30th SW located at Patrick Air Force Base (AFB) and Vandenberg AFB, respectively. In particular, Randy Nyman, ACTA, supplied significant input data to the modeling effort; e.g., debris library and failure scenarios. Stan Adelfang, Jere Justis, and Wade Batts, CSC at MSFC, provided invaluable meteorological and modeling input data and advice. Robert Bennett, ATK Thiokol, provided expert responses to the author's questions, data, and procedures.

Given the valuable support provided by these and others persons not mentioned, note that in some cases, their perspectives on the issues discussed may differ from those presented here. The results and conclusions in this Technical Publication are those of the authors.

Available from:

NASA Center for AeroSpace Information
7121 Standard Drive
Hanover, MD 21076–1320
(301) 621–0390

National Technical Information Service
5285 Port Royal Road
Springfield, VA 22161
(703) 487–4650

TABLE OF CONTENTS

LIST OF FIGURES

LIST OF FIGURES (Continued)

LIST OF TABLES

LIST OF ACRONYMS AND SYMBOLS

ACGIH	American Conference of Governmental Industrial Hygenists
AIHA	American Industrial Hygiene Association
CAIB	*Columbia* Accident Investigation Board
CCAFS	Cape Canaveral Air Force Station
EPA	Environmental Protection Agency
EPCRA	Emergency Planning and Community Right-to-Know Act
ERPG	Emergency Response Planning Guideline
ET	external tank
EWR	Eastern and Western Range
HCl	hydrogen chloride
IDLH	immediately dangerous to life and health
ILL	impact limit line
KSC	Kennedy Space Center
LANL	Los Alamos National Laboratory
LARA	Launch Area Risk Analysis
LATRA	Launch Area Toxic Risk Analysis
LCC	launch commit criteria
MSFC	Marshall Space Flight Center
NASA	National Aeronautics and Space Administration
NIOSH	National Institute of Occupational Safety and Health
OSHA	Occupational Safety and Health Administration
QRAS	Quantitative Risk Assessment System
REEDM	Rocket Exhaust Effluent Diffusion Model

LIST OF ACRONYMS AND SYMBOLS (Continued)

SRB	solid rocket booster
SRM	solid rocket motor
SW	Space Wing
TP	Technical Publication
USAF	United States Air Force

NOMENCLATURE

E_c	expected casualty
L	length
U_0	lowest sounding level wind speed
u^*	computed friction velocities

TECHNICAL PUBLICATION

TOXIC GAS EXPOSURE RISKS ASSOCIATED WITH POTENTIAL SHUTTLE CATASTROPHIC FAILURES

1. INTRODUCTION

From the earliest days of the National Aeronautics and Space Administration's (NASA's) Shuttle program, toxic chemicals, primarily hydrogen chloride (HCl) released by burning of the solid propellant in the two solid rocket boosters (SRBs), have been carefully monitored concerns. Each SRB consists of a main core referred to as the solid rocket motor (SRM) where the solid propellant is contained and cast in a pattern that carefully controls the burn rate. The SRMs each contain 502 metric tons (553 tons) of solid propellant that consists of ≈70 percent ammonium perchlorate (oxidizer), 16 percent finely ground aluminum powder (fuel), a binder referred to as PBAN, iron oxide (catalyst), and a curative agent. The final assembly of each SRB consists of the SRM, avionics, flight termination system, parachute assembly, nose cone, etc. Combined, the two SRBs burn an average of 10 metric tons (9 tons) solid propellant per second for the first 2 min of flight. A more complete description of the SRBs and their respective combustion products can be found in the Space Shuttle Environmental Impact Statements (NASA 1978).[1,2]

In 1998, the United States Air Force (USAF) 45th Space Wing (SW), prompted by the rates of failure early in launch in the Titan and Delta programs, instituted more stringent launch commit criteria (LCC) and proposed that the same HCl LCC be included in the Shuttle LCC. The proposal addressed both onsite visitors and offsite public and was specific to possible consequences of theoretical catastrophic failure scenarios rather than to normal launches. This proposal led to a review by a joint NASA/USAF team, new Memoranda of Agreement (NASA/USAF, 2000)[3,4] between Kennedy Space Center (KSC) and the 45th SW, and a detailed case study of a meteorological scenario by modeling experts at the Los Alamos National Laboratory (LANL) (Linn et al., 2001).[5]

During initial review, which the authors supported, it was determined that two diverse types of health and safety standards are applicable to potential Shuttle aborts. One standard is the expected casualty (E_c) criteria as described and required by Eastern and Western Range (EWR) 127–1 (EWR, 1997).[6] The root logic of this standard, expressed in Public Law 81–60, requires safe operation of the ranges; i.e., "From a safety standpoint (test flights of missiles) will be no more dangerous than conventional airplanes flying overhead" (U.S. Congress, 1949).[7] The focus of evaluating compliance with this standard has been the threat from inert falling fragments and both primary and secondary blast effects from a failed space launch. One approach to demonstrating adequate public safety is to extend the E_c evaluation to include the risk of toxic gas exposure that might result from a launch failure. It may not be necessary to include the toxic gas threat in the E_c evaluation if the threat can be effectively mitigated. This would have to be in accordance with the second type of standards—air quality and safety standards—applicable to manufacturing or handling large quantities of toxic materials. These could be used as a basis for mitigation of potential HCl exposure.

It was also apparent from the initial review that analytical tools proposed for E_c evaluation and implementation of the USAF recommendations were lagging the general state of the art, even though the USAF had made considerable effort to upgrade and tailor them to the specific Eastern Range situation. American industry manufactures, transports, and stores large quantities of hazardous chemicals in the midst of the public every day, and public safety is maintained by vigilant industrial safety practices and emergency response planning, procedures, and preparedness. The current screening effort was undertaken to reevaluate the issues using modern U.S. Environmental Protection Agency- (EPA-) accepted analysis techniques and a broadened perspective. The contents of this report provide the basis for determining improved options for protection of the public and the KSC and Cape Canaveral Air Force Station (CCAFS) workforce. Note that this investigation was conducted over a period of several years and prior to the *Columbia* accident and subsequent release of the *Columbia* Accident Investigation Board (CAIB) report. Recent safety initiatives in response to the CAIB report are not reflected here.

This study addresses these issues using the U.S. EPA-recommended model referred to as CALPUFF. CALPUFF results were compared to those produced by the USAF model, REEDM, which was developed early in the Shuttle program for projecting air quality and acid rain out from nominal launches. In addition, model performance was evaluated against results of a KSC-sponsored study at the Los Alamos National Laboratory (LANL) using a computer-intensive wild-fire model.

CALPUFF and the LANL model are capable of multipuff modeling of multiple sources. REEDM is only a single-source, single-puff model. This study revealed significant deficiencies in REEDM when applied to the catastrophic failure problem. Comparison of results and parameter sensitivities all indicate that CALPUFF performed effectively. CALPUFF results indicate that if a Shuttle abort were to occur over land, within the first 25 s of launch, serious levels of HCl exposure could occur out to distances of at least 10 km. Coupled with the possibility that the abort may occur off of the nominal ground track, this is sufficient range to include all major onsite visitor viewing areas as well as some populated offsite locations. Due to the findings of this report, a preliminary survey of potential mitigation alternatives was performed. Initial results indicate that there are potential mitigation measures that could be implemented that are sufficiently protective and cost effective.

2. PROBLEM DEFINITION AND APPROACH

2.1 The Regulatory Environment

Safety and environmental protection issues related to toxic gas release from a Shuttle failure is a specific situation that must be addressed in the light of a variety of existing laws and executive orders, as well as Department of Defense, EPA, and Occupational Safety and Health Administration (OSHA) guidelines, regulations, and accepted industrial practices. This body of precedents can be divided into two categories, each of which provides a different perspective on the criteria and methods for public and worker safety and environmental protection: (1) Range safety requirements, especially the expected casualty standards of EWR 127–1 (EWR, 1997);[6] and (2) air quality standards including both "mobile source" and "fixed source" or facility regulations as defined by Executive Order[8] (EO 2000), prior executive orders, and the Emergency Planning and Community Right-to-Know Act (EPCRA) of 1986 (U.S. Congress 1986).[9–11] Central issues concerning applicability of these precedents to specific questions at hand with the intent of providing effective protection to the public are summarized below.

2.1.1 Air Quality Standards

Air quality regulations are generally divided into two groups according to whether the source is fixed or mobile. The Shuttle is a mobile source; however, there are advantages to considering fixed source criteria and regulations as guidelines for issues addressed in this TP. A Shuttle abort would result in one or two debris field(s) from the SRBs which would then be characterized by modeling input parameters as "fixed," and model output can be more straightforwardly compared to existing air quality standards. Facilities operating within these standards provide acceptable levels of public and worker safety, and area HazMat responders would utilize this protocol. Also, KSC routinely handles and stores large quantities of toxic and/or hazardous substances and is in compliance with these regulations for other accidents (nonlaunch related). For these reasons, the current study was undertaken as a preliminary assessment of Shuttle failure toxic gas issues as one would approach them from a facility (fixed source) point of view.

2.1.2 Range Safety, EWR 127–1

EWR 127–1 and related regulations and guidelines are viewed by the USAF 45th SW as defining the primary guiding principle in this situation (EWR 1997).[6] Thus, the focus is on cumulative E_c risk which is ≤30 casualties per million flights (30×10^{-6}).This criterion was derived from the principle that the ranges should be operated in a manner that is as safe to the public as general or commercial aviation. "Casualty" is considered to include either death or injury (at least 1-day disability) from the direct effects of an accident, falling fragments, blast, etc (EWR 1997).[12,13]

Open questions remain as to whether or not risk from potential HCl exposure should be included in the E_c calculation, and if so, how the toxic gas release from a potential abort and exposure consequences should be calculated.[14] For example, what is the appropriate criteria for HCl at which the exposed population would become casualties? One approach would be to use the National Institute of Occupational Safety and Health (NIOSH)/Occupational Safety and Health Administration (OSHA) immediately dangerous to

life and health (IDLH) value of 50 ppm HCl as an exposure criterion. An alternative would be the older American Industrial Hygiene Association (AIHA) Emergency Response Planning Guideline–3 (ERPG–3) level (also described as an IDLH level) of 100 ppm. In either case, the criterion could be challenged as insufficiently restrictive.

A better choice would be the AIHA ERPG–2 level which is described as the "maximum airborne concentration below which it is believed that nearly all individuals could be exposed for up to 1 hr without experiencing or developing irreversible or other serious health effects or symptoms which could impair an individual's ability to take protective action." This level is 20 ppm. However, this level is also open to challenge as insufficiently protective since it may allow harm to the individual which, though reversible, leaves him/her disabled for more than 1 day. It also exceeds the OSHA permissible exposure level and the American Conference of Governmental Industrial Hygienists (ACGIH) threshold limit value, both of which are "ceiling" levels of 5 ppm. Ceiling levels are maximum concentrations, independent of exposure duration, above which personal protective equipment is required.

Whatever criteria is established, the model results presented here indicate the area in the affected near field where the toxic gas criteria is exceeded will exceed the fragment field area by a substantial margin. The blast field should largely overlap the fragment field, so when calculating E_c for a combined blast-plus-fragment-plus-toxic gas threat, the potential toxic gas contribution would be the largest of the three. Other key factors in the calculation—accident probability and population distribution—are the same for each threat.

2.2 Objectives and Approach

The primary objectives of this study are as follows:

(1) To identify the range of possible failure scenarios, and from them, select the worst cases; i.e., maximum credible exposures, and those scenarios requiring unique mitigation approaches, thus providing an indication of the scope of issues.

(2) To run a screening analysis using an appropriate (multipuff) EPA-approved toxic dispersion model and covering a large meteorological database to develop an indication as to the range and relative frequency of potentially harmful HCl exposure levels; i.e., toxic gas concentrations as a function of location.

(3) To derive an assessment of the need for mitigation, mitigation options, and potential new requirements from the information developed under objectives (1) and (2).

The three objectives are for a preliminary assessment sufficient to ascertain what significant issues exist, define the need for additional work, determine an indication of the required scope, and determine a methodology for a full assessment and mitigation of the issues. To help place the study in perspective, the technical issues identified and authors' judgment as to their importance and complexity are summarized in table 1.

Table 1. Technical issues with their respective importance and complexity.

Parameters	Importance	Complexity	Comments
Accident scenario			
Vehicle element initiating	Minor	Moderate	Must include all alternatives
Location	Major	Moderate	
Probability of occurrence	Minor	High, non-T	More important for E_c approach
Probability of location	Major	Low to moderate	High precision not needed, except for E_c—proximity of two SRBs
Source term			
Fragment number and size distribution	Minor	Low	Results are not very sensitive
Fragment shape	Minimal	Moderate	Not likely to be important
Area covered (fragment spread)	Moderate	Moderate	Only important for small spread (very early accidents, two SRBs)
In-water fragments	Major	Low	Half-in, half-out remains question
Burn rate	Moderate	Low	
Combustion chemistry	Moderate	Low	
Aerosol production	Moderate	Moderate	Atmospheric humidity dependence
Air entrainment	Moderate	High	
Heat loss via radiation	Moderate	High	Interacts with aerosol issues
Meteorology			
Vertical thermodynamic profile	Major	Low	Address by using large database
Surface winds	Major	Low	Address by using large database
Winds aloft	Minor	Low	Address by using large database
Humidity	Moderate	Low	Address by using large database
Persistence and predictability	Minor	Moderate	
Dispersion model selection			
Specific to locale	Moderate	Moderate	Very important for operations
Specific to source term	Moderate	Low	Critical work is complete
Multipuff capability	High	Low	Critical work is complete
Risk of accident model	Minor	Very high	Becomes highly important for E_c
Population distribution model	Minor	Low	More important for E_c
Health and safety criteria			
Gaseous HCl	Moderate	Low	Well enough defined except for E_c
Aerosol/HCl	Moderate	High	Resolve by conservative approach
Other toxics, synergistic effects	Moderate	Moderate	Resolve by conservative approach

Key to Importance Categories:

Minimal: The impacts are not expected to be measurable or are too small to cause any safety risk or environmental degradation.

Minor: Impacts which should be measurable but which are too small to affect public or worker safety and emergency response planning. Variations in environmental impact are not likely to be significant.

Moderate: Likely to cause clearly measurable variations which should be accounted for in safety evaluations and emergency response planning, but which are unlikely to be primary drivers to safety risk assessment, mitigation efforts, or emergency response planning.

Major: Factors which are likely to be primary drivers to the safety evaluation and/or necessary mitigation procedures and emergency response planning.

Key to Complexity Categories:

Low: The issue is technically well understood and application to this situation is either complete or could be accomplished with an effort of a few man-months.

Moderate: The issue is technically manageable to the level required for effective safety evaluation, mitigation, and emergency response planning, but significant resources would be needed to be resolved.

High: Technical complexity such that adequate resolution is either beyond the current state-of-the-art, or extensive long-term studies would be required. (Cost of studies would probably exceed $500 K.)

Non-T: Issues where nontechnical factors (public affairs, legal, regulatory, etc.) play a significant part.

Section 3 provides an identification and breakdown of the important accident scenarios that could potentially lead to toxic cloud effects and an assessment of the probabilities that these scenarios might be realized. Section 4 discusses the source terms, meteorological conditions, and sensitivity to environmental parameters that determine the consequences; i.e., HCl gas concentrations that could potentially result from these scenarios. Results of the analyses, based on the CALPUFF code, are presented in section 5 along with comparisons to results from the Rocket Effluent Exhaust Diffusion Model (REEDM) code (currently used at KSC and the 45th SW) and the LANL study (Linn et al. 2001).[5] Findings from these results are presented in section 6 along with potential mitigation alternatives.

2.3 Exposure Criteria for Hydrogen Chloride

HCl is a strong oxidizer and forms a strong acid when mixed with water. It is considered a hazardous substance because it readily produces chemical burns upon exposure to eyes or upper respiratory track, lungs, or skin. Thus, health issues associated with HCl are generally related to acute exposure rather than long-term cumulative effects. The exposure criteria listed in table 2 are for short-term peak (ceiling) exposure levels. In the opinion of the authors, the more recent OSHA and NIOSH criteria are the appropriate guidelines for consideration of public and worker safety associated with a Shuttle launch. Results of this study have been expressed with respect to these levels. The older AIHA's ERPG levels differ from the OSHA and NIOSH levels by factors of 2 to 4. These differences are comparable to variations from model input parameters and accuracy discussed in section 4 and are not so great that they would change the basic findings and conclusions of this study.

Table 2. Emergency response guidelines for anhydrous HCl. All HCl gas concentrations are ceiling levels.

NIOSH/OSHA Immediately dangerous to life and health	50 ppm
OSHA and American Conference of Governmental Industrial Hygienists Ceilings Exposure to concentrations above this level require respirator protection	5 ppm
NIOSH Ceiling	5 ppm
AIHA ERPG–1 The maximum airborne concentration below which it is believed that nearly all individuals could be exposed for up to 1 hr without experiencing other than mild, transient adverse health effects or without perceiving a clearly defined objectionable odor.	3 ppm
AIHA ERPG–2 The maximum airborne concentration below which it is believed that nearly all individuals could be exposed for up to 1 hr without experiencing or developing irreversible or other serious health effects or symptoms which could impair an individual's ability to take protective action.	20 ppm
AIHA ERPG–3 The maximum airborne concentration below which it is believed that nearly all individuals could be exposed for up to 1 hr without experiencing or developing life-threatening health effects.	100 ppm

3. EMERGENCY SCENARIOS

Safe operation of the Shuttle is one of NASA's highest priorities. However, it must also be recognized that some residual risk will always remain because of the complexity of the systems and hazardous nature of the propellants. During final prelaunch and launch processes, there are many possible sequences of events that potentially could lead to a catastrophic Shuttle failure with multiple burning solid propellant fragments. For emergency preparedness, it is necessary to consider possible sequences that could lead to potentially unacceptably high public and/or worker exposure to toxic gases.

3.1 Abort Scenarios

Any catastrophic launch-related failure would involve all elements of the Shuttle. Therefore, a main issue becomes one of identifying the list of possible outcomes that could potentially expose the public and/or workers to dangerously high levels of HCl, as indicated in the logic flow diagram in figure 1.

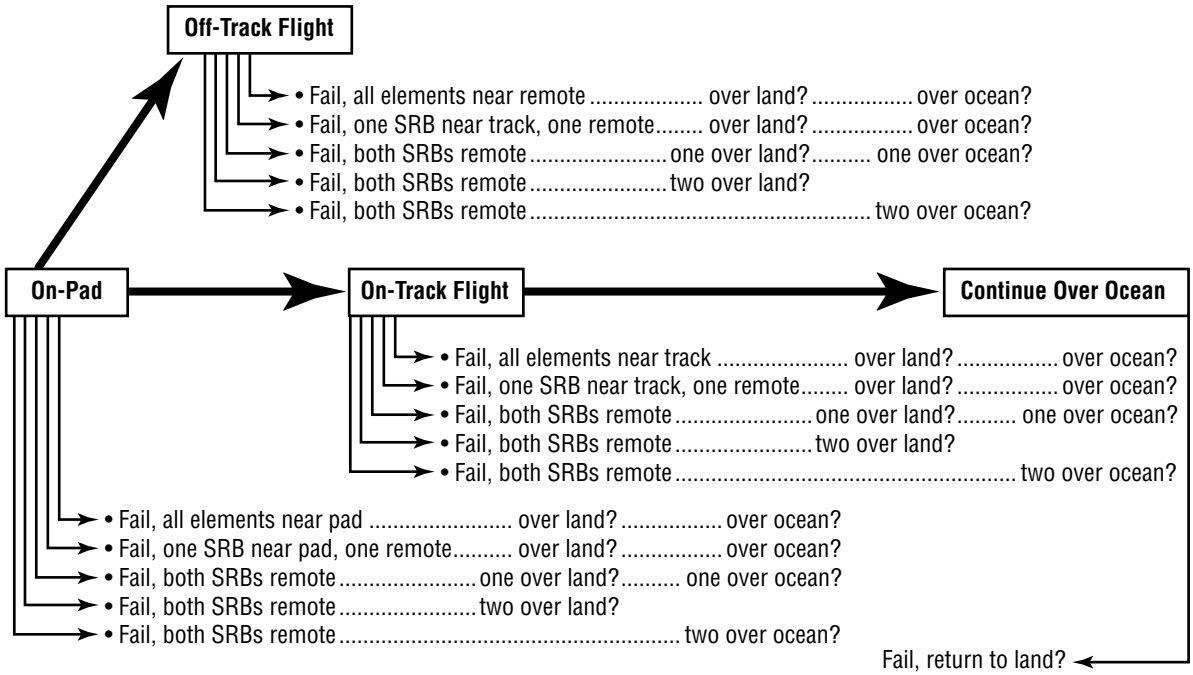

Figure 1. Failure tree.

Experience from the *Challenger* accident (NASA, 1986)[15] and the analysis contained in appendix A indicate that burning propellant fragments that fall into the ocean will be quenched by the cooling capability of the water. Thus, only scenarios where one or both SRB fragment fields fall on land are of interest from the toxic cloud hazard point of view for the purposes of this study. Also, both launch pads are

centered within 1 km of the beach, so there is little difference between "on-pad" and "on track, still over land" cases. Various possibilities in figure 1 can be grouped as follows:

(1) Both SRB fragment fields colocated with the liquid propellant; i.e., liquid oxygen/H_2, fire on or near the pad or nominal track.

(2) One SRB fragment field colocated with the liquid propellant fire on or near the pad/nominal track; the second SRB fragment field is remotely located inland.

(3) Both SRB fragment fields remotely located from the pad/nominal ground track—one over the ocean and one inland.

(4) Both SRB fragment fields remotely located inland at separate locations.

(5) Both SRB fragment fields remotely located inland in near proximity to one another, perhaps overlapping.

Each of the five cases involves SRB fragments and, consequently, burning solid propellant on land at locations that may be either near or remote from onsite workers and visitors. The question that must be asked is this: Can any of these cases be eliminated; i.e., clearly be identified as nonrealistic or highly improbable by the physics of potential catastrophic failures? Unless eliminated, they should be considered "credible" scenarios and appropriate emergency response planning measures taken.

After examining this issue within the scope of this effort, none of the above scenarios were eliminated. Several facts suggest these cases are credible for the purposes of this work. For example, analysis by GE Astro Space (app. B) and experience with the *Challenger* accident indicate that SRB cases are sufficiently robust that they would withstand the overpressures generated by a deflagration of the orbiter and external tank. Thus, nearly all scenarios involving deflagration of the central elements result in at least one—perhaps two—intact SRBs that would fly freely away from the initial failure location until impact or range destruct action renders them nonpropulsive. Exceptions are prelaunch accidents where the SRBs may remain unignited and off-track trajectories where the entire vehicle impacts the ground or ocean. Considering the SRB thrust of 11.79 MN, a gross mass of 590,000 kg, and a maximum range trajectory, it is estimated that the delay in range destruct action must exceed 16 to 17 s, twice the expected value of 7 s, before the fragment field could reach the Causeway, over 9 km from the pad. Thus, the on-track scenarios should lead to SRB impacts within ≈2 km of the point(s) where they break free. Distances and relative locations of the launch pads, important viewing areas, and impact limit lines (ILL) are illustrated on the map provided in figure 2.

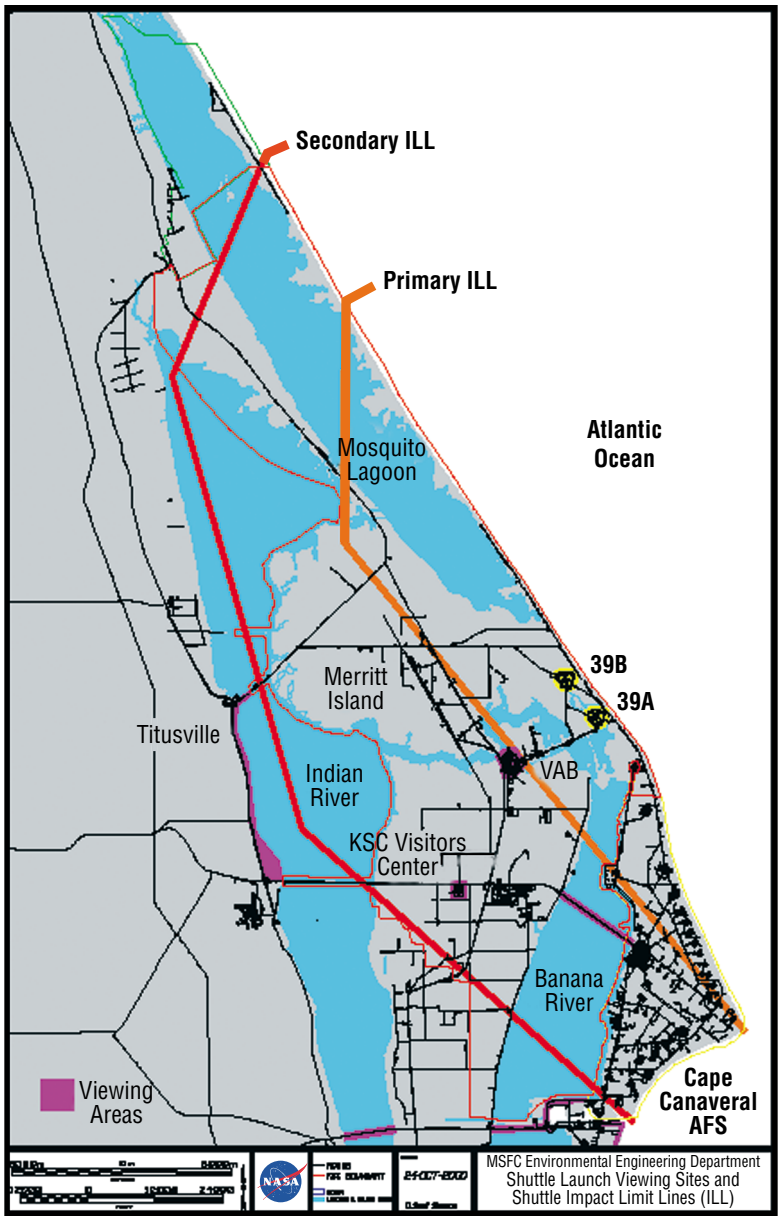

Figure 2. Map of the KSC/Cape Canaveral area, showing the Shuttle launch sites (yellow), important viewing areas (purple), and the primary (orange) and secondary (red) impact-limit lines.

Table 3. An example of Shuttle lift-off altitude, velocity, and pitch angle data for the first 25 s of flight.

Mission Elapsed Time (s)	Geodetic Altitude (m)	Relative Velocity (m/s)	Pitch Angle (deg)
0.00	–7.2	0.0	90.00
1.04	–5.9	3.9	89.88
2.08	1.1	9.7	89.74
3.12	14.3	15.7	89.73
4.16	33.6	21.8	89.81
5.20	59.4	28.3	89.86
6.24	92.1	35.0	89.90
7.28	132.0	42.0	89.95
8.32	179.2	49.2	89.73
9.36	233.9	56.5	88.96
10.40	296.2	64.0	87.50
11.44	366.5	71.6	85.39
12.48	444.7	79.4	82.13
13.52	531.0	87.2	79.32
14.56	625.3	95.2	76.22
15.60	727.5	103.4	73.41
16.64	837.6	111.8	70.59
17.68	955.4	120.4	69.62
18.72	1,081.1	129.3	69.51
19.76	1,214.7	138.6	69.83
20.80	1,356.5	148.0	70.24
21.84	1,506.8	157.6	70.38
22.88	1,665.4	167.1	70.43
23.92	1,832.3	176.4	70.49
24.96	2,007.3	185.5	70.50

A representative motion profile of the Shuttle during the first 25 s of flight is provided in table 3 which was derived from the STS–105 flight. The vehicle lifts vertically for 7 s. At that time it begins its roll and, slightly later, pitch maneuver. The roll-pitch sequence is completed at $L + 16$ to $L + 20$ s, depending upon the desired orbital inclination. The pitch angle tends to bias the SRB trajectories, if there was to be a failure during this stage of flight, toward the ocean. However, as the velocity data in table 3 indicate, there is still not a lot of oceanward momentum, and the mechanics of the breakups would probably dominate initial trajectories taken by the SRBs. As time increases beyond 25 s, the vehicle's ballistic trajectory (given a failure) would point toward an ocean landing, and the oceanward momentum would continue to become more and more important as flight time increases. However, the failure time—when it finally becomes impossible for fragments to reach land—is not surpassed until ≈100 s into flight.

One simplification that can be made to reduce the required analysis is to assume that scenario (5)—the case of two SRBs leaving fragment fields colocated or near each other—can be treated as a linear combination of two single SRB outputs; i.e., simply doubling the output from the one SRB case. Doubling the number of fragments in a location doubles the amount of gases released. Therefore, if the plumes from individual fragments do not interact as they rise, doubling the resulting output is a good assumption. However, doubling the number of fragments also doubles the heat released within the area, which tends to carry the gases higher into the atmosphere where they are less of a hazard. This effect is expected to be important when the fragments are close enough that the rising plumes interact.

For accidents at 15 s after launch assumed to be on nominal track, the maximum fragment number density is roughly 0.008 m^{-2}, or one fragment for every 128 m^2 in the densest portion of the pattern. The mean fragment size burning surface is estimated to be 0.41 m^2 (and the median area is one-fourth of this value). These dimensions imply that while the typical maximum dimension of the fragments is <1 m, the typical separation is almost 20 m. In this case, there would be little interaction between the plumes in the initial rise phase, and twice the single SRB fragment field case output should be a fair approximation for purposes of the current study. For accident cases before 15 s, the fragment field would be more compact, and the approximation would not be as good. The approximation would overestimate resulting gas concentrations.

The most serious consequences seem to be associated with the cases where the intact vehicle flies off track for some period of time. If the track is inland and the vehicle is determined to be beyond all possibility of control, the flight termination system would be activated when the vehicle threatens the primary ILL, a process that requires an estimated 7-s minimum. However, if it is determined that the vehicle is still under some level of control, the vehicle would be allowed to continue flight until it threatens the second ILL, at which time the flight termination system would be activated. Under this scenario, propellant fragments could be spread anywhere within the primary and secondary ILLs, in much closer proximity to onsite workers and visitors. While this scenario is less likely to occur than the on-track failures, it provides the dominant toxic cloud threat.

3.2 Risk of On-Land Fragments

To obtain a preliminary assessment of the relative risks for the types of accident outcomes and locations of fragment fields, contacts were made with the MSFC Quantitative Risk Assessment System (QRAS) team and ATK Thiokol Corporation. Databases of failure modes in the prelaunch and $T = 0$ to $L + 25$-s timeframe were assessed for scenarios leading to an off-trajectory flight. As indicated by the memo from B. Belyeu (app. C), no significant risk was identified for the prelaunch phase. For the $T = 0$ to $L + 25$-s phase, it was estimated that ≈35 percent of the total risk could be associated with scenarios involving off-nominal flight trajectories of the total vehicle. This estimate is in rough agreement with the 21 percent used in the USAF's Launch Area Risk Analysis (LARA) model (W. Snyder, personal communication, June 25, 2001). No discernment was made with respect to direction of flight. If trajectories are inland, these scenarios could lead to simultaneous breakup of both SRBs and the external tank (ET) initiated by the Range Safety Flight Termination system, or one SRB or the central vehicle elements could fail spontaneously due to an internal system failure. In the first case, one would expect the fragment fields from the two SRBs to be colocated, or at least near each other and in close proximity to the remnants of the ET and orbiter. In the second case, one or both SRBs would, in most cases, break free and remain propulsive for a few seconds until flight termination action is effected. The likely outcome is two fragment fields separated by some distance. The latter case would be similar to the *Challenger* accident, which occurred much later in flight (L + 72 s). In that instance, both SRBs broke free and remained propulsive for ≈38 s. Their flight trajectories took them out to sea; therefore, flight termination was not initiated immediately.

The total risk of failure in the first 25 s of flight estimated by the QRAS team (app. C) was 2.1×10^{-4}; the risk of off-track failure was estimated at 7.5×10^{-5}. (Products from QRAS and similar analysis approaches are most useful for determining the relationships or relative risks between differing scenarios. They do not provide a high-confidence estimate of absolute risk since the results are sensitive to the assumptions and historical data used in their development. QRAS models are routinely revised and

updated.) For the purposes of this study, it was assumed that all directions of flight were equally likely for the off-track failure scenario, a plausible assumption since there is little oceanward momentum in the initial seconds. This estimate implies that ≈0.42 of these accidents would result in over-land trajectories, and risk of on-land propellant fragments would be $(0.42 \times 7.5 \times 10^{-5}) = 3.2 \times 10^{-5}$ per launch. The risk exceeds "one in a million," a level which is generally considered as the criteria where the risk approaches natural background risk. The issue is aggravated by several factors. The on-track, free-flying SRB scenarios are not included, nor is consideration that there are two SRBs involved in each accident. Further, from a facility perspective, and unlike primary range safety considerations expressed in EWR 127–1, the problem of toxic gas release should be calculated on an annual or multiyear basis, requiring multiplication of the above figures by the annual or multiyear number of launches.

The USAF 45th SW assessed the risk of on-land fragments for the Range Safety panel based on the LARA model. The USAF found total risk of one or more fragments landing close to the primary ILL of 6×10^{-3} per launch; likewise, it was 1×10^{-3} for the area between the primary and secondary ILLs. The LARA included the entire launch process, not just the initial 25 s of flight. It is also based on a total risk of failure per launch that is ≈5 times the QRAS estimate. The large risk indicated close to the primary ILL is probably the result of inclusion of the on-track scenarios plus the larger total failure probability. The high per-launch risk indicated between the primary and secondary ILLs does not have a ready explanation. Considering a factor of 5 higher total probability of failure still leaves more than an order of magnitude discrepancy unexplained. The after 25-s portion of the flight may contribute more than expected.

4. SOURCE TERMS AND METEOROLOGY

In this TP, the work was focused on potential consequences of the toxic byproduct HCl release from combustion of solid propellant that would follow a catastrophic Shuttle accident while the vehicle is still in the immediate vicinity of KSC or CCAFS. The accident may be either prelaunch (while the Shuttle is still resting on the launch pad) or during the initial seconds of flight when the solid propellant fragments are most likely to fall on land. To simplify the analysis, it is noted that for a vehicle that is on course at the time of the accident/SRB destruct, essentially all fragments fall offshore if the accident is after $L + 25$ s (app. D). Also, the mass of propellants involved would be less than the earlier accident scenarios. Thus, only accidents in the initial 25 s, with focus on $L + 2.5$ and $L + 15$ s were analyzed. It is assumed cases arising from post 25-s accidents would be less severe and less likely to leave on-land fragments, but they would not be qualitatively different than those studied.

By far, the most dominant hazardous substances that would be released from a Shuttle accident are HCl and chlorine gas. Normally, HCl comprises ≈21 percent of the burn products from Shuttle solid propellant. For burning in the open atmosphere, as assumed here, with a 3:1 air-to-propellant ratio by weight, the NASA Lewis Equilibrium Combustion Code indicates HCl and chlorine would be approximately 4.3 and 1 percent, respectively, of the total products (includes the entrained air). Other toxic gases released by the propellant burn include nitric oxide and carbon monoxide at approximately 0.9 and 0.3 percent, respectively, with lesser amounts of other products. The vehicle also carries 10,900 kg of monomethylhydrazine and nitrogen tetroxide that may be released in an accident (Isakowitz, 1999).[16] In addition, substances with varying degrees of toxicity would be released by burning material and vegetation on the ground in the KSC vicinity. Each of these materials would exacerbate potential hazardous effects. For purposes of this work, identification of the significant cases that would comprise a "scenario matrix" for emergency response planning, HCl and chlorine considered together as HCl is the accepted methodology since Cl would have an approximate half life of 7 min in the atmosphere before reduction to HCl (NASA 1979).[17]

Aluminum oxide comprises ≈7.5 percent of the total burn products and is released as a very fine particulate. It plays an important role in HCl transport and deposition in the body. Much of this material would remain airborne in the form of hydrophilic aerosol in the inhalation size regime. Propellant burned in the ambient environment, especially at high humidity, is known to form copious amounts of hollow, spherical aerosol particles of low density (Dawbarn, 1980).[18] The hydrophilic nature of the aerosol has long been known because of comparison of Aitken and cloud condensation nucleus counts in exhaust clouds from Shuttle and Titan launches (Anderson and Keller, 1983; Radke et al., 1979).[19,20] The aerosol would tend to absorb the HCl gas and water from ambient air, leading to formation of an acidic aerosol. The acid concentration is not well known, and it may be expected to change rapidly with conditions (mixing with ambient air, temperature, humidity, etc.). In the early stages, acid concentrations are calculated to be at least in the 0.1 to 2 N range (Anderson and Keller, 1983).[19] Over time, the acid would be neutralized by reactions with trace gases, such as ammonia, in the atmosphere (Radke et al., 1982).[21]

4.1 Source Matrix

The discussion so far has centered on elements of the source term—initial release conditions—that are common to all scenarios. This section focuses on the matrix of possibilities, illustrated in table 4, that categorize the primary variables and secondary factors which influence model results. Selection of the modeling approach summarized in table 4 is driven by two factors: (1) The fact that this is intended as a screening study with limited objectives, and (2) results of the sensitivity analysis, summarized in table 5, which provide an indication of how results vary with input parameters.

Table 4. Primary variables (left column) and other variable factors that affect the source term. The approach blocks define the steps taken to reduce the problem to a manageable size.

Source Term	Variations: One or two SRMs and time of the accident affects the total mass, fragment size, and dispersal of the solid propellant. There would always be two SRMs involved; but in some cases, they would end up at separate locations so that only one SRM could affect a receptor. Approach: Primary attention is given to (1) an early accident at $t = L + 2.5$ s (the earliest time for which fragment distribution data are available) and (2) a later $t = L + 15$-s accident with more fragment spread. The cloud rise algorithms used do not account for interactions between adjacent fragments, so this primarily captures the propellant mass, fragment size, and dispersal variations. Doubling the concentrations from the single SRM cases, especially the $t = L + 2.5$-s case, gives a conservative estimate of the two SRM outcomes.
Meteorology	Variations: Wind speed, direction, stability, temperature, humidity, turbulence, etc. Approach: Wind direction was effectively eliminated by using complete rings of receptors at 5-deg increments and focusing on the maximum concentration detected on each ring. Results are based on a full 5-yr data set, two or more soundings per day with soundings that indicated “no go” meteorological conditions unsuitable for Shuttle launch excluded.
Location (relative to sensitive receptors)	Variations: Accident: On the launch pad, nominal ground track, off-track inland, off-track inland with source partially in water, or off-track out to sea. Receptors: VIP visitor viewing, NASA Causeway, Visitor’s Center, Day Care Center, Titusville, Port Canaveral, etc. Approach: Model runs based on receptors set in concentric circles centered at the accident location. The primary rings were set at 2.5 km, characteristic (assuming an on-pad or on-track accident) of the near field and VIP viewing area, 10-km characteristic of the NASA Causeway, and 20 km characteristic of Titusville and other offsite locations. Results indicate strong variations between the 2.5- and 10-km circles. Therefore, rings at 4, 6, and 8 km were used for additional analyses intended to help elucidate the off-track scenarios.

Table 5. Summary of sensitivity study analyses. Baseline input parameters are listed in the second column and baseline results are listed in bold on the top "Baseline Results" row. Variations indicated in the third column were made one at a time, and the results of each set of runs (447 meteorology cases) are displayed in the corresponding row.

Parameter	Baseline	Variation	Percent >10 ppm at Range (km)			Percent >50 ppm at Range (km)		
			2.5	10	20	2.5	10	20
	Baseline Results		**97.1**	**62.0**	**1.3**	**79.0**	**0.4**	**0.0**
Plume emissivity	0.8	0.6	97.1	61.5	1.3	79.0	0.4	0.0
		1.0	97.1	62.4	1.6	79.2	0.2	0.0
Mean surface temperature	22 ˚C	8 ˚C	97.1	73.0	1.1	89.1	1.1	0.0
Accident time	L + 15 s	L + 2.5 s	96.6	66.0	4.5	83.9	5.8	0.0
Mixing parameters	Calculate	Pasqu – G	99.8	92.4	19.9	89.3	7.8	0.4
Plume type	Slug	Puff	96.9	61.7	1.3	79.2	0.2	0.0
Probability density function	Off	On	86.1	61.3	1.3	70.2	0.4	0.0

Since the objective is to provide a screening analysis, the primary output of interest is the probable consequences; i.e., the frequency, given an accident does occur with on-land propellant fragments, that significant HCl concentration levels would be encountered at a given range from the accident epicenter. Results are used to identify the probable consequences that drive the emergency response planning process. This consideration sets a limit on how much accuracy is required of the modeling effort. It is important to analyze a relatively large meteorological data set to obtain statistically significant results. A full 5-yr set of meteorological data was analyzed for this study. The set consists of 4,471 rawindsonde soundings taken at KSC during the years 1965 through 1969. Usually two soundings per day were taken with additional soundings taken when launches were planned. This data set was selected because of the high data quality. Soundings with surface conditions that would be "no-go" for Shuttle launch—for reasons other than those addressed in this TP—were excluded.

A sense of the significance of the size of the meteorological data set can be gained from figure 3. The 5-yr data set was ranked by surface temperature and then divided into 10 nearly equal subsets of ≈447 soundings each. These subsets were identified by the mean surface temperature for each group. Figure 3 shows three histograms for HCl peak concentration 10 km from the source for model runs with all parameters identical except the meteorological soundings. The three subsets are Go281, Go295, and Go302; the numbers indicate the mean surface temperature (K) of the data set. Go281 was the coldest set of the 10; Go295 was near the middle; and Go302 was the hottest set. Thus, these sets span the range of surface temperature. The histograms are very similar, both presenting the same qualitative picture of the range of peak HCl concentrations as a function distance from the epicenter of fragments. The scenario modeled is for a single SRM with the failure at L + 15 s. Other model parameters were "baseline," as listed in table 5.

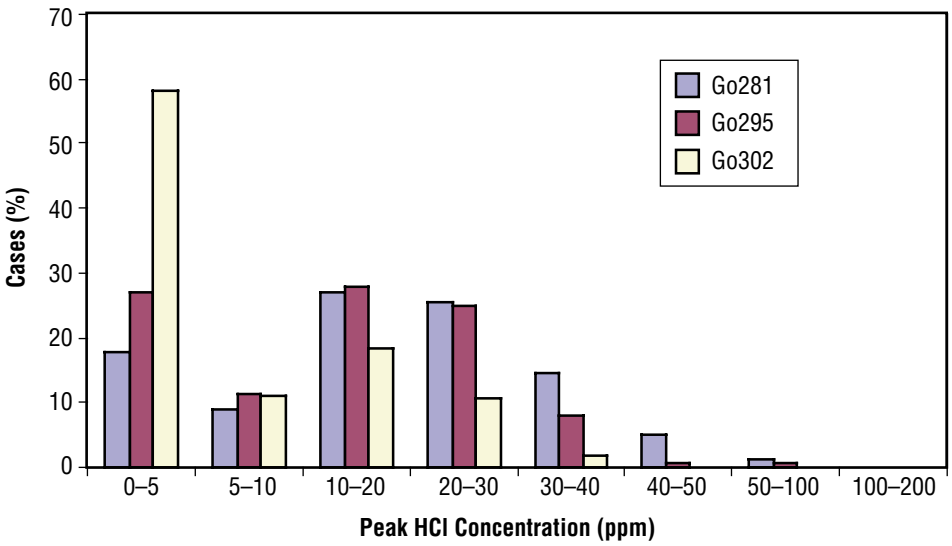

Figure 3. Variations in probability distribution of peak HC1 concentrations for different meteorology data sets. Assumed accident time of 15 s after launch, 10-km range to receptor, 447±1 soundings per set. The breathing zone peak concentration is indicated by the *x* axis (actually 0.05 to 56 ppm).

While meteorological data are the most important factor in determining the HCl concentration that would be encountered at a given distance from the accident fragment field(s), there are other parameters which enter into the CALPUFF model runs and analyses. The approach taken in this work was to select what are believed to be the "best"; e.g., most realistic, values for each. The approach is discussed with additional detail in appendices D and E. Table 5 summarized the influence of several of the most important parameters. Of the parameters listed, the strongest effect is from using the well-known Pasquill-Gifford mixing parameterization rather than calculating the mixing parameters from the sounding. An important observation is that the sensitivity cases tend to indicate more severe outcomes—as a rule—than the baseline. Due to these results, it appears unlikely that current results overestimate the consequences.

Variations in table 5 should also be interpreted in light of recognized limitations on the accuracy of models of this type. Paragraph 10.1.2 of *Guideline on Air Quality Modes* (Bureau of National Affairs, Inc., 1996)[22] states "…. and (2) the models are reasonably reliable in estimating the magnitude of highest concentrations occurring sometime, somewhere within an area. For example, errors in highest estimated concentrations of ± 10 to 40 percent are found to be typical, i.e., certainly well within the often quoted factor-of-two accuracy that has long been recognized for these models." Model parameter inputs used in this study are believed to be the best available representation of the actual circumstances to be expected, and the variations in the sensitivity study are a fair representation of the uncertainties.

Another important source term issue concerns the question of what happens when burning solid propellant fragments land in the water. This issue is important not only because of the immediate proximity of the ocean, ≈1 km from the center of Pads 39A and 39B, but also because of the Indian River ≈11 km to the west, the Banana River 4 to 7 km south, and Mosquito Lagoon 4 to 7 km northwest of the Pads. There

are also numerous ponds and channels nearby. If the fragments were to remain burning while submerged, HCl and other gases would be released into the atmosphere in a much cooler, wet aerosol-laden form. This form of release would result in a less buoyant toxic cloud than one evolving from the very hot fragments burning on land; thus it would be more likely to stay near the ground in concentrated form, posing a greater hazard. Data from analytical studies, testing of small quantities of solid propellant at ambient pressures (app. A), and experience with the *Challenger* failure indicate that rapid heat loss to the water would quench the flame (El Dorado Engineering 2000 (app. A); NASA 1986[15]). Small propellant pieces are routinely burned submersed in water at high pressure (>400 psi) and a pail full of 1/4-in chips immersed in water also burned nearly to completion. In addition, observations of single pieces, whether small or large, are that they quickly extinguish under water, or at the water line if they were only partially submerged. Direct proof is that many large (and small) propellant fragments with evidence that they had been burning were recovered following *Challenger* (NASA, 1986).[15] In summary, high pressure increases the burn rate, and multiple small chips heat one another, but without these enhancements, solid propellant extinguished in water.

5. CALPUFF RESULTS

Distributions of peak HCl concentration at ranges of 2.5, 10, and 20 km from the epicenter of the fragment field are illustrated in figures 4–6. The figures show results for accidents initiated at 2.5 and 15 s after launch. Both accident times were run against the same 5-yr meteorology (4,471 cases) using the baseline selection of model inputs as described in section 4 and summarized in table 6. For the earlier accident time, the fragment field is more concentrated, and there is slightly more propellant than the later (L + 15 s) cases. Maps illustrating the fragment fields are shown in appendix D. Additional details on modeling methods are provided in appendix F.

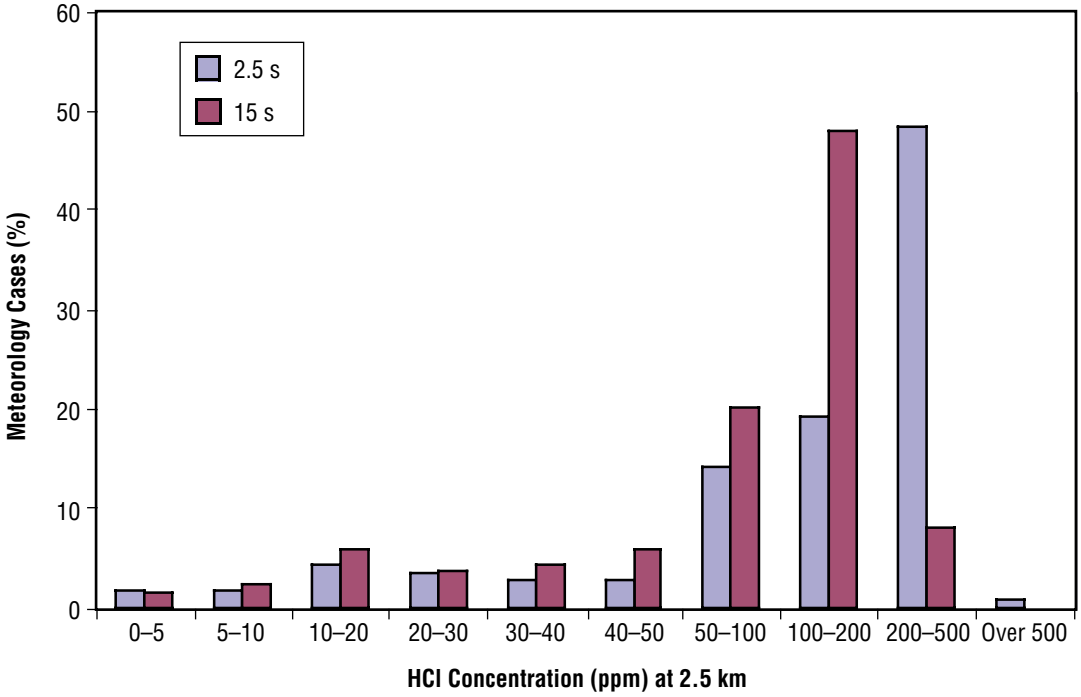

Figure 4. Distribution of peak breathing zone HCl concentrations at 2.5 km from the fragment field epicenter.

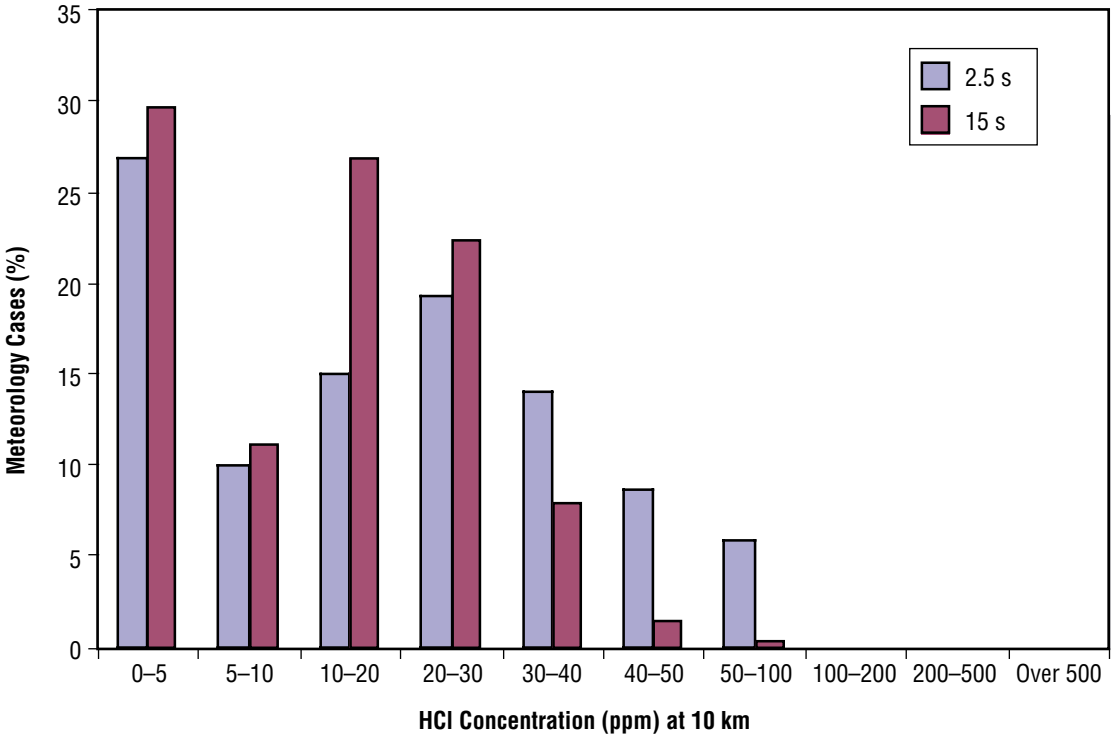

Figure 5. Distribution of peak breathing zone HCl concentrations at 10 km from the fragment field epicenter.

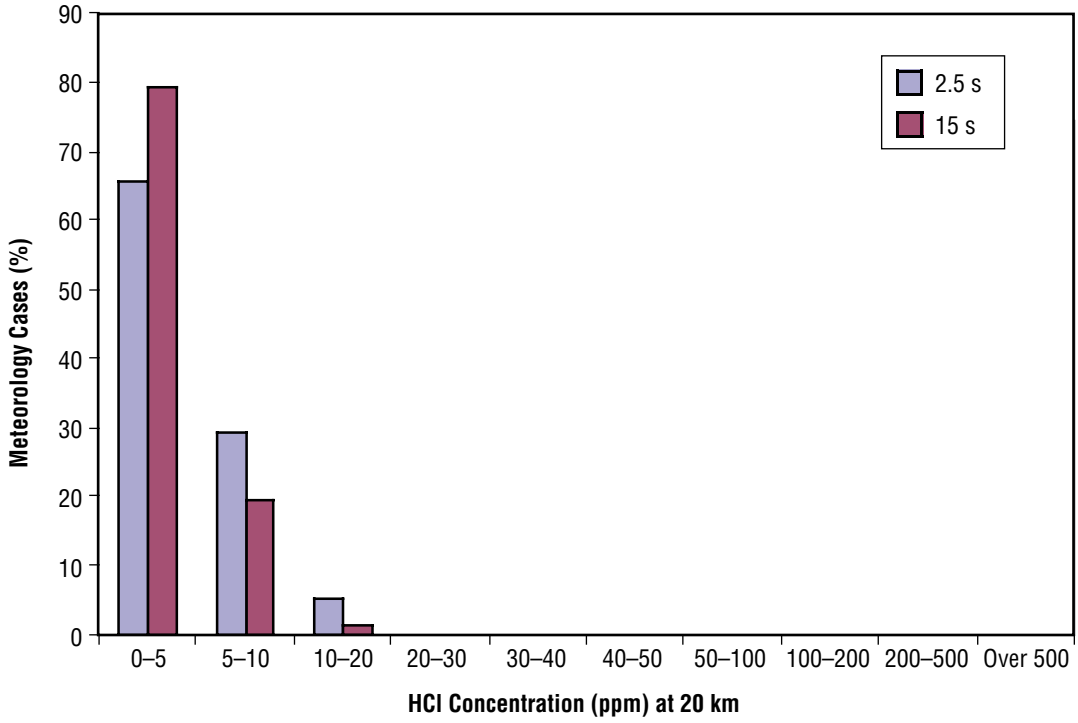

Figure 6. Distribution of peak breathing zone HCl concentrations at 20 km from the fragment field epicenter.

Table 6. Summary of baseline input parameters for the CALPUFF analysis.

CALPUFF Input Parameter	Baseline Value
Duration of diffusion process modeled	4 hr
Plume emissivity (radiation from hot rising gases)	0.8
Mixing (turbulence) parameters	Calculated (app. F)
Plume type (slug or puff)	Slug
Probability density cloud rise option	Off
Receptor elevation	Surface (zero meters)
Receptor locations	Concentric rings at 2.5, 10, and 20 km

For source terms from 2.5 to 15 s, results do not differ significantly in terms of the objectives of this study. HCl concentrations within 10 km of the fragment field epicenter—and downwind—were found to be high enough to be of concern from an emergency response perspective.

To further clarify dependence on distance from the source in the critical region between 2.5 and 10 km from the accident epicenter, an additional analysis of the 5-yr meteorology database, $L + 15$-s scenario was made with results reported at 4, 6, and 8 km from the epicenter. Combined results are displayed in figure 7, and statistics for all of the 15-s accident cases are summarized in table 7. The 2.5-s accident case was not run at intermediate distances, but it is reasonable to expect that it would be more severe than the 15-s cases based on comparison of the statistics at 2.5, 10, and 20 km. At these ranges, the 2.5-s case median peak HCl concentrations were 200, 19, and 3.3 ppm, respectively. The means of the peak HCl concentrations were 190, 21, and 3.9 ppm at the same respective locations.

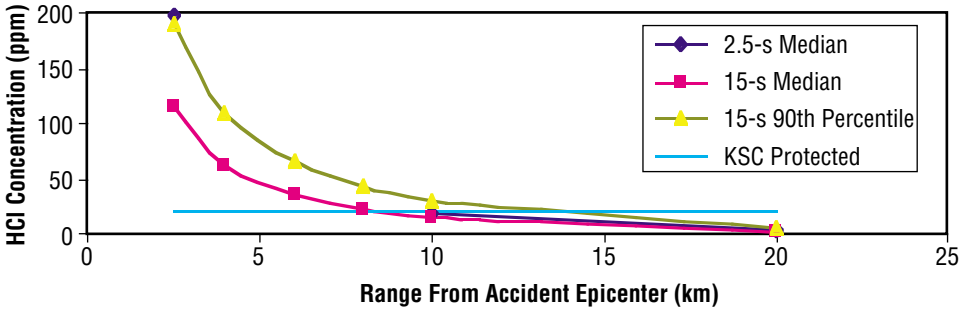

Figure 7. Statistics of peak breathing zone HCl concentrations as a function of range from the fragment field epicenter. The horizontal line is at 20 ppm.

Table 7. Statistical summary of peak HCl concentrations (ppm) as a function of range from the fragment field epicenter. Statistics derived for 4,471 "go" meteorology cases and an accident time of $L + 15$ s.

Range	2.5 km	4 km	6 km	8 km	10 km	20 km
1st percentile	4.1	1.5	0.6	0.3	0.2	0.04
5th percentile	13.0	4.9	1.9	1.1	0.7	0.15
10th percentile	31.0	9.4	4.0	2.0	1.3	0.28
Mean	110.0	61.0	34.0	22.0	15.0	3.00
Median	110.0	63.0	35.0	22.0	14.0	2.60
90th percentile	190.0	110.0	65.0	43.0	30.0	6.30
95th percentile	220.0	130.0	75.0	49.0	34.0	7.40
Maximum	380.0	220.0	140.0	98.0	65.0	15.00

5.1 Rocket Exhaust Effluent Diffusion Model and Los Alamos National Laboratory Model Comparisons

In order to improve understanding of the CALPUFF results and context in terms of prior results obtained in KSC- and USAF-sponsored work on this subject, several comparisons were made with the REEDM and with the single meteorological case used in the LANL study. Figures 8–11 show CALPUFF peak HCl concentration results plotted against REEDM results for 1,342 meteorological cases from the Go281, Go295, and Go302 meteorology files. If the models were giving similar results, the data points would cluster around the equal value line. Instead, for the 4-km case (fig. 8), the points cluster near the *y* axis, indicating a substantial number of instances where CALPUFF is returning high values of HCl peak concentration at the same time that REEDM is returning low values. The difference is greater than is apparent because many points lie on top of each other in the thick of the cluster. The distribution functions in figure 12 are a better illustration of how different the models perform. At greater distances from the source—figure 10 (for 10 km) and especially figure 11 (20 km)—the models begin to yield more comparable results. This convergence is clearly the case as can be seen in the statistics of the distributions compared in table 8. At 4 km, mean and median values for peak HCl concentrations from CALPUFF exceed the REEDM values by a full two orders of magnitude. At 10 km, the spread is one order of magnitude, and at 20 km, it is only a factor of 3 to 4. However, on a case-by-case basis, there is still not a good match—no clustering around the equal value line. Rather, model results seem to be uncorrelated. It should be noted that REEDM version 7.08 was utilized for this analysis. However, spot checks with six soundings made with the more recent version 7.09 (courtesy of D. Berlinrut, 45th SW) indicated very small differences from version 7.08 results.

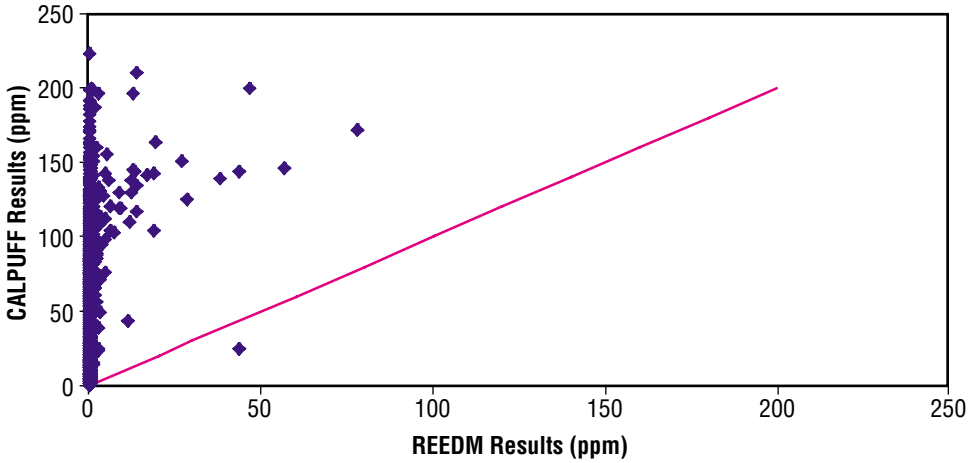

Figure 8. CALPUFF results plotted against REEDM results for the same 1,342 meteorology cases, 4 km from the source, 15-s accident time. Equal results would fall upon the diagonal line. This close to the source, REEDM shows very few significant concentrations, 95 percent are <5 ppm, whereas CALPUFF shows values >5 ppm in all but 14 percent of the cases in this sample.

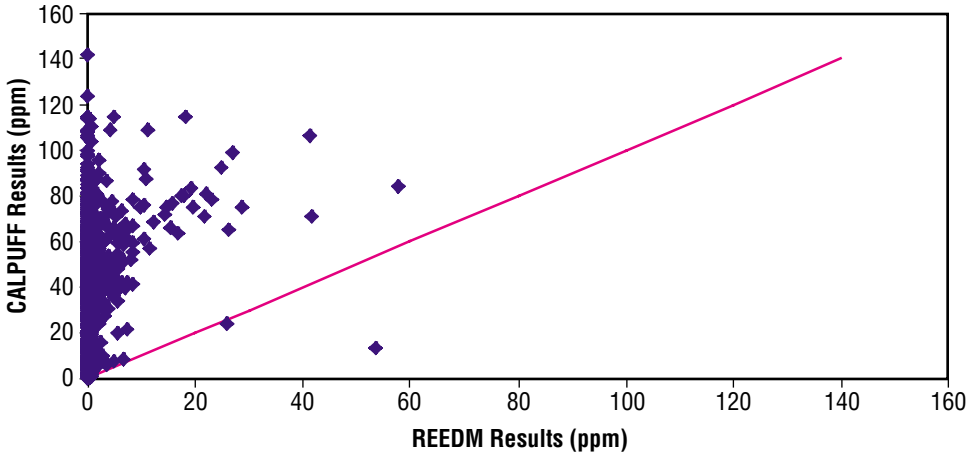

Figure 9. CALPUFF results plotted against REEDM results for the same 1,342 meteorology cases, 6 km from the source, 15-s accident time. Equal results would fall upon the diagonal line. CALPUFF indicates higher concentration in all but two or three cases.

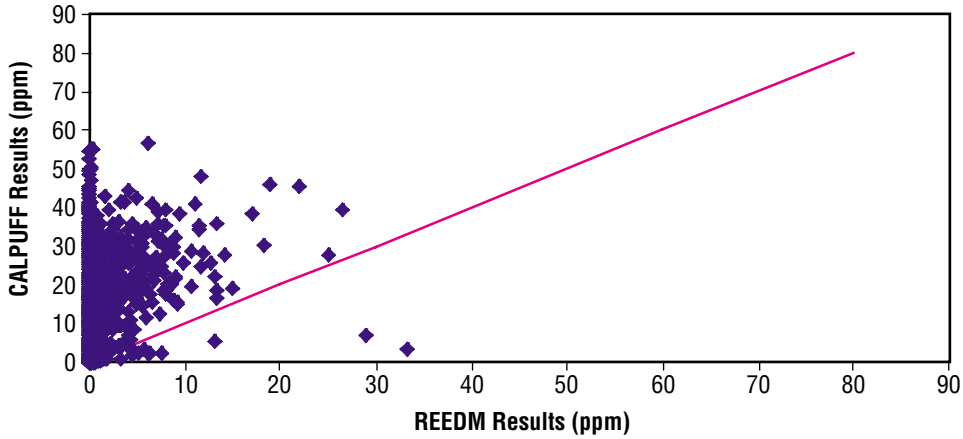

Figure 10. CALPUFF results plotted against REEDM results for the same 1,342 meteorology cases, 10 km from the source, 15-s accident time. Equal results would fall upon the diagonal line.

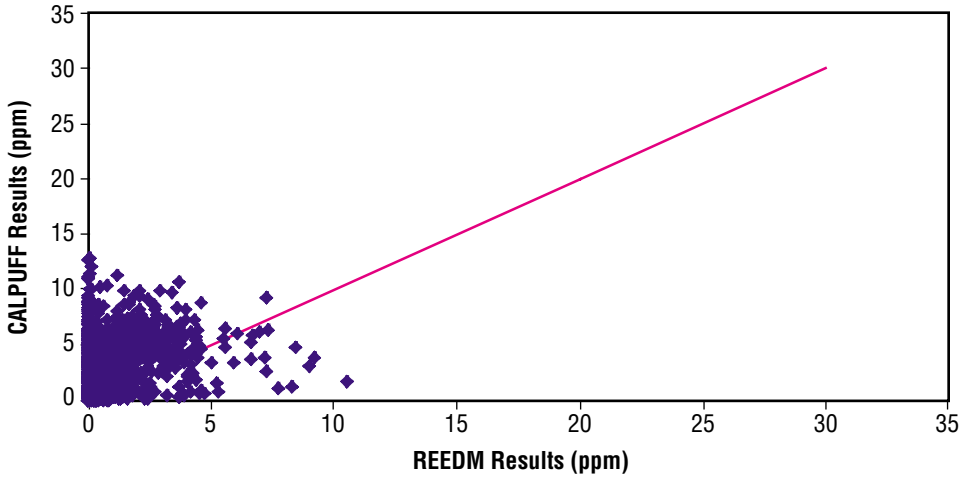

Figure 11. CALPUFF results plotted against REEDM results for the same 1,342 meteorology cases, 20 km from the source, 15-s accident time. Equal results would fall upon the diagonal line. In comparison to CALPUFF, REEDM still usually underestimates the concentration, but the difference is much less pronounced than in figures 8–10.

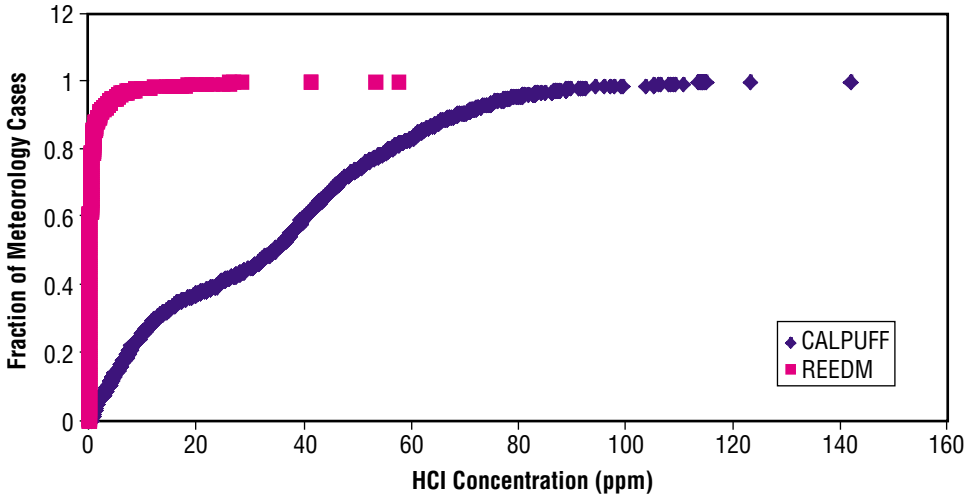

Figure 12. Comparison of cumulative distributions for 1,342 meteorology cases. HC1 peak concentrations at 6 km from the fragment field epicenter, while REEDM indicates ≈90 percent of the cases would not reach the 5 ppm OSHA ceiling—CALPUFF indicates the opposite.

Table 8. Comparison of statistics from REEDM (columns marked REED) version 7.08 and CALPUFF (columns marked CPUF) based on 1,342 meteorology cases. Values are peak HC1 concentration in parts per million. Notice that the REEDM and CALPUFF results become more similar as the range increases from 4 to 20 km, left to right across the table.

	REED 4 km	CPUF 4 km	REED 6 km	CPUF 6 km	REED 8 km	CPUF 8 km	REED 10 km	CPUF 10 km	REED 20 km	CPUF 20 km
Means	0.66	61	1.00	34	1.20	21	1.30	14	0.96	2.8
Median	0.06	61	0.11	34	0.22	21	0.35	13	0.56	2.3
STD deviation	4.00	43	3.80	26	3.30	17	2.80	12	1.30	2.4
90th percentile	0.56	120	1.90	69	3.20	44	3.70	30	2.50	6.1
95th percentile	1.40	140	4.90	78	6.30	51	6.20	35	3.60	7.1

The key difference between CALPUFF and REEDM that leads to significantly different results near the source is that REEDM is a single-puff, single-source model. In REEDM, the burning propellant fragments are modeled as a single, disk-shaped source which gives rise to a single "puff" that represents the gas cloud. CALPUFF is a multipuff model that treats each fragment as a separate source, each of which generates a series of separate puffs. In any diffusion model, an extremely important computation is the relationship between the "stabilization height" (the height at which the puff(s) stabilize after their buoyant rise from the source) to the "mixing height," the level in the atmosphere that separates the turbulent lower atmosphere from the higher, more stratified air. Usually the mixing height is well defined by an inversion layer. Puffs or portions of puffs that rise above the mixing height will spread horizontally but there is no significant mechanism to bring the gases downward toward the surface. Thus, this gas makes

no contribution to the local gas concentrations at or near ground level—the breathing zone. On the other hand, puffs (gases) that stabilize below the mixing height are rapidly mixed downward by turbulence. This material dominates the local surface effects. In REEDM, with only a single puff that must end up either above or below the mixing height, there is a tendency toward binary results—very high or very low—near the source. The puff is split after stabilization into portions above and below the mixing height to give some compensation, but results still tend to be unrealistically binary.

Table 9. REEDM results for the November 23, 1995, case also studied by LANL.

	Abort Time				
	5 s	10 s	15 s	20 s	25 s
Initial cloud radius (m)	100	200	320	370	410
Stabilization height (m)	1,100	900	78	52	44
	Peak HCl Concentration (ppm)				
Range from source:					
2 km	0.05	0.03	245	390	410
4 km	0.03	0.04	240	260	235
6 km	0.05	0.08	150	148	130
8 km	0.10	0.18	96	92	82
10 km	0.18	0.36	65	61	55
20 km	0.84	1.80	15	14	12

REEDM results for the meteorology of November 23, 1995—the case that formed the focus of the LANL study—illustrate the point. Table 9 shows how REEDM handled this case for five different accident times. The later the accident the more spread out the fragment field, while the total amount of propellant diminishes slightly. The top of the table shows the initial cloud radius, indicative of the source size, and the stabilization height calculated by REEDM. In all cases, the mixing height was calculated to be 826 m, since it depends only on the meteorology. For the 5- and 10-s cases, the cloud is smallest and thus more buoyant, leading to puff stabilization heights above the mixing height. At 15 s, there is a very sharp transition; the larger and less buoyant puff rises only to 78 m, less at later accident times. The effect on peak HCl gas concentration in the near field is dramatic, as illustrated in the lower portion of the table. There is an unrealistic—nearly four orders of magnitude—transition in the predicted concentrations between the 10- and 15-s cases. The multipuff, multisource approach of CALPUFF precludes this sharp discontinuity.

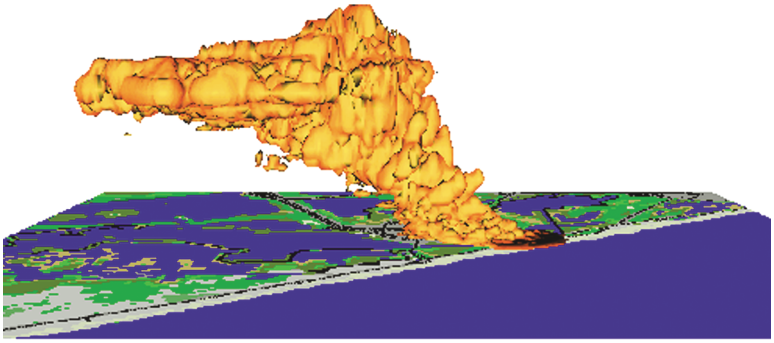

Figure 13. 20 ppm HCl concentration isosurface from the LANL analysis[3] for a single, disk-shaped source similar to the source assumed in REEDM. November 23, 1995, meteorology, 15-s accident time, 500 s after the fragments hit the ground, 20-m horizontal resolution.

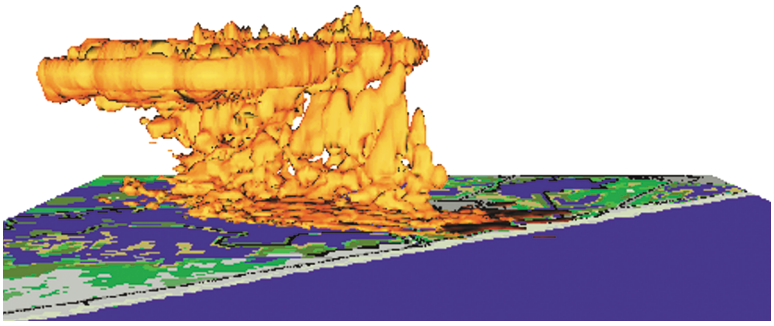

Figure 14. 20 ppm HCl concentration isosurface from the LANL analysis[3] for a multifragment source; otherwise, the same conditions as figure 13. Note the much greater extent of the horizontal dispersion near the surface.

It is important to note that the primary use of REEDM is to model toxic gas diffusion from nominal launches. For nominal launches, the source is a single concentrated source, so the REEDM modeling is more realistic for this application, even in the near field. In the LANL study, the 15-s accident with November 23, 1995, meteorology was looked at for both the distributed multifragment source and a single, disk-like source as assumed by REEDM. The cloud from the disk-like source shows a clear tendency to rise higher (fig. 13) compared to the multifragment source (fig. 14). The LANL results were read from the color-scale graphs that lack the fidelity of tabular data. Peak concentrations 3 m above ground level at the 4-km range is ≈20 ppm for the multifragment case and ≈5 ppm at 10 km. These values are intermediate between the REEDM values for the 10- and 15-s cases at the same ranges.

CALPUFF peak HCl concentration for the 15-s accident and the November 23, 1995, meteorology was 360 ppm at 2.5 km. At 10 km, the CALPUFF peak was 58 ppm at the surface, decreasing monotonically to 50 ppm at 58 m above the surface. In comparison, the LANL result was <5 ppm at 3 m (the lowest elevation reported), increasing to over 50 ppm at 58 m. Similarly, at 20 km, CALPUFF showed a nearly uniform 9 ppm over this height range while LANL showed a strong increase, from <5 ppm at 3 m to over 25 ppm at 58 m. Figure 31 of the LANL report shows a vertical cross section near Port of Canaveral, at about the 20-km range. The HCl gas is all contained in a diagonal sheet which, judging from the discussion of this figure on page 21 of the same report, must be no more than ≈30 m thick. This result represents little vertical diffusion from the source and may be a spurious result.

6. FINDINGS AND CONCLUSIONS

6.1 Study Results

One conclusion dominates the results from this screening analysis. The multitude and separation of propellant fragments, many of them relatively small, that would result from a catastrophic Shuttle failure over land almost always leads to significant toxic gas concentrations in the near field. As illustrated in figure 7, HCl peak concentrations in the "immediately dangerous to life and health" range would occur downwind for over half the meteorological situations out to a distance of over 4 km from the fragment field epicenter, and the possibility of encountering concentrations at this level remains of concern out to distances of at least 10 km. HCl concentrations that require effective mitigation (levels in the 5 to 50 ppm range) should be anticipated for just over 70 percent of meteorological situations downwind at a range of 10 km; even at 20 km, the expectation is 20 to 30 percent. These results indicate a serious safety hazard and a very different picture than previously believed, based on the results from REEDM "early in flight" catastrophic abort scenarios.

These results for the anticipated "consequences," given an accident of the types modeled, is based on analysis of a 5-yr meteorological database (4,471 cases) using CALPUFF, an EPA-recommended and commonly used model for similar air quality applications. Sensitivity studies with respect to variations in source term and model parameters, as described in section 4, leave little doubt about the basic magnitude of the conclusion. One might anticipate that refinements in the modeling and description of the source terms could alter single meteorology case results by perhaps a factor of 2 to 4. It is highly unlikely that a change of approximately two orders of magnitude that would be needed to alter the basic conclusion could be realized. Examination of the parameters list (table 1) indicates that essentially all of the parameters expected to be of "major" or "moderate" importance were looked at in the sensitivity studies and found to be incapable of changing the basic conclusion. The exception is the aerosol issue that would produce HCl exposure potentials of even higher magnitudes. This work plus the verification from the LANL study and earlier review team work all support the conclusion that results from prior REEDM analysis are faulty and significant HCl concentrations must be expected in the near field following an accident involving deflagration of the SRMs over land.

While the estimated magnitudes of the anticipated consequences following an over-land catastrophic failure are relatively firm, the estimation of the probability that such an event could occur is more problematic. The only existing model known to the authors is the USAF's Launch Area Toxic Risk Analysis (LATRA) which relies on REEDM. NASA estimates using the QRAS indicate that the risk of catastrophic failure in the $L = 0$ to 25-s timeframe is of the order 2×10^{-4}; estimates using the database and ground rules favored by the 45th SW would increase this number up to an order of magnitude. In any case, estimates of this type are always difficult and subject to large uncertainty. In addition, many accidents within the first 25 s after launch will not result in an SRB fragment field over land, but some accidents at times even as late as 100 s could still result in an SRB turning around and impacting on land. There is no clear cutoff, so that an extensive modeling of the many failure modes and possible dynamic effects would be needed to quantify the risks. The complexity of the issues is such that much uncertainty would always remain even after a substantial effort was expended.

Given a failure, QRAS analysis indicates that ≈35 percent of the time the abort would be "off-nominal flight trajectory"; i.e., the intact vehicle would fly at an undesired trajectory until, assuming control of the vehicle is not recovered, either further failures occur or flight termination action is initiated, resulting in catastrophic breakup. USAF estimates for this conditional probability are roughly the same, ≈21 percent. These scenarios are the most serious because the undesired trajectory may be carrying the vehicle inland such that the SRB fragment field would land somewhere within the secondary ILL. See figure 2 for the relationship of the ILLs and locations where public and worker populations are to be found. Therefore, no matter what the wind direction, there is the possibility that workers or the public could be located downwind and within the near field of the accident location. The remaining 65 percent of the scenarios involve a catastrophic failure of one or more of the vehicle elements while it is still on the nominal trajectory. In these cases, either one or both of the SRMs can be expected to remain as an intact free-flier and propulsive until ground impact or the flight termination system breaks up the motor(s). In these cases, the fragment field(s) are most likely to be centered within 2 km of the initial failure location. This scenario could shorten the distance to the worker and viewing public at the VIP viewing area, the Vertical Assembly Building, NASA Causeway, etc., but at least 4 km or more separation should remain. Thus, this scenario is less critical than the intact vehicle off-nominal flight scenario.

Based on the findings presented above, it is concluded that REEDM should no longer be used to predict near-field HCl exposure levels, nor should any further investment be made in REEDM upgrades when CALPUFF and other quality models are available at no cost through the EPA. Mitigation decisions should be based on results from a multipuff, multisource model and consideration of far, off-nominal ground tracks which would encompass sensitive inland sites. Note that the USAF has a currently funded project to replace REEDM.

6.2 Perspectives on Mitigation

It is clear from these results that toxic gas concentrations in the near field—within ≈10 km from the SRB fragment field(s)—are problematic for many, if not most, meteorological conditions. Thus, there is little to be gained in further pursuing meteorology-based LCC; i.e., holding the launch during weather conditions that could lead to a projected unsafe condition. This finding is true for protection of both onsite and the offsite viewing public, since the secondary ILL is within 1 km of the offsite public in several areas.

Another approach that appears to be inadequate is reliance on probability arguments and an E_c approach, although this aspect needs to be addressed because of range safety requirements; e.g., EWR 127–1. The basic probability of occurrence for an accident is high. A convincing argument would have to be developed that the risk was several orders of magnitude less than current estimates before the risk could be considered insignificant. Likewise, for the risks that the fragment field could be located on land, leaving workers or the public in the near field. Considering the basic assumptions and key parameters of risk calculations and the dependence on historical databases, no projected risk reduction is expected in the near term. Risk of a catastrophic abort is within the "credible" range.

Two mitigation approaches that are typically used for toxic gas accident mitigation are evacuation and sheltering. These approaches hold promise for providing at least a partial solution in this case. The USAF has tested and classified all of their buildings on the CCAFS for their ability to protect workers from launch-related toxic gases. By requiring workers to remain inside approved buildings and turning off

circulation of outside air into the building during the critical period, the USAF is usually able to continue operations without special holds and still maintain worker safety. This approach should be effective for NASA workers as well, although the protection afforded by existing buildings should be reassessed in light of these study results. A larger investment would be needed to provide shelter for visitors, especially for the viewers at the NASA Causeway.

Evacuation and barricading also offer promise for contributing to a mitigation strategy, although with limitations, because of the large number of people potentially involved and the fact that the fragment field location is unknown beforehand, making it uncertain how much time can be expected to be available between the abort and when the public would potentially be exposed. Plans should be in place to barricade roads for up to 10 km downwind from the fragment field, wherever it may be located, and to provide alternative routes for emergency vehicles and public egress. Evacuation may also be effective for workers and small pockets of people. For large concentrations of the viewing public, such as the several thousand viewers at the NASA Causeway, sheltering may be the only viable option. Detailed studies of the failure scenarios and associated probabilities and flight mechanics could be useful in defining the probability contours of where the fragment fields may be located. These data would be helpful in preparing evacuation and barricading plans.

Another mitigation option is reexamination of the ILLs and flight termination criteria. The longer the vehicle flies and the higher it goes, the more propellant is burned at a high altitude above the mixing layer and the more dispersed the fragment field is likely to be. It may also be feasible to use prelaunch meteorology to define keep-out zones within the existing ILLs to provide range destruct protection to population concentrations such as the NASA Causeway and some offsite viewing areas.

An augmentation of mitigation approaches described above is the use of disposable acid gas masks that can be acquired for as little as $10 each per a preliminary survey. Gas masks could be made available on buses and where workers or the public are within potential zones of excessive HCl exposure.

APPENDIX A—ANALYSIS OF PROPELLANT QUENCHING IN WATER

COMBUSTION STUDY FOR SOLID PROPELLANT IN WATER

June 15, 2000

PREPARED FOR:

DR. BECKY McCALEB
NASA

PREPARED BY:

EL DORADO ENGINEERING, INC.
2964 WEST 4700 SOUTH, SUITE 109
SALT LAKE CITY, UTAH 84118
TELEPHONE: 801-966-8288
FAX: 801-966-8499

A Simplified Model to Predict Nonadiabatic Propellant Flame Temperature

By
*Mardson Q. McQuay, Professor
Brigham Young University
Mechanical Engineering Department, 435 CTB
Provo, UT 84602
801-378-4980
Email: mq01@byu.edu

Submitted to
Eldorado Engineering
June 11, 2000, Revised

*New Affiliation:
Mardson Q. McQuay
Registered Patent Attorney
Oblon, Spivak, McClelland, Maier, & Neustadt, P.C.
1940 Duke Street
Alexandria, VA 22314

Executive Summary

A simplified, one-dimensional, steady, heat-transfer model was developed to predict the flame temperature of composite solid propellant fuels under nonadiabatic conditions in order to simulate and to investigate whether or not it would continue to burn in contact with water. A traditional, one-dimensional model of a solid propellant under adiabatic conditions, including preheat, gasification, induction, and reaction zones,[1,2] was modified and extended to include a radiative heat loss boundary condition in the calculation of the final combustion temperature. The model includes a zero-order, high activation energy thermal decomposition initiation reaction in the condensed phase (preheat and gasification zones) followed by a second-order, low activation energy chain reaction in the gas phase. This approach basically eliminates the induction region of standard models leaving only the reaction zone in the gas phase.[3] The assumptions made in the present model prevent ignition and extinction to be captured because of the time-dependent nature of these phenomena.

Flame temperatures predicted with the inclusion of radiative heat loss to the water at ambient pressure are still significantly higher than the relatively low auto-ignition temperature of solid propellant (around 500K), suggesting that these energetic materials may continue to burn under water. In the case of AP and HMX propellants, comparing flame temperatures under adiabatic and non-adiabatic conditions (for a water temperature of 400 K), the predicted flame temperatures dropped from 3630 to 2350 and from 2750 to 1850 K, respectively. However, limited validation of these simplified predictions against available experiments and the opinion of experts are inconclusive, indicating the need for both the development and use of more complex models and performance of additional experimental tests at the conditions of interest.

---

[1] R.A. Strehlow, Combustion Fundamentals, McGraw Hill, NY, 1984, page 455.

[2] M.W. Beckstead, Model for Double-Base Propellant Combustion, *AIAA Journal*, 18(8): 980-985(1980).

[3] M.J. Ward et al., Steady Deflagration of HMX With Simple Kinetics: A Gas Phase Chain Reaction Model, *Combustion and Flame*, 114:556-568 (1998).

Nomenclature

A_c Condensed phase frequency factor
B_g Gas phase frequency factor
c_p Specific heat at constant pressure
D Gas phase diffusion coefficient
D_g Gas phase Damköhler number
E_g Activation energy for the bimolecular gas phase reaction
E_c Activation energy for the zero-order solid phase decomposition reaction
k Thermal conductivity
m Mass flux
MW Molecular weight
q Heat release rate per unit mass
R Universal gas constant
T Temperature
x_g Characteristic gas phase flame thickness

Greek Symbols

ρ Density
σ Radiation constant

Subscripts

c Condensed phase
g Gas phase
r Reference
s Surface
o Initial
f Final
w Water
~ Dimensional quantity

Model Description

The one-dimensional, heat transfer model implemented here solves energy and species equations in the solid and gas phase regions using temperature-dependent, simplified chemistry. Several simplifying assumptions were made including: (1) equal molecular weights for the various species involved; (2) mass diffusion in the gas phase described by Fick's law; (3) temperature independent thermodynamic properties; (4) unity Lewis number; (5) equal specific heats for the solid and gas phases; (6) neglect of mass diffusion in the solid phase and radiation heating of the solid by the flame; (6) ideal gas behavior in the gas phase and incompressible solid phase; (7) neglect of turbulent effects (i.e., laminar flow) and (8) steady state conditions. Variables used here to describe the model are defined in the nomenclature section of this report. Under these assumptions the energy equation and appropriate boundary conditions in the solid phase are:

$$\tilde{m}\tilde{c}_p \frac{d\tilde{T}}{d\tilde{x}} = \tilde{k}_c \frac{d^2\tilde{T}}{d\tilde{x}^2} + \tilde{q}_c \tilde{w}_c \tag{1}$$

$$\tilde{T}(0) = \tilde{T}_s; \quad \tilde{T}(\tilde{x} \to -\infty) = \tilde{T}_0. \tag{2}$$

The approach used here to solve this equation is to divide the solid phase in two regions was proposed by Legelle[4] and summarized by Williams.[5] The first region is controlled by thermal convection and diffusion and the second by thermal diffusion and chemical reaction. The solutions in these two subdomains are merged together by use of an activation energy asymptotic analysis and assuming a zero-order gasification reaction in the solid. The reaction rate for this propellant gasification reaction is given by Equation (3) below and the reaction rate expression obtained from this solution is that shown in Equation (4)

$$\tilde{w}_c = \tilde{\rho}_c \tilde{A}_c \exp(-\tilde{E}_C / R\tilde{T}) \tag{3}$$

$$\tilde{m}^2 = \frac{\tilde{A}_c R \tilde{T}_s^2 \tilde{k}_c \tilde{\rho}_c \exp(-\tilde{E}_c / R\tilde{T}_s)}{\tilde{E}_c \left[\tilde{c}_p (\tilde{T}_s - \tilde{T}_0) - \tilde{q}_c / 2\right]}. \tag{4}$$

---

[4] G. Lengelle, Thermal Degradation Kinetics and Surface Pyrolysis of Vinyl Polymers,, *AIAA Journal*, 8:1989-1998(1970).

[5] F.A. Williams, Combustuon Theory, Addison-Wesley Co., Redwood City, CA. 1985.

Note in the above equation that the solid surface temperature is part of the solution and will also be needed in the solution of the governing equations in the gas phase; therefore, the solution will be iterative in nature.

In the gas phase conservation equations of energy and species are given by:

$$\tilde{m}\tilde{c}_p \frac{d\tilde{T}}{d\tilde{x}} = \tilde{k}_g \frac{d^2\tilde{T}}{d\tilde{x}^2} + \tilde{q}_g \tilde{w}_g \tag{5}$$

and

$$\tilde{m}\frac{dY}{d\tilde{x}} = \tilde{\rho}_c \tilde{D} \frac{d^2Y}{d\tilde{x}^2} - \tilde{w}_g \tag{6}$$

where a second-order overall reaction is assumed for which the reaction rate is given by equation (7)

$$\tilde{w}_g = \tilde{\rho}_g^2 \tilde{B}_g Y \tilde{T}^{-2} \exp(-\tilde{E}_g / R\tilde{T}); \quad where \quad \tilde{\rho}_g = \frac{\tilde{P}MW}{R\tilde{T}}. \tag{7}$$

Control volume balances at the solid/gas interface and on the entire system (solid and gas phases) provide additional equations for the solid surface temperature and flame temperature as:

$$\tilde{T}_s = \tilde{T}_0 + \frac{\tilde{q}_c}{\tilde{c}_p} + \frac{\tilde{k}_c}{\tilde{m}\tilde{c}_p}\left[\frac{d\tilde{T}}{d\tilde{x}}\right]_{\tilde{x}=0} \tag{8}$$

and

$$\tilde{T}_f = \tilde{T}_0 + \frac{1}{\tilde{c}_p}\left(\tilde{q}_c + \tilde{q}_g\right). \tag{9}$$

Under the assumption of $Le = 1$ the energy and species relationships, Equations (5) and (6), have identical forms and are written in dimensionless form as:

$$m\frac{dY}{dx} = \frac{1}{Le}\frac{d^2Y}{dx^2} - D_g Y \exp\left(\frac{-E_g}{T_f - Yq_g}\right) \tag{10}$$

and

$$m\frac{dT}{dx} = \frac{d^2T}{dx^2} - D_g(T_f - T)\exp\left(\frac{-E_g}{T}\right) \tag{11}$$

where: (1) the nondimensional variables used are

$$T = \frac{\tilde{T}}{\tilde{T}_f - \tilde{T}_0}; \quad x = \frac{\tilde{m}_r \tilde{c}_p}{\tilde{k}_g}\tilde{x}; \quad m = \frac{\tilde{m}}{\tilde{m}_r}; \quad E = \frac{\tilde{E}}{R(\tilde{T}_f - \tilde{T}_0)}; \quad q = \frac{\tilde{q}}{\tilde{c}_p(\tilde{T}_f - \tilde{T}_0)}; \tag{12}$$

(2) the gas phase Damköler number is defined as

$$D_g = \frac{P^2 MW^2 \tilde{B}_g \tilde{k}_g}{(\tilde{m}R)^2 \tilde{c}_p}; \tag{13}$$

and (3) the species mass fraction and temperature profiles are related as follows:

$$Y = \frac{\tilde{c}_p(\tilde{T}_f - \tilde{T}_0)}{\tilde{q}_g} = Y = \frac{c_p(T_f - T_0)}{q_g}. \tag{14}$$

If one assumes that the activation energy in the gas phase is small, i.e., $E_g \to 0$, the solution for the energy equation is a simple exponential function given by Equation (15), involving a characteristic dimension for the flame, x_g, as shown in Equation (16)

$$\frac{Y}{Y_s} = \frac{T - T_f}{T_s - T_f} = \exp\left(-\frac{x}{x_g}\right) \tag{15}$$

$$x_g = \frac{2}{\sqrt{m^2 - 4D_g} - m}. \tag{16}$$

In nondimensional terms the three equations to be solved are Equations (16), (17), and (18) for the three unknowns, T_f, T_s, and m. Note that Equations (17) and (18) are the nondimensional counterparts of Equations (4) and (8), where the flame temperature expression in Equation (9) (in nondimensional terms) has also been used to obtain the expression in Equation (18).

$$m^2 = \frac{A_c \tilde{T}_s^2 \exp(-E_c / T_s)}{\tilde{E}_c\left[T_s - T_0 - q_c/2\right]} \tag{17}$$

$$T_s = T_0 + q_c + \frac{q_g}{mx_g + 1}. \tag{18}$$

In order to include a radiative heat loss to simulated a large heat loss to the water, the energy balance to the entire system is modified as

$$\tilde{T}_f = \tilde{T}_0 + \frac{1}{\tilde{c}_p}\left(\tilde{q}_c + \tilde{q}_g\right) - \frac{\sigma}{\tilde{m}\tilde{c}_p}(\tilde{T}_f^4 - \tilde{T}_w^4). \tag{19}$$

In nondimensional form Equations (19) and (18) become, respectively:

$$T_f = T_0 + q_c + q_g - \frac{\sigma(\tilde{T}_{fR} - \tilde{T}_0)^3}{m\tilde{m}_r\tilde{c}_p}(T_f^4 - T_w^4) \tag{20}$$

and

$$T_s = \frac{mx_g(T_0 + q_c) + T_f}{1 + mx_g}. \tag{21}$$

This highly nonlinear system of equations is to be solved iteratively as shown on the computer program enclosed in Appendix A. In the next section the results and discussion of results are presented followed by a section summarizing the conclusions.

Results and Discussion

The model was evaluated with thermodynamic data for AP[6] and HMX[7] propellants. These data are summarized below.

Input Parameters for AP Propellant

$\tilde{q}_c = 4180\ kJ/kg$ $\quad \tilde{k}_c = 0.2\ W/m-K$

$\tilde{q}_g = 485\ kJ/kg$ $\quad \tilde{E}_c = 176\ KJ/mol$

$\tilde{c}_p = 1.4\ kJ/kg-K$ $\quad \tilde{\rho}_c = 1840 Kg/m^3$

$\tilde{k}_g = 0.07\ W/m-K$ $\quad MW = 97.1 kg/mol$

$\tilde{A}_c = 9.10X10^{12}\ 1/s$ $\quad \tilde{B}_g = 1.6X10^{-3}\ \ m^3/kg-s-K^2$

Input Parameters for HMX Propellant

$\tilde{q}_c = 3018\ kJ/kg$ $\quad \tilde{k}_c = 0.2\ W/m-K$

$\tilde{q}_g = 400\ kJ/kg$ $\quad \tilde{E}_c = 176\ KJ/mol$

$\tilde{c}_p = 1.4\ kJ/kg-K$ $\quad \tilde{\rho}_c = 1800 Kg/m^3$

$\tilde{k}_g = 0.07\ W/m-K$ $\quad MW = 34.2 kg/mol$

$\tilde{A}_c = 1.637X10^{15}\ 1/s$ $\quad \tilde{B}_g = 1.6X10^{-3}\ \ m^3/kg-s-K^2$

Figure 1 shows the variation of flame temperature and burn rate as a function of water temperature for both propellants. Both burn rate and flame temperature decrease as the water temperature is reduced. For AP and HMX at ambient pressure the adiabatic flame temperatures for the properties considered here are 3630 and 2740 K, respectively. As shown in Fig. 1, for a water temperature equal to the adiabatic flame temperature, there is no heat loss by radiation and the calculated flame temperature is equal to the adiabatic flame temperature, as one would expect. The burn rate also decreases as the water temperature decreases. At a water temperature of 400 K the flame temperatures reached for AP and HMX are slightly above 2300 and 1800 K, respectively.

---

[6] M.W. Beckstead, Modeling AN, AP, HMX, and Double Base Monopropellants, 26th JANNAF Combustion Meeting, Vol. IV, CPIA, No. 529, 1989.

[7] M.J. Ward et at., Steady Deflagration of HMX With Simple Kinetics: A Gas Phase Chain Reaction Model, *Combustion and Flame*, 114:556-568 (1998).

Figure 2 shows the variation of propellant surface temperature with water temperature for both propellants. The flame temperature variations are also included in this figure for reference. The surface temperatures vary only slightly for both propellants as the water temperature is reduced from a value equal to the adiabatic flame temperature down to 400K. However, as observed in Fig. 1, the drop in burn rate was significant. The reason for this behavior is the neglect of radiative heating of the solid and the strong dependency of the gasification process on surface temperature, which is primarily controlled by the activation energy for the zero-order reaction in the model. In the absence of radiative heating of the solid propellant the only source of energy from the gas phase to the solid is heat conduction at the surface as shown in Equation (8). This behavior also explains the weak predicted dependency of surface temperature on flame temperature. As previously explained, radiation heating of the solid phase was neglected. This would most probably limit the observed drop in burn rate because higher surface temperatures would be predicted. Also, the energy equation for the water has not been solved; therefore, the effect of radiative volumetric heating of the water has not been included and radiative heat transfer was treated as blackbody radiation assuming flame and water emissivities equal to one.

The one-dimensional, steady approach used here assumes an infinitely large propellant burning at steady state; therefore, the effect of any unsteady process (such as ignition and extinction) and propellant size has not been simulated. One would expect the effect of size and/or curvature to scale with α/m, where α is the thermal diffusivity of the solid. Curvature would only be important if the thermal layer in the solid, which follows the scaling just mentioned, is large compared with the particle size. It is expected that for small initial pieces of propellant the size would play a more dominant role in whether or not the flame would extinguish.

A comparison of flame temperature predictions using this simplified model to the relatively low auto-ignition temperature of solid propellants (around 500K) suggests that these energetic materials would continue to burn if immersed in water. However, if one is to reach such a conclusion based on the model results presented here, it must be at least qualitatively supported and verified by experiments performed in the same operating conditions. This validation procedure is always necessary when using mathematical models to predict actual phenomena—here, it is particularly important because of the very limiting assumptions used in the model, including primarily the neglect of ignition, extinction, and turbulence phenomena. Nonetheless, as described below, examination of existing published and unpublished experiments and discussion with a few experts in this field produces somewhat conflicting information.

In solid propellant manufacturing companies the evaluation of burn rate for each batch manufactured is done in a process called acoustic emission strand burning.[8] In this process a small piece of propellant (a 4" long 1/4" square piece) is placed under water and pressurized to pressures between 500 to 3000 psi. An igniter wire connected to one end of the propellant bar ignites it and the propellant burn rate is then measured as the bar burns under water. Although this procedure shows that solid propellants burn under water at elevated pressures, similar tests do not exist at ambient pressures.

An experimental program was conducted at the Air Force Propulsion Laboratory[9] to investigate whether or not burning in place could be a suitable means of disposing of solid propellant. It was shown that water controlled ambient pressure combustion of solid propellant and only minor burning was observed for large pieces below water level. Burning of large propellant pieces partially immersed in water stopped at the water line. Only minor burning was observed for large pieces below water level, and combustion always extinguished before much of the propellant below was consumed. Although burning did not transfer between propellant blocks touching underwater, burning would transfer to other blocks that were exposed a short distance away. A slow, sputtering combustion was obtained when a burning block was sprayed with water at a certain spray intensities, in which the propellant pieces extinguished when the initial block became a few pounds in size. Also, combustion proceeded to completion in a bucketful of water-immersed propellant chips, which had been soaked for three days in water. With a flame height of about five feet the twenty pounds of quarter inch thick chips burned almost to completion with a steady controlled flame.

During the time that the work reported here was conducted, Dr. R.R. Bennett from Thiokol also performed some limited and informal tests to investigate whether or not solid propellants would burn under water under ambient pressure.[10] RSRM propellant sliced into ~1/2-inch cubes were ignited with a hot wire and placed burning in 2-inch diameter x 5-inch tall metal filled half full with water, when one surface was entirely aflame. As described by Dr. Bennett, "there was a good deal of turbulent bubbling in the water for about a second, whereupon the propellant was extinguished." The experiment was repeated with the same result. A second experiment was conducted in which most of the water was removed from the can, leaving it at a depth of about 3/8-inches. A propellant cube was placed in the water, with the upper reacting portion extending out of

[8] Dr. R.R. Bennett, Thiokol. personal communication, January, 2000.

[9] 1983 JANNAF Propulsion Systems Hazards Subcommittee Meeting, Vol. 1, Los Alamos National Laboratory, Los Alamos, NM, 13-15 July.

[10] Dr. Bennett's results have been reported in a letter dated June 8, 2000 to Ralph Hayes, president of Eldorado Engineering.

the water. When the propellant burned down to the surface of the water, there was some bubbling and the propellant was rapidly extinguished. Dr. Bennett concluded from these simple experiments that RSRM propellant could be extinguished by water when burning at ambient pressure. Whether it will do so regardless of its configuration is not known, but without data to the contrary, he felt that it is likely that the propellant will be extinguished upon submersion in water.

Personal communication with Dr. Bennett before he conducted these limited tests also indicated that he was of the opinion that solid propellants would not sustain combustion under water at ambient pressure. Nonetheless, conversation with other solid propellant scientists resulted in opinions contrary to that of Dr. Bennett.[11]

It is intuitive, and clearly supported by the experimental tests discussed above, that water should at a minimum slow down the burning of solid propellants. However, the results of the Air Force tests seem to suggest that under certain conditions burning may proceed to completion. Also, these conflicting experimental results seem to suggest that size, concentration of propellant (amount of propellant present compared to the amount of water), etc should also be considered controlling variables on any extensive experimental tests to resolve the question of interest here. Further, in a dynamic situation, the penetration velocity of the burning propellant in water should also be an important variable because of the higher probability that at least locally the flame would be expected to extinguish at the moment of impact with the water.

[11] Personal communication with Prof. Merrill Becksteak from BYU and Dr. Steve Son from Los Alamos National Laboratory.

Conclusions and Recommendations

A simplified thermal model was developed to predicted the flame temperature of solid propellants under nonadiabatic conditions under simplifying assumptions, including: (1) equal molecular weights for the various species involved; (2) mass diffusion in the gas phase described by Fick's law; (3) temperature independent thermodynamic properties; (4) unity Lewis number; (5) equal specific heats for the solid and gas phases; (6) neglect of mass diffusion in the solid phase and radiation heating of the solid by the flame; (6) ideal gas behavior in the gas phase and incompressible solid phase; (7) neglect of turbulent effects (i.e., laminar flow) and (8) steady state conditions. Under these assumptions the flame temperature and burn rate of AP and HMX were shown to drop significantly. However, a comparison of flame temperature predictions using this simplified model to the relatively low auto-ignition temperature of solid propellants suggests that these energetic materials would continue to burn if immersed in water. Nevertheless, although it is intuitive and clearly supported by the experimental tests discussed herein that water should at a minimum slow down the burning of solid propellants at ambient pressures, published and unpublished experimental tests lead to somewhat conflicting conclusions of whether or not solid propellant would continue to burn under water at ambient pressure, conflict that is also observed in the opinion of experts in the area. Therefore it is the main conclusion of the present study that the problem should be further investigated numerically and experimentally before a final conclusion is reached on whether or not, or under what conditions, solid propellants would continue to burn under water. Propellant size, a variable expected to be important on a more complex numerical analysis of this problem, was not accounted for in the present study. The inclusion of propellant size would require the derivation of the model presented here in spherical coordinates, a step that would not be justified given other limiting assumptions in the model such as steady-state conditions. Inclusion of time dependency seems to be a more important improvement in the model so as to allow ignition and extinction issues to be studied in a longer-term research effort.

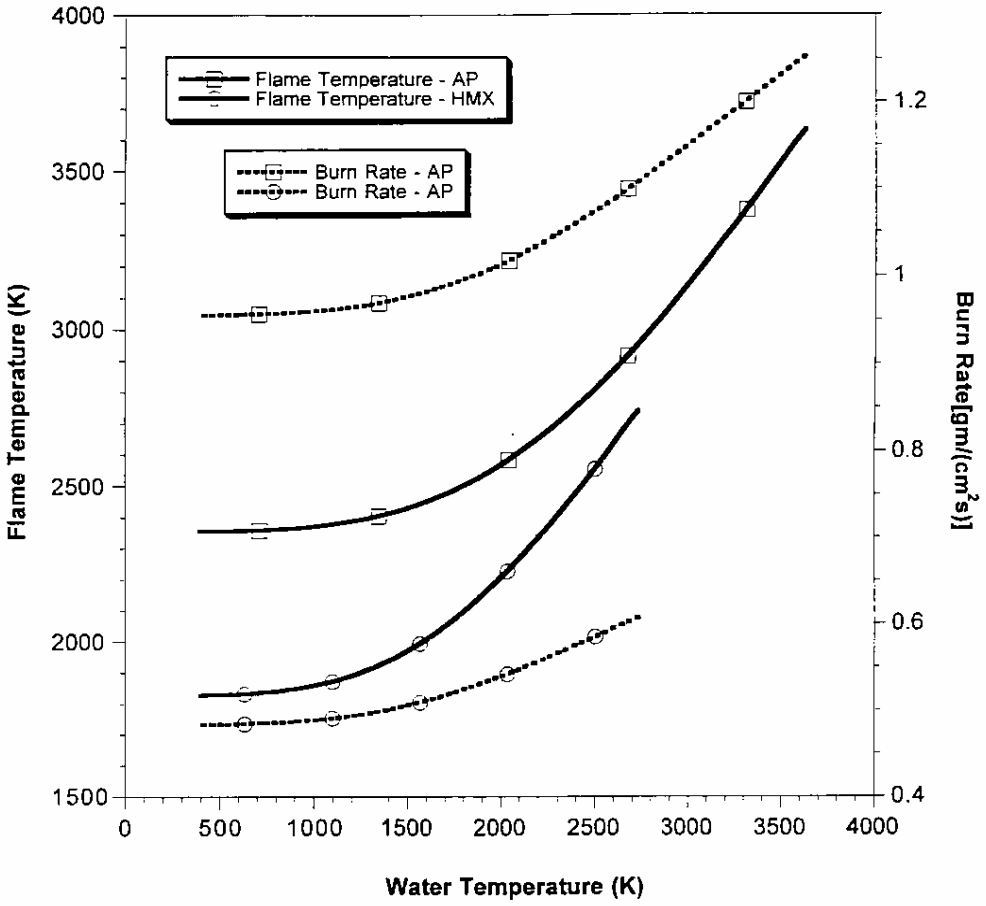

Figure 1 - Variation of flame temperature and burn rate with water temperature.

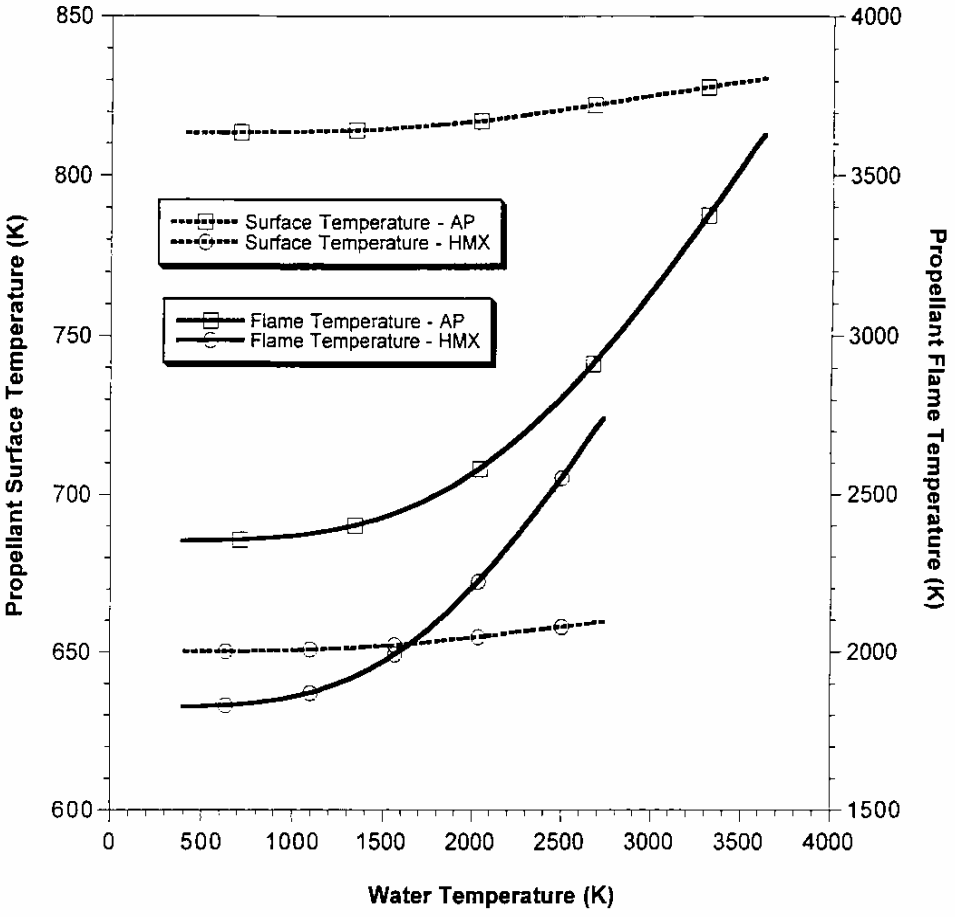

Figure 2 - Variation of surface and flame temperatures with water temperature.

Thiokol Propulsion
A Division of Cordant Technologies, Inc
P O Box 707, M/S 243
Brigham City, Utah 84302-0707
(435)863-2271 (Fax)

Thiokol Propulsion
From Cordant Technologies

June 8, 2000
33B0-CY00-L081

Ralph Hayes, President
El Dorado Engineering Inc.
2964 West 4700 South, Suite 109
Salt Lake City, UT 84118

Dear Ralph,

As you requested, I have reviewed the report entitled "A Simplified Model to Predict Nonadiabatic Propellant Flame Temperature," by Prof. M. Q. McQuay. While I am not really qualified to evaluate the mathematics of the combustion model presented, I would like to comment on some of the results and references. In his paper, Prof. McQuay references a discussion that he and I had, and describes the results of some of the propellant testing that we do at Thiokol. He cites our practice of conducting propellant ballistic testing under water at pressures of 500 to 3000 psi, and uses this as evidence to substantiate his conclusion that a burning solid propellant will continue to burn if immersed in water. I warned him that our tests are typically conducted at high pressures (>400 psi), and that the propellant may not sustain combustion at ambient pressure.

Since I had never personally evaluated the effects of submersing burning propellant in water, I decided to conduct some simple experiments on my own. On June 1, 2000, Steve Cutler (a propellant engineer who reports to me) and I took some RSRM propellant and sliced it into ~1/2-inch cubes. We obtained a 2-inch diameter x 5-inch tall metal can and filled it about half full with water. Using a hot wire, we ignited a propellant cube. When one surface was entirely aflame, it was dropped into the water. There was a good deal of turbulent bubbling in the water for about a second, whereupon the propellant was extinguished. The experiment was repeated with the same result. A second experiment was conducted in which most of the water was removed from the can, leaving it at a depth of about 3/8-inch. A propellant cube was placed in the water, with the upper portion extending out of the water. Once again, the propellant was ignited and allowed to burn. Again, when the propellant burned down to the surface of the water, there was some bubbling and the propellant was rapidly extinguished. It appears from these simple experiments that RSRM propellant can be extinguished by water when burning at ambient pressure. Whether it will do so regardless of its configuration is not known, but without data to the contrary, I feel that it is likely that the propellant will be extinguished upon submersion in water.

From my observations, it appears that the flow and heat exchange of the combustion products, steam and liquid water near the propellant flame would be a difficult phenomenon to accurately model because there is such a tremendously turbulent flow.

Please feel free to call if you have any further questions.

Sincerely,

Dr. Robert R. Bennett
Thiokol Propulsion, MS 243
P.O. Box 707
Brigham City, UT 84302

CC: M. Q. McQuay

APPENDIX B—SOLID ROCKET BOOSTER CAPABILITY TO WITHSTAND DEFLAGRATION OVERPRESSURES

Appendix B
SRB CAPABILITY TO WITHSTAND DEFLAGRATION OVERPRESSURES

Some of the most complete and detailed analyses of Shuttle aborts were undertaken to provide risk assessments for the potential dispersion of radioactive material in support of the launch approval process for the Galileo and Ulysses missions in the late 1980's and early 1990's. These extensive assessments were performed on behalf of the Programs and by the Interagency Nuclear Safety Review Panel. While the focus of this work was on the potential for dispersion of the radioactive material from the payload, they also provide useful insight into various failure scenarios. In particular, flying fragments from a disintegrating SRB could pose a threat to the containment of the radioactive payload; therefore breakupof the SRBs was modeled in the analyses. According to the results of the "Final Safety Analysis Report for the Ulysses Mission," (GE Astro Space, 1990) Appendix A, there are several cases which are likely to produce intact SRBs which remain free-flying until range destruct action is taken or the SRB impacts the ground. One example is the "Aft Compartment Explosion Scenario, 0 to 10s MET" in which "rupture of the 17-inch ID LOX and LH2 lines, plus a possible puncture of the external tank, can be anticipated as a result of an SSME propulsion system failure and ensuing aft compartment explosion." This case is expected to result in two free-flying SRBs. Another example is the "SRB Case Rupture Scenario, 0 to 10s MET." In this case a single SRB explodes and sends fragments into the orbiter and external tank. However, this intervening structure is expected to provide sufficient protection to the opposite SRB that it remains intact and flies free until range destruct. Likewise, the SRB case rupture after 10 s mission elapsed time also results in a single SRB free-flier. While the probabilistic aspect of this study is no longer current, it is interesting to note that the failure probabilities for these cases were found to be in the 1E-4 range.

Analyses of these cases are complex and probabilistic in nature, and no attempt to describe them is provided herein. The reader is referred to GE Astro Space, 1990. However, the plausibility that SRBs can survive is illustrated by noting that the SRM metal case is stiffened by internal working pressures in the 900 to 1000 psi range early in the flight; one would not expect the case to be significantly affected by external pressures until they exceed this level (ATK Thiokol, private communication, Oct., 2001). The strength of the blast wave is determined by how much fuel–oxidizer mixing takes place before detonation, the separation distance between the source of the blast and the SRB, and the presence of other surfaces that can reflect the wave and cause enhancements to the pressure. Response of the SRB depends not only on the static overpressure, but also on the static overpressure impulse, peak reflected pressure, dynamic pressure and dynamic pressure impulse. An indication of the probable magnitude of these parameters can be found in the following table excerpted from Table B-2 of GE Astro Space, 1990, Appendix B. Note that the pooling and mixing of the fuel and oxidizer is likely to occur on the mobile launch platform or in the flame trench, well below the SRBs.

Height feet	Percentile	Blast Parameter				
		ΔP_{stat} psi	P_{dyn} psi	P_{refl} psi	I_{stat} psi-s	I_{dyn} psi-s
20	50	41	36	167	0.25	0.076
	10	106	123	552	0.71	0.19
	1	206	294	1271	1.34	0.36
	0.1	349	524	2407	1.83	0.60
40	50	18	15	67	0.19	0.071
	10	59	59	261	0.61	0.22
	1	114	146	605	1.23	0.38
	0.1	203	318	1249	1.93	0.69

Reference:
GE Astro Space, 1990. ìFinal Safety Analysis Report for the Ulysses Mission,î Volume II, (Book 2) Accident Model Document ñ Appendices. Prepared for the U.S. Department of Energy under contract DE-AC01-79ET32043. Document No. 90SDS4203.

APPENDIX C—QUANTITATIVE RISK ASSESSMENT SYSTEM ANALYSIS RESULTS FROM B. BELYEU

To: Jeffrey Anderson, ED44

From: Becky Belyeu, HEI QS10

Subject: Request for QRAS analysis of Shuttle failure risks

Date: April 20, 2001

Per your request, QS10 has performed a quick assessment of the QRAS models and information regarding the risk of catastrophic failure during pre-launch and T+0 to T+25 seconds, and also risk of a failure causing an off-nominal trajectory during the same time frames. Although this is not modeled in QRAS, we have taken the failure rates of applicable failure modes during the time frames of interest and summed up those failure rates to obtain estimated vehicle-level numbers.

Pre-launch scenarios

There are only a few catastrophic failure modes that are specifically modeled in QRAS for the propulsion elements. Those failure modes result in a risk of 1.33e-05 or approximately 1 in 75,000. Orbiter models for pre-launch are not complete. For this assessment, the Orbiter contribution to the risk of catastrophic failure before liftoff is assumed negligible as most failures of the Orbiter would only result in a launch scrub.

The risk of a failure resulting in an off-nominal trajectory before liftoff is assumed to be remote for all elements.

T+0 to T+25 seconds after liftoff

The risk of catastrophic failure is estimated to be 2.13E-04 or approximately 1 in 4,700. (Note this is different from the 1 in 5,600 that we gave you in Oct. 2000. This is due to updated modeling). This also assumes Orbiter contribution is negligible during that time frame. (Orbiter catastrophic risk during entire ascent is approximately 1 in 18,000).

For the risk of failure causing off-nominal trajectory during this timeframe, the failure modes for the propulsion elements were assessed as to which were credible to cause this kind of effect. As would be imagined, the RSRM failure modes dominate the risk. The SRB servoactuator failure is also considered. The estimated risk of a failure resulting in off-nominal trajectory is 7.53E-05 or approximately 1 in 13,500. Again, this assumes Orbiter contribution to be negligible to the risk. There are other failure modes which could potentially occur, for instance the SSME gimbal bearing sticking, the failure of SRB holddown posts causing extreme tilt such that the TVC could not regain control, or interface failure modes between the Orbiter and SRB related to power busses, controllers, etc, but the risk is considered to be remote due to high levels of redundancy or extremely remote probability of occurrence.

Please note that this analysis has been performed as a special study and not part of the QRAS PRA project. The numbers provided have been derived through extensive extrapolation of the QRAS baseline data and their accuracy is hard to assess.

Becky Belyeu

Becky Belyeu

APPENDIX D—FRAGMENT FIELD MAPS

(Graphics by Scott Stevens, Intergraph Corporation)

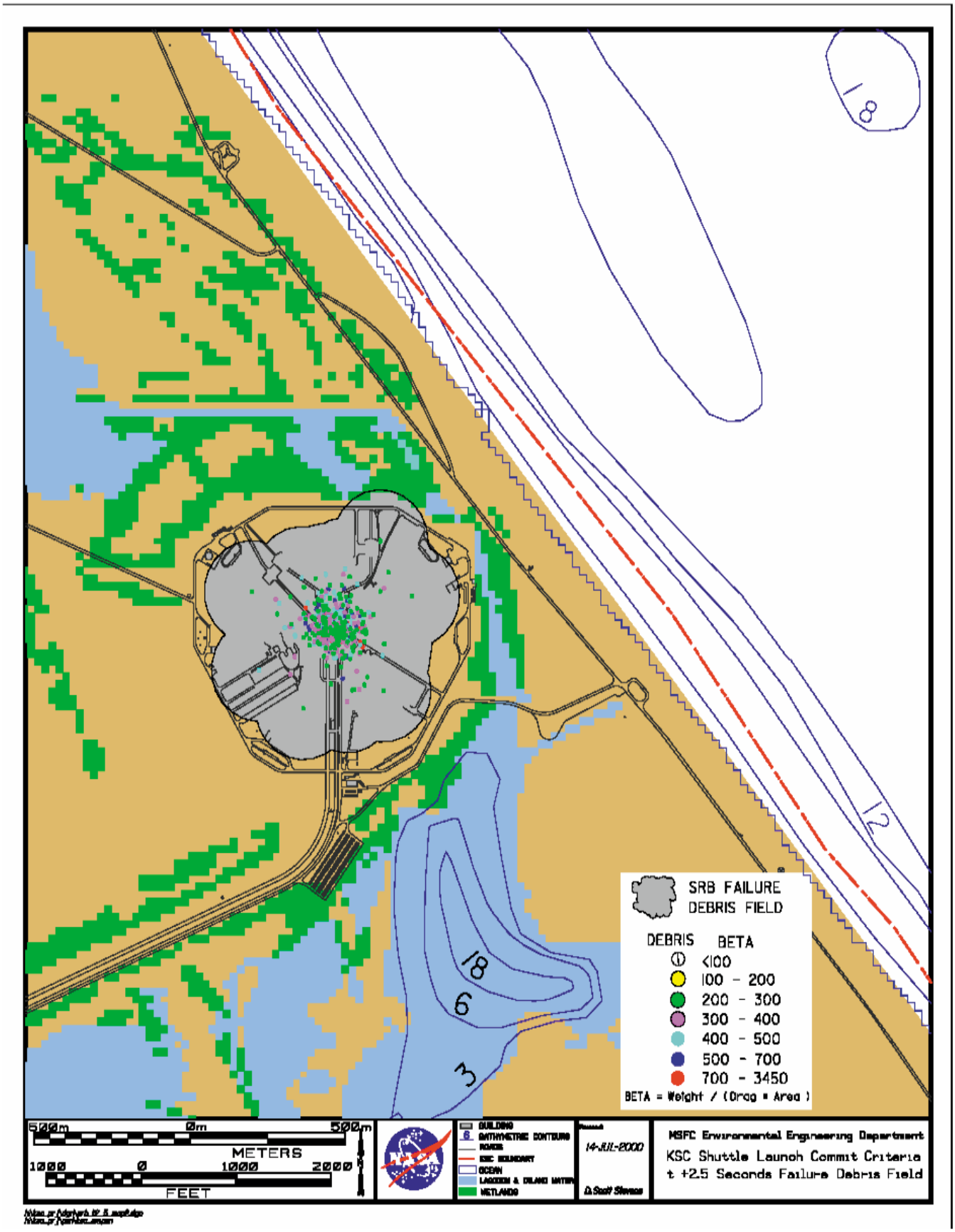
18
12
18
6
3
SRB FAILURE
DEBRIS FIELD
DEBRIS BETA
<100
100 - 200
200 - 300
300 - 400
400 - 500
500 - 700
700 - 3450
BETA = Weight / (Drag * Area)
500m
0m
500m
METERS
1000
0
1000
2000
FEET
BUILDING
BATHYMETRIC CONTOURS
ROADS
KSC BOUNDARY
OCEAN
LAGOON & INLAND WATER
WETLANDS
14-JUL-2000
MSFC Environmental Engineering Department
KSC Shuttle Launch Commit Criteria
t +2.5 Seconds Failure Debris Field

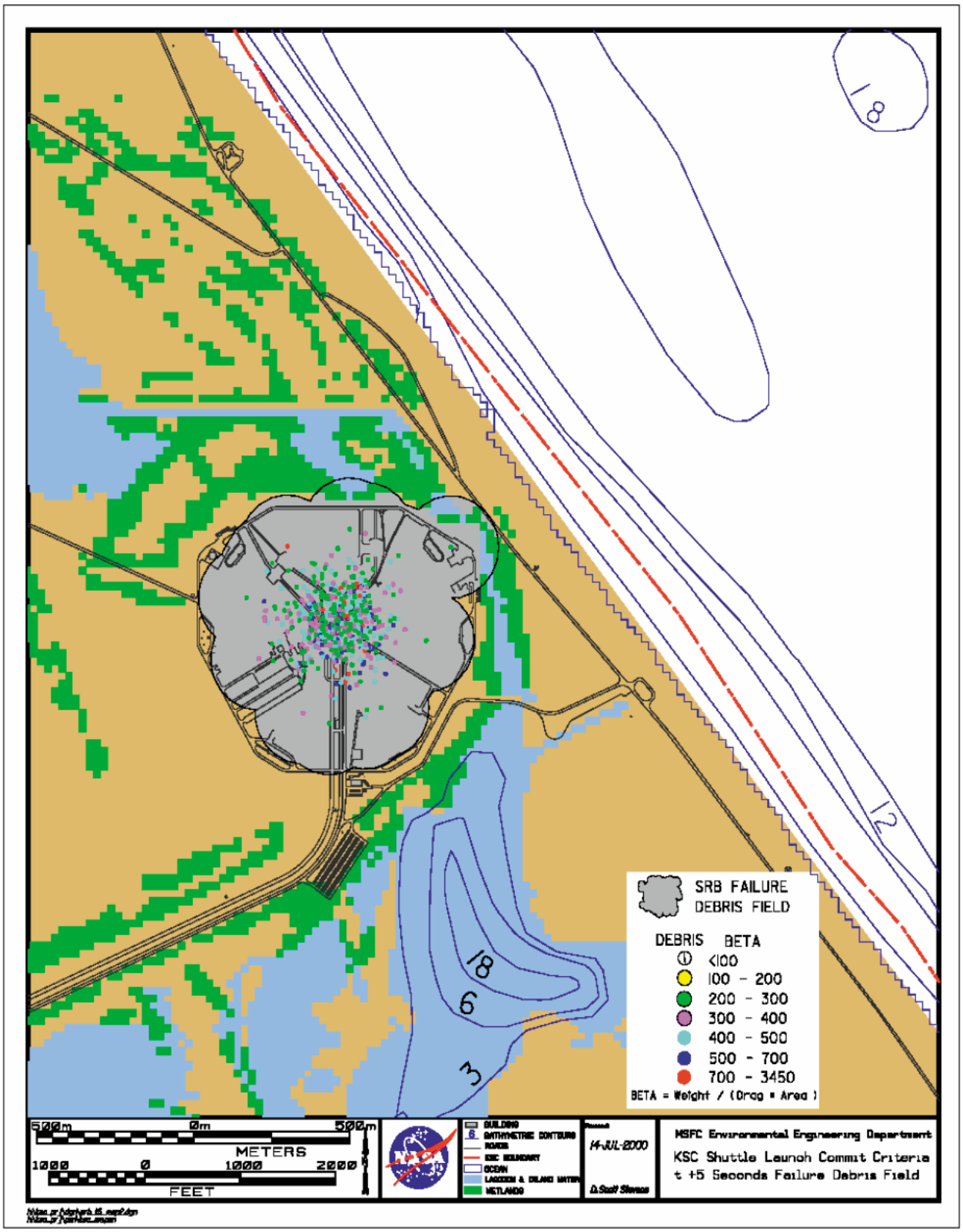
18
12
18
6
3
SRB FAILURE
DEBRIS FIELD
DEBRIS BETA
<100
100 - 200
200 - 300
300 - 400
400 - 500
500 - 700
700 - 3450
BETA = Weight / (Drag * Area)
500m
0m
500m
METERS
1000
0
1000
2000
FEET
BUILDING
BATHYMETRIC CONTOURS
ROADS
KSC BOUNDARY
OCEAN
LAGOON & INLAND WATER
WETLANDS
14-JUL-2000
MSFC Environmental Engineering Department
KSC Shuttle Launch Commit Criteria
t +5 Seconds Failure Debris Field

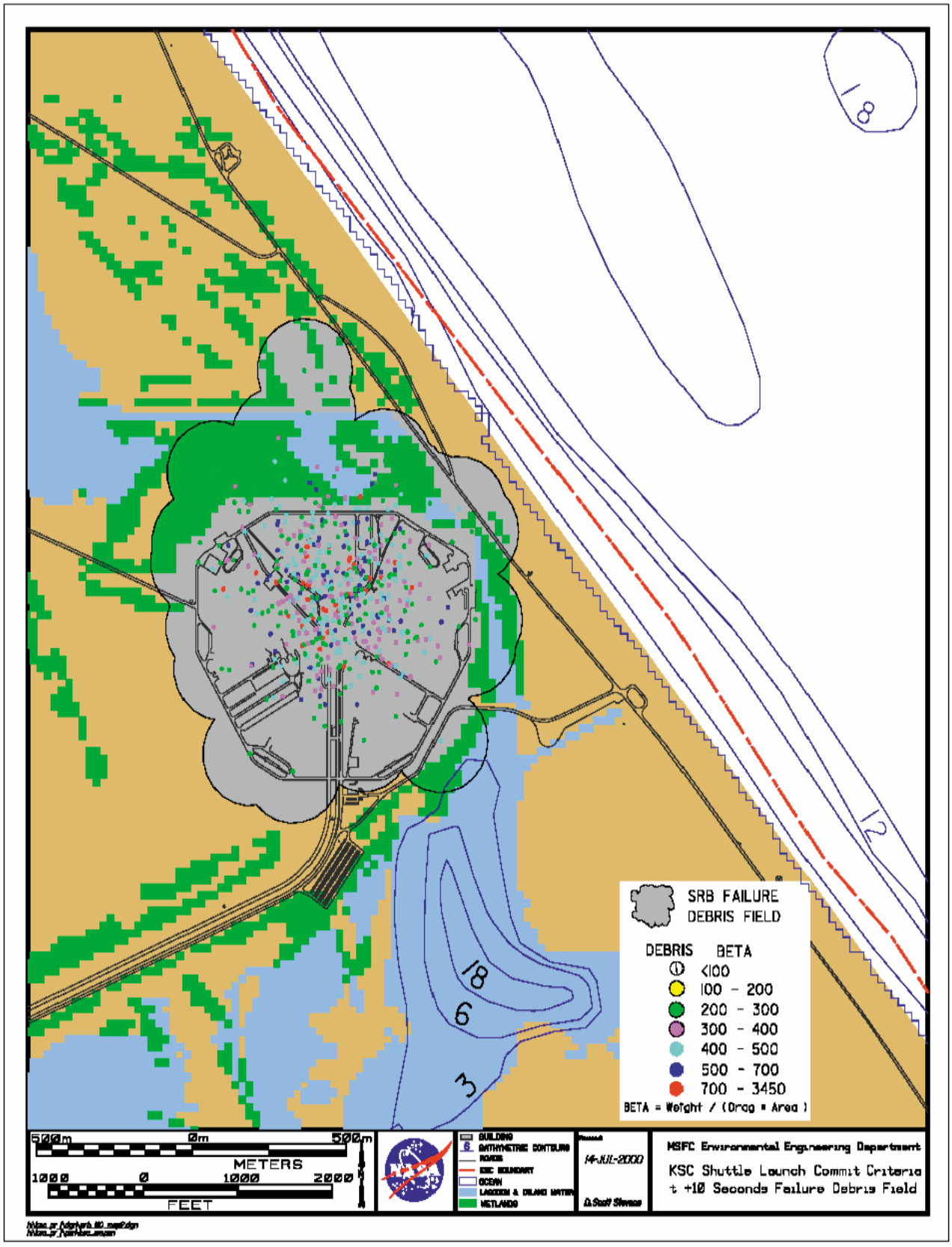
18
12
18
6
3
SRB FAILURE
DEBRIS FIELD
DEBRIS BETA
<100
100 - 200
200 - 300
300 - 400
400 - 500
500 - 700
700 - 3450
BETA = Weight / (Drag * Area)
500m
0m
500m
METERS
1000
0
1000
2000
FEET
BUILDING
BATHYMETRIC CONTOURS
ROADS
KSC BOUNDARY
OCEAN
LAGOON & INLAND WATER
WETLANDS
14-JUL-2000
MSFC Environmental Engineering Department
KSC Shuttle Launch Commit Criteria
t +10 Seconds Failure Debris Field

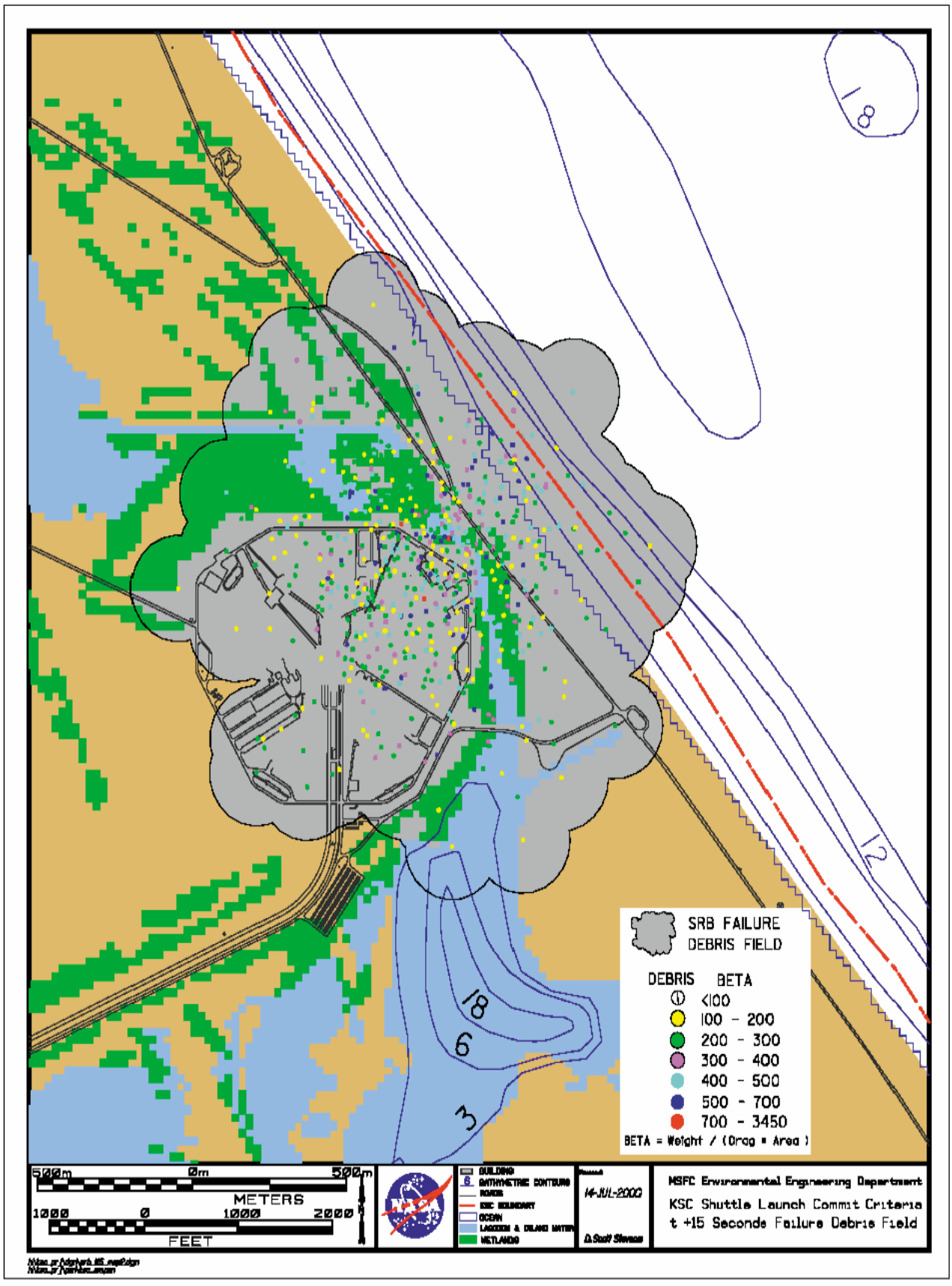
18
12
18
6
3
SRB FAILURE
DEBRIS FIELD
DEBRIS BETA
<100
100 - 200
200 - 300
300 - 400
400 - 500
500 - 700
700 - 3450
BETA = Weight / (Drag * Area)
500m
0m
500m
METERS
1000
0
1000
2000
FEET
BUILDING
BATHYMETRIC CONTOURS
ROADS
KSC BOUNDARY
OCEAN
LAGOON & INLAND WATER
WETLANDS
14-JUL-2000
MSFC Environmental Engineering Department
KSC Shuttle Launch Commit Criteria
t +15 Seconds Failure Debris Field

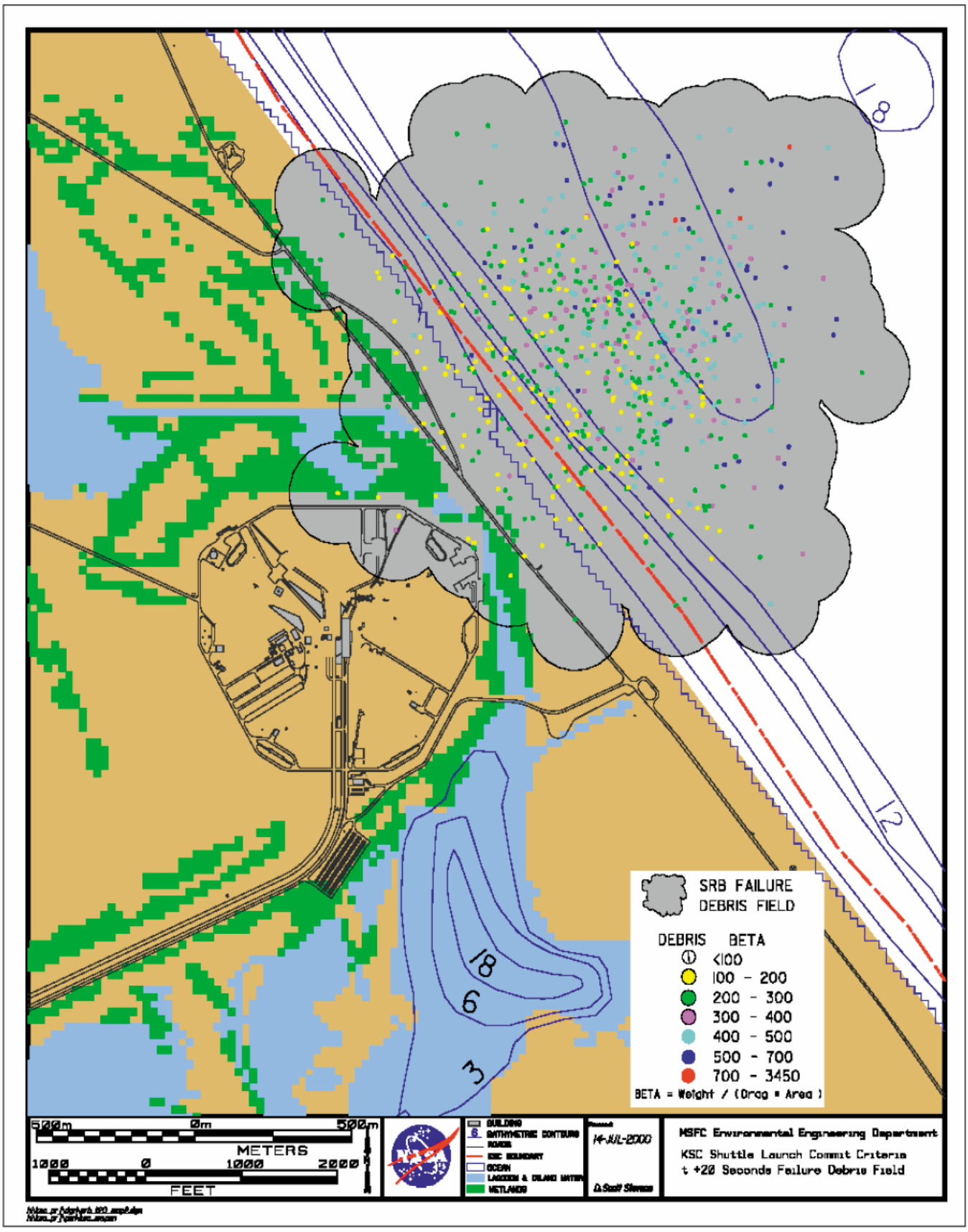
SRB FAILURE
DEBRIS FIELD
DEBRIS BETA
<100
100 - 200
200 - 300
300 - 400
400 - 500
500 - 700
700 - 3450
BETA = Weight / (Drag * Area)
18
12
18
6
3
500m
0m
500m
METERS
1000
0
1000
2000
FEET
BUILDING
BATHYMETRIC CONTOURS
ROADS
KSC BOUNDARY
OCEAN
LAGOON & INLAND WATER
WETLANDS
14-JUL-2000
MSFC Environmental Engineering Department
KSC Shuttle Launch Commit Criteria
t +20 Seconds Failure Debris Field

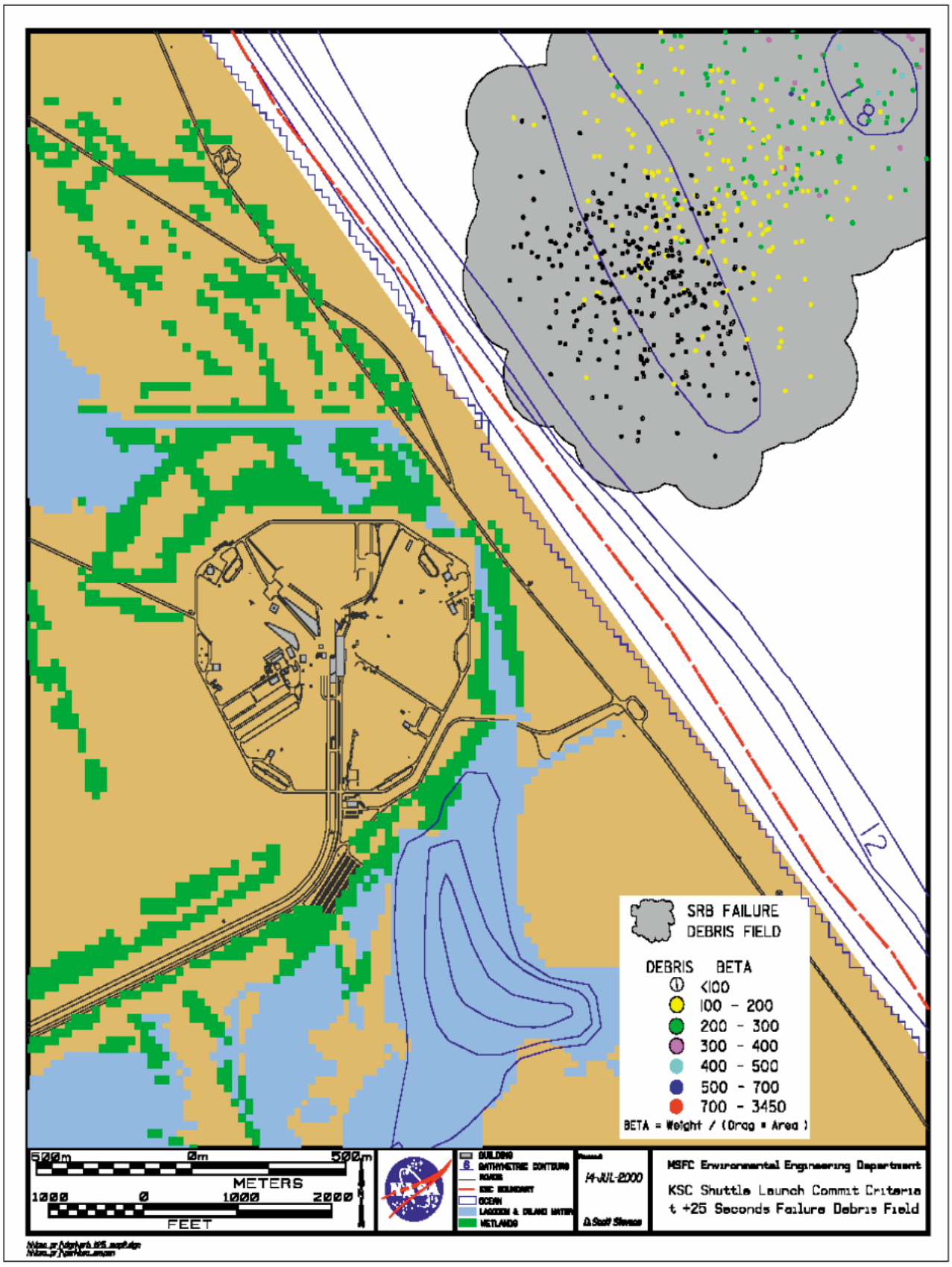
SRB FAILURE
DEBRIS FIELD
DEBRIS BETA
<100
100 - 200
200 - 300
300 - 400
400 - 500
500 - 700
700 - 3450
BETA = Weight / (Drag * Area)
500m
0m
500m
METERS
1000
0
1000
2000
FEET
14-JUL-2000
MSFC Environmental Engineering Department
KSC Shuttle Launch Commit Criteria
t +25 Seconds Failure Debris Field

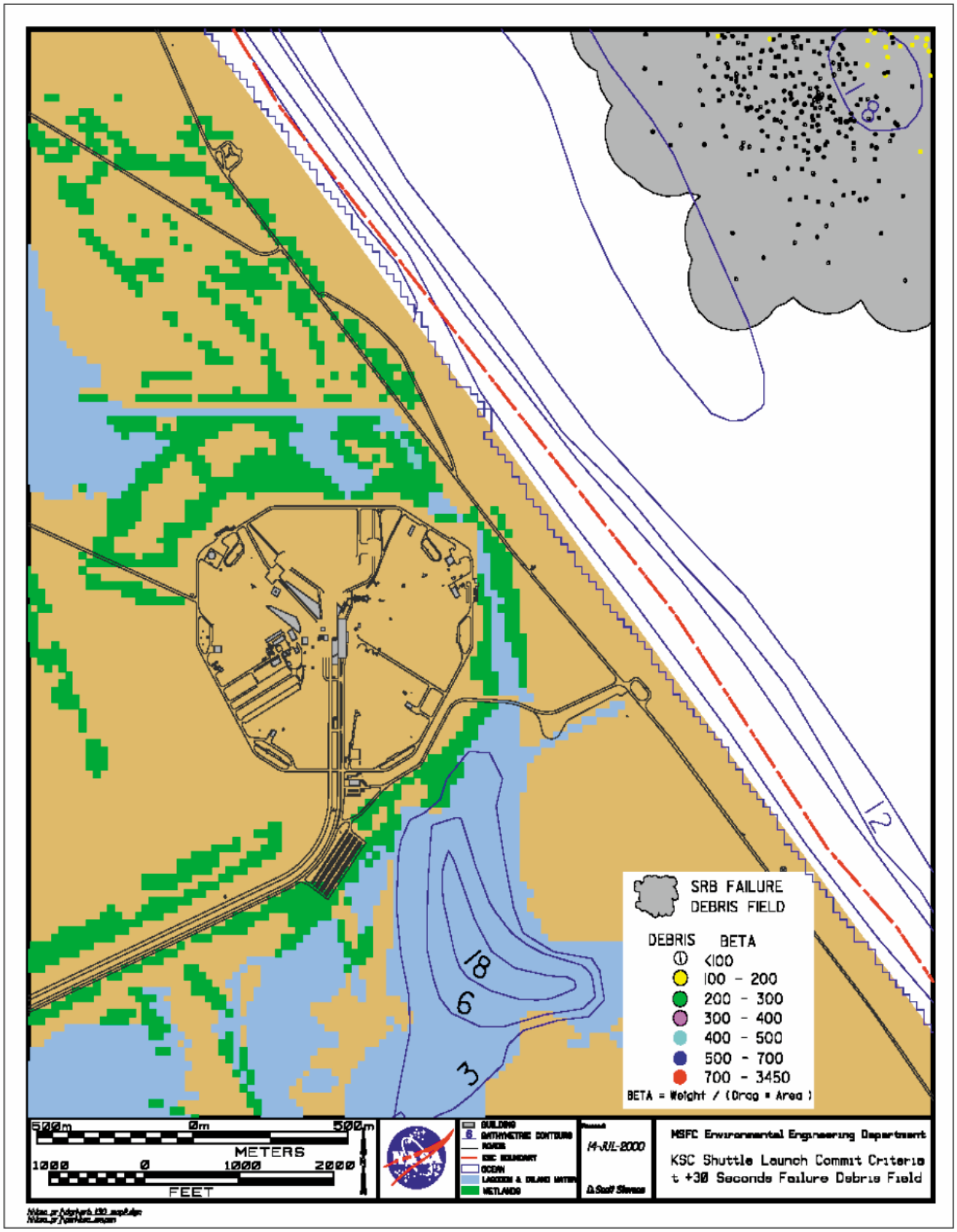
SRB FAILURE
DEBRIS FIELD
DEBRIS BETA
<100
100 - 200
200 - 300
300 - 400
400 - 500
500 - 700
700 - 3450
BETA = Weight / (Drag * Area)
18
12
6
3
500m
0m
500m
METERS
1000
0
1000
2000
FEET
BUILDING
BATHYMETRIC CONTOURS
ROADS
KSC BOUNDARY
OCEAN
LAGOON & INLAND WATER
WETLANDS
14-JUL-2000
MSFC Environmental Engineering Department
KSC Shuttle Launch Commit Criteria
t +30 Seconds Failure Debris Field

APPENDIX E—CH2MHILL ANALYSIS

Launch Commit Criteria Modeling Assistance, Analysis Summary

PREPARED FOR:	Rebecca McCaleb / Manager, Environmental Engineering Department B. Jeffrey Anderson / Environments Group
PREPARED BY:	Mark Bennett / CH2M HILL
COPIES:	Nannette Woods / CH2M HILL J.P. Martin / CH2M HILL
DATE:	May 6, 2001 Revised October 4, 2002 to incorporate minor corrections identified in the MSFC review by Batts, Adelfang, Leahy, and Justus.

This technical memorandum provides background and analysis summary of results for PC-based modeling for the dispersion of hydrogen chloride from the catastrophic failure of a Space Shuttle early in flight. The overall purpose of the work is to support the development of a Launch Commit Criteria (LCC) and complimentary Emergency Response Planning for the launch of a Space Shuttle.

1. Model Selection

1.1. Problem Definition

Model selection involved defining the physical problem to be modeled, deciding on the key components of the problem that needed to be included in the modeling, and then screening the models available against these criteria. The physical problem to be modeled is the dispersion of hydrogen chloride gas from multiple burning solid rocket propellant fragments. The details about the burning fragments are not modeled in this work, but rather, the description of the sources (i.e., the burning solid rocket propellant fragments) was taken from information supplied by the USAF. All fragments are completely burned within 30 minutes.

The key components from the physical problem that needed to be included in the modeling are plume rise from buoyant sources, including each of the approximately 600 burning fragments as an individual source, model dispersion from short-term sources, and include vertical variations of wind speed and direction. Another requirement was that the model include state-of-the-science algorithms for dispersion models that can be run on PCs. Furthermore, it was felt that it would be preferable to have a regulatory model as regulatory models undergo a high level of scrutiny and have undergone comparison to field data.

1.2. Models Evaluated

Models in the U.S. Environmental Protection Agency's Guideline on Air Quality Models (Appendix W to Part 50 of Section 40 of the Code of Federal regulations) were reviewed. None of the preferred air quality models satisfied the selection criteria. However, EPA was then reviewing the CALPUFF model for potential nomination to its list of preferred air quality models. The CALPUFF model satisfied the

selection criteria. After review (Environmental Protection Agency, 1998; Irwin, 1997; Strimaitis et al., 1998) EPA proposed designating CALPUFF as a preferred model in the April 21, 2000 Federal Register Notice (65FR21506-21546).

1.3. CALPUFF

A general description of the CALPUFF modeling system is given below. This is followed by a description of those features used in the modeling done for the LCC work.

CALPUFF is a multi-layer, multi-species non-steady-state puff dispersion modeling system that simulates the effects of time- and space-varying meteorological conditions on pollutant transport, transformation, and removal. CALPUFF is intended for use on scales from tens of meters from a source to hundreds of kilometers. It includes algorithms for near-field effects such as building downwash, transitional buoyant and momentum plume rise, partial plume penetration, subgrid scale terrain and coastal interactions effects, and terrain impingement as well as longer range effects such as pollutant removal due to wet scavenging and dry deposition, chemical transformation, vertical wind shear, overwater transport, plume fumigation, and visibility effects of particulate matter concentrations. (Scire, et al., 1998a; Scire, et al., 1998b).

1.3.1. Sources

CALPUFF can model point, area, volume, or line sources of pollutants. As one of its features, CALPUFF was designed to model forest fires via area sources. Consequently, for the LCC modeling the burning fragments were described as so-called "arbitrarily varying" buoyant area sources. For area sources CALPUFF requires source location and shape, release height, base elevation, initial vertical distribution (σ_z), and emissions rates for each pollutant as input. For sources that vary temporally in a non-periodic fashion, data is entered via an external file. Area sources specified in the external file are allowed to be buoyant and their location, size, shape, and other source characteristics are allowed to change in time. It was by this method that the burning fragments were modeled. Details are provided in Section 2.

1.3.2. Meteorological Data

Different forms of meteorological input can be used by CALPUFF. The time-dependent three-dimensional meteorological fields generated by the diagnostic meteorological model CALMET (which is a component of the CALPUFF modeling system), is the preferred form for regulatory application. However, two so-called "single station" meteorological data forms are also accepted by the CALPUFF model. For the LCC modeling the single-station format used by the Complex Terrain Dispersion Model Plus Algorithms for Unstable Situations (CTDMPLUS), which is an EPA preferred air quality model, was used. This allows a vertical variation in the meteorological parameters but no spatial variability. Details are provided in Section 2.

1.3.3. Plume Behavior

Momentum and buoyant plume rise is treated according to the plume rise equations of Briggs (1974, 1975) for non-downwashing point sources, and Zhang (1993) for buoyant area sources. Effects of partial plume penetration into elevated temperature inversions are included.

1.3.4. Horizontal and Vertical Dispersion

Turbulence-based dispersion coefficients provide estimates of horizontal and vertical plume dispersion based on measured or computed values of σ_V and σ_W, respectively. The effects of buoyancy-induced dispersion are included. Optionally, vertical dispersion during convective conditions can be simulated with a probability density function based on Weil et al. (1997). Options are available to use Pasquill-Gifford (rural) and McElroy-Pooler (urban) dispersion coefficients. Initial plume size from area sources is allowed.

1.3.5. Terrain Effects

The CALPUFF dispersion modeling system contains numerous methods to include the effects of both terrain and landuse; however, for the LCC modeling a flat terrain was assumed. It is felt that this a reasonable approximation given the relatively flat terrain surrounding the Cape Canaveral Air Force Station (CCAFS) Shuttle launch sites. Furthermore, this allows the results to be generally applicable to any location in the area. This is also in line with the application of the results for emergency response planning as the location of the burning fragments would not be known beforehand.

1.3.6. Source-Receptor Relationships

CALPUFF contains no fundamental limitations on the number of sources or receptors. Parameter files are provided that allow the user to specify the maximum number of sources, receptors, puffs, species, grid cells, vertical layers, and other model parameters. Its algorithms are designed to be suitable for source-receptor distances from tens of meters to hundreds of kilometers.

1.3.7. CALPUFF, Version 6

In the fragment data provided by the USAF, all fragments have burn times of less than 15 minutes. As the CALPUFF modeling system was designed to primarily meet regulatory requirements, the standard version of the code, Version 5, does not have the ability to accept and process changes in emission sources that occur over times shorter than one hour. However, the time-stepping algorithms within CALPUFF allow it to take very short time steps if necessary. Consequently, the authors of CALPUFF, Earth Tech, Inc., were contracted to modify the code. Modifications made to CALPUFF and CALPOST Version 5 to create Version 6 allow the dispersion modeling system to accept emissions data with temporal variations as small as 1 second, and report average concentrations for intervals as short as 1 minute.

CALPUFF Version 6 also allows the user to change the value of the variable EPSRAD via the CALPUFF control file. EPSRAD is the emissivity used in the radiative heat loss component of the energy equation of the numerical rise module for buoyant area sources (Scire and Strimaitis, 1999).

2. Methodology

The three components needed to run the CALPUFF dispersion modeling system are the source terms, the meteorological data, and the various modeling options used. The details of the these three components are given below. Furthermore, in order to examine a statistically significant sample of possible meteorological conditions, data covering a five year period were used. These sounding were screened for “no-go” conditions by the Environmentals Group at NASA’s Marshall Space Flight Center (MSFC). With the no-go cases removed, 4471 rawindsonde soundings were left in the set. In order to efficiently run CALPUFF for such a large set, a batching system was developed using a set of Visual Basic macros executed via Microsoft Excel.

2.1. Modeling Domain and Receptor Locations

The modeling analysis was performed with the Universal Transverse Mercator (UTM) coordinate system. The modeling used for the analysis was in the shape of a square extending 60 km in the east-west direction and 60 km in the north-south direction. The domain was centered at 3,165 km northing and 539 km easting, which is approximately the location of the launch pad 39A at CCAFS.

The CALPUFF analysis used an array of discrete receptors. The receptors were spaced at 5 degree intervals on three rings. The rings were centered on the center of mass of the fragments, and thus the center of the rings changed for each abort time modeled. The radii of the rings were 2.5, 10, and 20 kilometers.

2.2. Source Terms

Variables in the area source file are provided to the CALPUFF program as an input file whose default name is BAEMARB.DAT, for Buoyant Area Source Emissions File with Arbitrarily Varying Emissions (Scire et al. 1998a; Scire and Strimantis, 1999). This file contains buoyant area source emissions data for sources with detailed, arbitrarily varying emissions parameters. The data for this input file are derived from the debris fragment data and the results of NASA-Lewis model calculations for the burning of propellant. Both the debris fragment data and the NASA-Lewis model calculations were provided by the USAF.

The fragment debris data supplied by the USAF is for launch failure times from 2.5 to 45 seconds. For each failure time the data records contain estimates of the number of fragments, the initial mass, impact mass, the impact location, burn time, and area of the impact fragments. The required BAEMARB input parameters are given in Table 1.

Table 1 BAEMARB input data

Input File Parameter	Description	Value*	Units
CID	Source Identifier	Taken directly from debris data file	dimensionless
VERTX	X-coordinate of each of the four vertices defining the perimeter of the area source	Estimated using the fragment area, the east and west displacement of the fragments from the launch pad, and the latitude and longitude of the launch pad	kilometer
VERTY	Y-coordinate of each of the four vertices defining the perimeter of the area source	Estimated using the fragment area, the north and south displacement of the fragments from the launch pad, and the latitude and longitude of the launch pad	kilometer
HT	Effective height of the emissions above the ground	0	meters
ELEV	Elevation of ground	0	meters MSL
TEMPK	Temperature of area source plumes	2328.35	degrees Kelvin
WEFF	Effective rise velocity	$\frac{\text{Specific Volume} \times \text{weight}_{\text{initial}}}{\text{burn time} \times \text{Area}}$	meters per second
REFF	Effective radius for rise calculation	$r_p = \sqrt{\frac{A}{\pi}}$	meters
SIGZ	Initial Vertical Spread	1.	meters
QEMIT	Emission rates for each area sources	Initial mass of fragment divided by amount of time fragment is allowed to burn	g/s

*Some input data require other parameters. Table 2 provides values and data that are required as part of input data in Table 1.

The effective radius of the plume was estimated using a circular cross-section with an equivalent area. The effective rise velocity was estimated by assuming the volume of emissions produced initially flows through an area equal to that of the largest face of the fragment. The specific volume comes from a NASA-Lewis calculation which assumed a 3-to-1 ration of air to combustion products.

Table 2 BAEMARB input file supporting data

Description	Value	Units	Reference
X-coordinate of the launch pad	538.688	kilometer	USAF
Y-coordinate of the launch pad	3,164.455	kilometer	USAF
Weight fraction of HCl in propellant	0.2163		USAF
Specific volume of combustion product and air	6.167	cubic meters per kilogram	USAF
Area (A)	Fragment area	square meters	USAF

This method of generating the terms needed for the CALPUFF BAEMARB.DAT file from the fragment data provided by the USAF was implement via a FORTRAN computer program. The source code for that program is provided as Attachment 1.

2.3. Meteorological Data

As mentioned above, the primary meteorological data, in the form of vertical soundings, was supplied by MSFC. In addition to this vertical profile, CALPUFF requires certain other meteorological data be specified: the frictional velocity (u*), Monin-Obukhov length (L), and mixing height. The method used to derive these values from the vertical soundings is given in Attachment 2.

This method was reviewed in a May 23, 2000 technical discussion from Frank Leahy (Raytheon ITSS); a July 7, 2000 memorandum from Kirk Stopenhagen (CH2M HILL); and a July 28, 2000 technical discussion from Frank Leahy (Raytheon ITSS). The Stopenhagen and Leahy methods were chosen at the August 18, 2000 meeting as the methods to finish the development of the meteorological data files. Lack of clarity due to the notation used in the Leahy memo led to the error that was corrected in 2002. The necessary minor corrections have been incorporated into this revised report.

The method of generating the CTDMPLUS-format meteorological files from the soundings provided by NASA's MSFC was implemented by means of Visual Basic macros executed via Microsoft Excel.

2.4. CALPUFF Modeling Options

The variables used in the CALPUFF control file are primarily the default values for the model. A description of the main modeling options and the "base case" values used are given in Table 3. A sample control file from a base case run is given in Attachment 3.

Table 3 CAPUFF modeling options

Variable	Description	Base case value
NSECDT	Length of time-step in seconds	60
IRLG	Length of run in time-steps	240
METFM	Format of meteorological data	4 (for CDTMPLUS-compatible format)
MSLUG	Near-field puffs modeled as elongated	1 (for yes)
MDISP	Method used to compute dispersion coefficients	2 (dispersion coefficients from internally calculated σ_V and σ_W using micrometeorological variables)
EPSRAD	Emissivity for radiative heat loss in energy equation used in numerical rise module for buoyant area sources	0.8 (the default value)

CALPUFF modeling options are discussed further with respect to sensitivity analysis in section 2.5.

2.5. Batching System

A batching system was developed so that large numbers of soundings can be processed efficiently. The batching system consists of a set of Visual Basic macros implemented via Microsoft Excel. Three worksheets in an Excel workbook are used as input to the batching system: CPUF, CTRL, and BAEMARB. The CPUF worksheet contains almost all the information that will be used to generate the control files for running first CALPUFF and then CALPOST. The only information missing is the date and time for the run, as this is specific to each sounding processed. The BAEMARB worksheet contains almost all the information needed to generate the BAEMARB.DAT file used in the CALPUFF run. Similar to the CPUF worksheet, the absolute date and time are missing. The CTRL worksheet contain control information for the batching system, such as the names of the input files.

Preparing the batching system to process a set of soundings consists of two steps. First, the CPUF and CTRL worksheets are completed. Second, one of the macros of the batching system reads the area source information output from the FORTAN program and creates the BAEMARB worksheet.

When run, the batching system executes the following steps.

- One sounding is read from the indicated set of soundings. Which sounding is determined by values in the CTRL worksheet. The specific date and time used in the subsequent steps match the date and time read from the sounding.
- Date and time specific surface and profile meteorological files are created. These are in the corresponding CDTMPLUS formats, which is the same as the CALPUFF SURFACE.DAT and PROFILE.DAT formats.
- A date and time specific buoyant areas sources file is created in the CALPUFF Version 6 BAEMARB.DAT format.
- Date and time specific control files for CALPUFF and CALPOST are created.
- An MS-DOS batch file is created to run first CALPUFF and then CALPOST. It is then executed. CALPUFF runs. Output from CALPUFF is used as input to CALPOST. CALPOST runs.
- Visual Basic macro reads the CALPOST output file and extracts the maximum hydrogen chloride concentration experienced at each receptor during the simulation. It then tabulates these values in a column in an Excel worksheet and labels the column with the date and the time of the sounding.

The batching system automatically carries out these steps for the range of soundings indicated in the CTRL worksheet.

3. Results

For each sounding modeled a time period of up to 4 hours was simulated. As mentioned previously, maximum fragment burn times are less than 30 minutes. Consequently, in some cases all the pollutant had left the 60 km by 60 km domain before 4 hours had been simulated. In these cases, the model automatically ended the simulation at that point.

The concentrations recorded by the model are the maximum time-weighted concentration experienced at the receptor during the simulation. All results reported here are for a time averaging period of one minute. As mentioned previously, the simulations used a maximum time step of sixty seconds. The CALPUFF code contains control algorithms that decrease the size of the time step if necessary.

The 4471 soundings provided by MSFC were sorted by surface temperature and divided into nine groups of 447 soundings each and one of 448. The average surface temperatures of the ten groups of soundings were 281 K, 287 K, 291 K, 293 K, 295 K, 296 K, 298 K, 299 K, 300 K, and 302 K.

3.1. Base Case

A baseline case was run using the 447 soundings in the group with average surface temperature of 295 K. The base case used the fragments for an abort after 15 seconds. As elongated puffs, so-called "slugs," better represent near-field results (Scire et al., 1998a), CALPUFF's option to use slugs in the near-field was used for the base case calculations. CALPUFF's option to calculate dispersion coefficients from the micrometeorological variables was used in the base case calculations. The default value of 0.8 was used for the emissivity (EPSRAD) was used in the base case calculations.

Histograms for the three rings of receptors of the maximum concentration found for each of the 447 soundings in the 295 K group are given in Attachment 4. As can be seen, only 6 of the 447 cases had maximum 1-minute time-weighted concentrations above 10 ppm for the receptors at 20 km. For the receptors at 10 km, 276 of the 447 soundings (61.7%) had maximum 1-minute time-weighted

concentrations above 10 ppm and 151 (33.8%) above 20 ppm. At 2.5 km, 268 (60.0%) had maximum 1-minute time-weighted concentration above 100 ppm. For the 447 cases, the maximum 1-minute time-weighted concentrations found on the 2.5 km, 10 km, and 20 km rings were 332 ppm, 55 ppm, and 13 ppm, respectively.

The entire set of 447 soundings in the 295 K group took roughly 24 hours to run on an 850 MHz computer.

3.2. Sensitivity Analysis

In order to examine the sensitivity of the results to the parameters chosen, runs were done using 447 soundings in the 295 K group while varying three parameters: the emissivity, the use of slugs vs. puffs, and the way the dispersion coefficients were calculated.

Emissivity

The 295 K group of soundings was run with an emissivity of 1 (i.e., EPSRAD = 1.0), rather than the default value of 0.8. This allows more heat from the initially very hot plume (T = 2328.35 K) to leave by radiative heat transfer. Consequently, lower stabilization heights, and thus higher ground level concentrations were expected. The histograms from the EPSRAD =1 runs are given in Attachment 5. As expected, ground level concentrations are higher for 87.5% of the cases at 2.5 km, 72.9% at 10 km, and 63.5 % at 20 km, but the magnitudes of the differences are slight. For example, for the receptors at 20 km there were 98 soundings with maximum 1-minute time-weighted concentrations above 5 ppm in both cases, but the emissivity = 1 set had one extra case above 10 ppm; not a significant difference. Furthermore, comparing the results on a sounding-by-sounding basis, the maximum 1-minute time-weighted concentrations on the 2.5 km, 10 km, and 20 km rings of receptors were on average only 0.9%, 0.8% and 0.8% higher than the corresponding concentrations in the base case.

Puffs vs. Slugs

In this comparison the 295 K group of soundings was run always using puffs (i.e., MSLUG = 0), rather than the using slugs for the near-field calculations. The histograms from the MSLUG =0 runs are given in Attachment 6. In a statistical sense the results are very nearly identical to the base case, typically within ± 1 %, even though in a few individual cases the difference could reach to the 20 to 40% range. Comparing the results on a sounding-by-sounding basis and then averaging the percent difference, the maximum 1-minute time-weighted concentrations on the 2.5 km, 10 km, and 20 km rings of receptors were 0.5% lower, 0.2% higher, and essentially unchanged from the corresponding concentrations in the base case.

Dispersion Coefficients

The 295 K group of soundings was run using the Pasquill-Gifford (PG) dispersion coefficient (i.e., MDISP = 3), rather than dispersion coefficients calculated from the micrometeorological variables. The histograms from the MDISP=3 runs are given in Attachment 7. The histograms indicate that overall for the sample of 447 sounding the PG dispersion coefficients give results with somewhat higher concentrations. However, when a comparison is made on a sounding-by-sounding basis, the maximum 1-minute time-weighted concentrations on the 2.5 km, 10 km, and 20 km rings of receptors were on average 84.5%, 414% and 487% higher than the corresponding concentrations in the base case. Furthermore, the standard deviations of the differences were 167%, 1067%, and 967%, respectively. This seems to indicate a weak case-by-case correlation between the PG results and the base case.

The Pasquill-Gifford method of determining stability class, and subsequently dispersion coefficients was developed 30 years ago. More recent methods use directly observed variables of the boundary layer to parameterize dispersion. These methods represent a significant advancement in the science of dispersion modeling. This is recognized by the EPA and is the primary reason they've

proposed replacing ISC, which uses the Pasquill-Gifford method, with AERMOD, which uses the micrometeorological method, as the primary model in their list of preferred models (65FR21506-21546).

3.3. 5 years for Base Case

The base case was run for all 4471 soundings spanning a 5-year period from 1965 – 1969. Histograms for the three rings of receptors of the maximum concentration found for each of the 4471 soundings are given in Attachment 8. As can be seen, 227 of the 4471 cases had maximum 1-minute time-weighted concentrations above 10 ppm for the receptors at 20 km. For the receptors at 10 km 2821 of the 4471 soundings (63.1%) had maximum 1-minute time-weighted concentrations above 10 ppm and 2148 (48.0%) above 20 ppm. At 2.5 km 3071 (68.7%) had maximum 1-minute time-weighted concentration above 100 ppm.

3.4. Meteorology for Delta II Explosion

A Delta II rocket exploded 12.5 seconds after liftoff from CCAFS on January 17, 1997. The clouds of combustion products from this explosion were observed to move in two primary directions. The lower elevation cloud moved southward and the upper elevation cloud moved eastward (NASA, 2000).

A meteorological sounding for the time of the Delta II launch was supplied by MSFC. CALPUFF was run using this meteorology and the base case parameters. Ground level concentrations indicated plumes moving in two directions, southward and eastward. Isopleths, in micrograms per cubic meter, are shown in Attachment 9. The higher concentrations of the southward plume indicate it was at a lower elevation; whereas the lower concentration of the eastward plume indicate it was at a higher elevation. This behavior is consistent with that observed from the Delta II explosion.

3.5. Meteorology used in Los Alamos study

A study of the dispersion of HCl from a Space Shuttle abort was done by Rodman Linn et al.(unpublished) of the Los Alamos National Laboratories. This study was done using the HIGHGRAD, FIRETEC, and RAMS numerical models. These are computationally intensive numerical models that require days of supercomputer time to simulate hours of dispersion time. This study used the USAF generated debris fragments for an abort at 15 seconds and a "worst-case" meteorology provided by the USAF 45th Space Wing Range Safety Office.

CALPUFF was run using this meteorology and the base case parameters. Maximum groundlevel concentrations at the 2.5 km, 10 km, and 20 km receptors were 359 ppm, 58 ppm, and nearly 9 ppm, respectively. This may be compared to the approximately 3 –5 ppm found at 9 – 12 km and 2 ppm found at 20 km in the Los Alamos report. Groundlevel isopleths from 1 – 10 ppm for the CALPUFF result are shown in Attachment 10.

4. Summary and conclusion

Results from the use of the CALPUFF (Version 6) dispersion modeling system to model HCl dispersion from a large number of burning solid rocket propellant fragments appear to be physically reasonable. Comparison to field studies would greatly improve the quality of the assessment of the modeling. Unfortunately, no relevant field data are know to exist.

The limited sensitivity studies done seem to indicate that results are fairly insensitive to changes in parameters that are not well know. Given the limited nature of the current sensitivity study, further analysis should be performed.

As mentioned previously, 4 hours of dispersion took approximately 3 minutes of computational time on an 850 MHz PC. Therefore, this modeling system could be used in real-time as part of a Launch

Commit Criteria and Emergency Planning system if real-time meteorology was used as input. The standard (i.e., 1-hour time step) version of CALPUFF has been used real-time to model pollutant dispersion. In these instances, high quality three-dimensional meteorological data from a prognostic meteorological model was used.

5. References

Briggs, G.A., 1974. Diffusion Estimates for Small Emissions. USAEC Report ATDL-106. U.S. Atomic Energy Commission, Oak Ridge, TN

Briggs, G.A., 1975. Plume Rise Predictions. Lectures on Air Pollution and Environmental Impact Analyses. American Meteorological Society, Boston, MA, pp. 59-111.

Environmental Protection Agency, 1998. Interagency Workgroup on Air Quality Modeling (IWAQM) Phase 2 Summary Report and Recommendations for Modeling Long-Range Transport Impacts. EPA publication No. EPA-454/R-98-019. U.S Environmental Protection Agency, research Triangle Park, NC.

Irwin, J.S. 1997. A Comparison of CALPUFF Modeling Results with 1997 INEL Field Data Results. In Air Pollution Modeling and its Application, XII. Edited by S.E. Gyrning and N. Chaumerliac. Plenum Press, New York, NY.

NASA, 2000. Delta II Explosion Plume Analysis Report. NASA Contractor Report NASA/CR-2000-208582.

Scire, J.S., and D.G. Strimantis, 1999. A User's Guide for the CALPUFF Dispersion Model: Version 6.0 Addendum. Earth Tech, Inc., Concord, MA.

Scire, J.S., D.G. Strimantis, and R.J. Yamartino, 1998a. A User's Guide for the CALPUFF Dispersion Model (Version 5). Earth Tech, Inc., Concord, MA.

Scire, J.S., F.R. Robe, M.E. Fernau, and R.J. Yamartino, 1998b. A User's Guide for the CALMET Meteorological Model (Version 5). Earth Tech, Inc. Concord, MA.

Strimaitis, D.G., J.S. Scire and J.C. Chang. 1998. Evaluation of the CALPUFF Dispersion Model with Two Power Plant Data Sets. Tenth Joint Conference on the Application of Air Pollution Meteorology, Phoenix, Arizona. American Meteorological Society, Boston, MA. January 11-16, 1998.

Weil, J.C., L.A. Corio, and R.P. Brower, 1997. A PDF dispersion model for buoyant plumes in the convective boundary layer. J. Appl. Meteor., 36: 982-1003.

Zhang, X., 1993. A computational analysis of rise, dispersion, and deposition of buoyant plumes. Ph.D. Thesis, Massachusetts Institute of Technology, Cambridge, MA.

ATTACHMENT 1

Source Code of FORTRAN File to Generate BAEMARB.DAT File for CALPUFF

ATTACHMENT 4

Baseline results from the sensitivity study, 447 meteorology cases from the file Go295

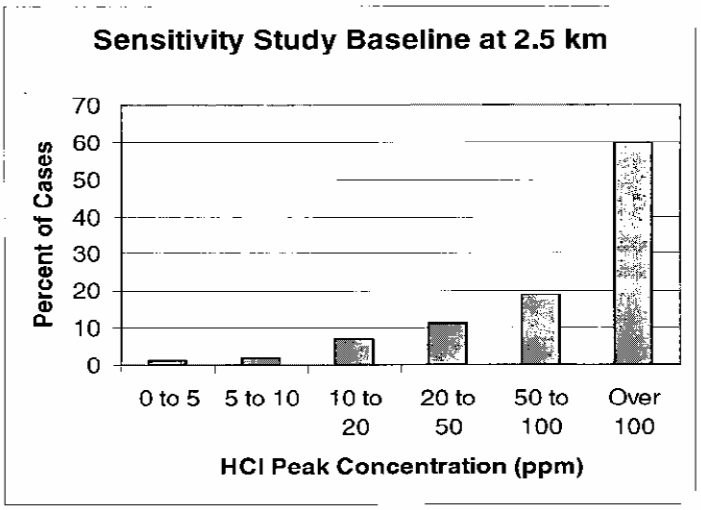

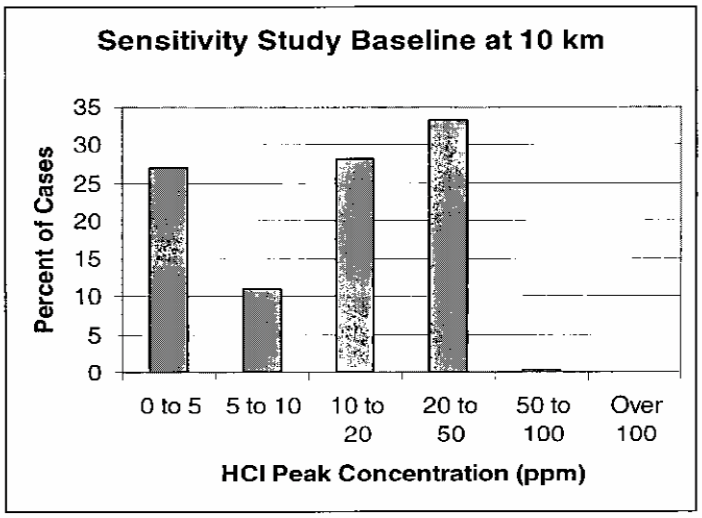
Sensitivity Study Baseline at 10 km
Percent of Cases
35
30
25
20
15
10
5
0
0 to 5
5 to 10
10 to 20
20 to 50
50 to 100
Over 100
HCl Peak Concentration (ppm)

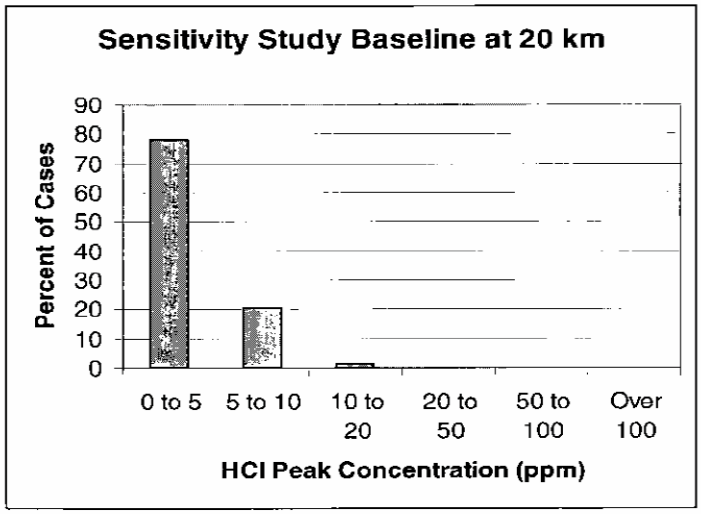
Sensitivity Study Baseline at 20 km
Percent of Cases
90
80
70
60
50
40
30
20
10
0
0 to 5
5 to 10
10 to 20
20 to 50
50 to 100
Over 100
HCl Peak Concentration (ppm)

Attachment 10: Updated (corrected) "Los Alamos" case results from CALPUFF. Map grid (x-y) coordinates are in kilometers, HCl isopleths are in ppm.
(Calculated October 4, 2002Find data in file "losalamossurfmap3.m")

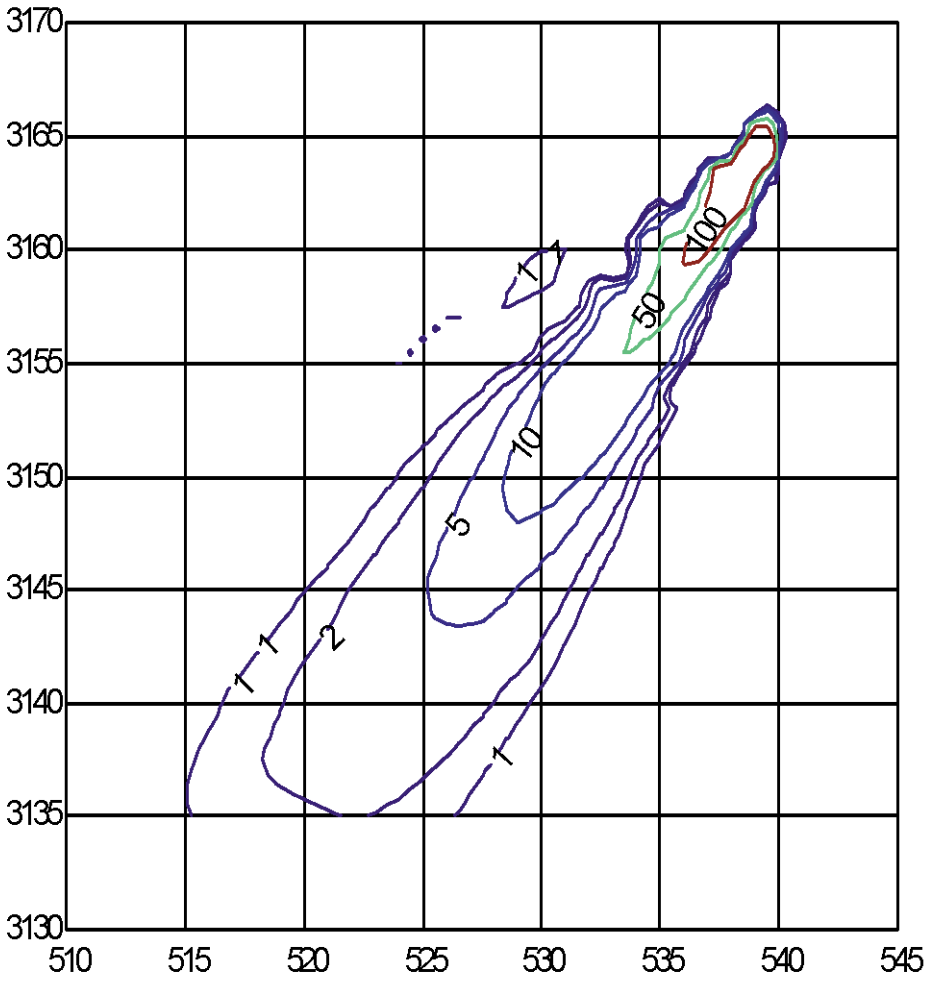

APPENDIX F—LEAHY REPORT ON TURBULENCE PARAMETERS

APPENDIX F.
Recommendations for Meteorological Input Parameters
For the CALPUFF Dispersion Model: Revision B

Frank Leahy
Raytheon ITSS
MSFC/Terrestrial and Planetary Environments Team
July 28, 2000

NOTE: Revision B completed on August 21, 2002 to correct equations B5 through B13 to indicate that ψ_M and ψ_H are functions of z/L.

This brief technical discussion is presented to review CALPUFF meteorological parameter methodology provided by Mr. Kent Norville of CH2M Hill (July 7, 1999). In the NASA CALPUFF analysis, rawinsonde data are used to provide a vertical profile of temperature, dew point temperature, pressure, and wind speed and direction. In addition, CALPUFF requires that the friction velocity (u_*), Monin-Obukhov length (L), and mixing height be specified. Two different methods will be described, Method A provided by CH2M Hill in the July 7, 1999 memorandum, and Method B provided by the author.

NOTE: Revision A contains corrections/additions to the original memorandum (May 23, 2000), which was instigated after receiving reviews from Mr. Kirk Stopenhagen of CH2M Hill/SEA (July 7, 2000). Many thanks to Mr. Stopenhagen for pointing out the need for clarification on some important points that were inadvertently omitted. The July 7, 2000 memorandum from Mr. Stopenhagen is attached at the end of this document.

Determination of Friction Velocity and Monin-Obukhov Length

Method A

The methodology was developed from information provided in *Atmospheric Science and Power Production, Chapter 5, Atmospheric Boundary Layer,* by D. Randerson (1984).

Friction Velocity

Randerson outlined several simple relationships that relate surface velocity to other parameters. Randerson estimated that the error from such an empirical relationship would be on the order of 20 percent. The Tennekes and Lumley (1972) smooth surface relationship was selected and is given by:

$$u_* \approx 0.03V \tag{A1}$$

where V is the average wind speed in the lowest layer. For this study, V was set to the lowest sounding wind speed. To prevent numerical problems, u_* is not allowed to be less than 0.001 meters/second.

Monin-Obukhov Length (L)

The Monin-Obukhov length is a measure of the thermal turbulence scale size near the ground and is given by:

$$L = -\frac{(u_*)^3 T}{kg\left(\overline{w'T'}\right)} \tag{A2}$$

where T is the temperature, k is the von Karman constant and is assumed to be 0.4, g is the acceleration due to gravity (9.8 m/s^2), and $\overline{w'T'}$ is the kinematic heat flux within the surface layer. The kinematic heat flux was estimated using:

$$\overline{w'T'} = -0.00097\ V\ \Delta T \tag{A3}$$

where V is the mean wind speed at 10 meters and ΔT is the difference between the surface temperature and the potential temperature at 10 meters. For this study, V was assumed to be the lowest sounding wind speed and ΔT was given by:

$$\Delta T = \frac{T_2 - T_1}{z_2 - z_1}(10 meters) \tag{A4}$$

where T_1 and T_2 are the temperatures at the surface and second measurement heights, respectively, and z_1 and z_2 are the elevation at the surface and second measurement heights. Although L can be infinite, L is limited to a maximum value of 10^5.

Method B

The methodology for determination of u_* and L was developed from information provided in Holtslag and Van Ulden (1983) and also Adelfang (1999).

Background

Holtslag and Van Ulden (1983) provided estimations for fluxes of heat and momentum that can be obtained from observed profiles of wind and temperature using the similarity relations for the atmospheric surface layer (Dyer, 1974). These relations are based on Monin-Obukhov similarity theory, which assumes stationary and horizontally homogeneous conditions. The flux of sensible heat H through the surface layer is related to u_* and the temperature scale θ_* by

$$H = -\rho C_p u_* \theta_* \tag{B1}$$

where C_P is the specific heat at constant pressure and ρ is the density of air. The Monin-Obukhov length (L) is related to the friction velocity and vertical heat flux by (Pielke, 1984, p. 142)

$$L = -\frac{u_*^3 \theta}{kg\ \overline{w'T'}} \tag{B2}$$

where k is von Karman's constant (0.4), g is the acceleration due to gravity (9.8 m/s^2), θ is the potential temperature at the lowest sounding level in Kelvin, and $\overline{w'T'}$ is the vertical heat flux within the surface layer. w' and T' represent perturbations of vertical velocity and temperature from the basic (mean) state. H is related to $\overline{w'T'}$ by (Pielke, 1984, p. 146)

$$\overline{w'T'} = \frac{H}{\rho C_p} = -u_* \theta_* \tag{B3}$$

Equation (B3) can then be substituted into (B2) to obtain

$$L = \frac{\theta u_*^2}{kg\ \theta_*} \tag{B4}$$

The friction velocity can be determined from (Holtslag and Van Ulden, 1983)

$$u_* = kU_{z1}\left[\ln\left(z_1/z_0\right) - \psi_M\left(z_1/L\right) + \psi_M\left(z_0/L\right)\right]^{-1} \tag{B5}$$

where U_{z1} is the wind speed at the first sounding level, z_1, and z_o is the surface roughness length. Typical values of z_o for Kennedy Space Center range from 0.1 – 0.7 m depending on wind direction (Fichtl et. al., 1970). The temperature scale θ_* is obtained from (Holtslag and Van Ulden, 1983)

$$\theta_* = k\Delta\theta\left[\ln\left(z_2/z_1\right) - \psi_H\left(z_2/L\right) + \psi_H\left(z_1/L\right)\right]^{-1} \tag{B6}$$

where $\Delta\theta$ is the potential temperature difference between two heights z_1 and z_2 in the atmospheric surface layer. According to Panofsky and Dutton (1984, pp. 133-137, 145-148), the correction parameters ψ_M and ψ_H are determined from:

$$\psi_M\left(z/L\right) = \int_0^{z/L} \frac{\left\{1 - \phi_M\left(z/L\right)\right\}}{z/L} d\left(z/L\right) \tag{B7}$$

and

$$\psi_H(z/L) = \int_0^{z/L} \frac{\{1-\phi_H(z/L)\}}{z/L} d(z/L) \tag{B8}$$

where

$$\phi_M(z/L) = \begin{cases} (1-16\,z/L)^{-1/4} & \mathrm{L}<0,\ \Delta\theta/\Delta\mathrm{z}<0 \\ \\ 1+5\,z/L & \mathrm{L}>0,\ \Delta\theta/\Delta\mathrm{z}>0 \end{cases} \tag{B9}$$

and

$$\phi_H(z/L) = \begin{cases} (1-16\,z/L)^{-1/2} & \mathrm{L}<0,\ \Delta\theta/\Delta z<0 \\ \\ 1+5\,z/L & \mathrm{L}>0,\ \Delta\theta/\Delta\mathrm{z}>0 \end{cases} \tag{B10}$$

Upon integration, B7 and B8 give

$$\psi_M(z/L) = \begin{cases} 2\ln\left\{\frac{1+x(z/L)}{2}\right\} + \ln\left\{\frac{1+x(z/L)^2}{2}\right\} - 2\tan^{-1}\{x(z/L)\} + \pi/2 & \text{for } \mathrm{L}<0,\ \Delta\theta/\Delta\mathrm{z}<0 \\ -5\,z/L & \text{for } \mathrm{L}>0,\ \Delta\theta/\Delta\mathrm{z}>0 \\ \\ 0 & \text{for } \mathrm{L}=\infty,\ \Delta\theta/\Delta z=0 \end{cases} \tag{B11}$$

$$\psi_H(z/L) = \begin{cases} 2\ln\left\{\frac{1+x(z/L)^2}{2}\right\} & \text{for } \mathrm{L}<0,\ \Delta\theta/\Delta\mathrm{z}<0 \\ -5\,z/L & \text{for } \mathrm{L}>0,\ \Delta\theta/\Delta\mathrm{z}>0 \\ \\ 0 & \text{for } \mathrm{L}=\infty,\ \Delta\theta/\Delta\mathrm{z}=0 \end{cases} \tag{B12}$$

where

$$x(z/L) = (1-16\,z/L)^{1/4} \tag{B13}$$

Methodology

1) Obtain potential temperature profile from input profile using Poisson's equation

$$\theta_z = T_z\left(\frac{1000mb}{p_z}\right)^{0.286} \tag{B14}$$

where p_z is the pressure at height z and T_z is the temperature at height z in Kelvin (^{o}C + 273.15).

2) Determine stability of the surface layer by computing the potential temperature gradient between the 2 lowest sounding levels

$$\frac{\Delta\theta}{\Delta z} = \frac{\theta_2 - \theta_1}{z_2 - z_1} \tag{B15}$$

where $\Delta\theta/\Delta z > 0$, $\Delta\theta/\Delta z < 0$, and $\Delta\theta/\Delta z = 0$ indicates stable, unstable, and neutral conditions, respectively. $\Delta\theta$ is used in B6.

3) Compute u_*, θ_*, and L by iteration of equations B4 through B6, and B11 through B13. First, set L to an arbitrary value (e.g., L = -100 for unstable case, L = 100 for stable case, $L = \infty$ for neutral case) and estimate u_* and θ_* with B5 and B6 with the use of B11 and B12. Let z_o be 0.25, z_1 be the first sounding level, and z_2 be the second sounding level. Using B4, a new value of L is computed and the process is repeated. According to Holtslag and Van Ulden (1983), this is done until L converges to values that do not change more than 5%. They state that usually no more than three iterations are needed to acquire convergence of L with 5% accuracy.

Comparison of Methods A and B

For this comparison, the lowest sounding level was taken to be 10 meters above ground level (AGL). The first sounding level is the surface observation level, which is taken from 10-meter towers at KSC. The analysis consisted of 299 soundings from the KSC database for April and May 1965-69 at 0 UTC. Using method B, the maximum number of iterations to compute L was 8, the minimum was 2, and the average number of iterations was 5.2. Iterations were performed until successive values of L did not change more than 1% to allow for a more accurate analysis.

A comparison of computed u_* as a function of U_o from both methods is depicted in Figure 1. In method B, the distribution of u_* for individual values of U_o is a result of the stability terms in equation B5. Figure 2 shows how the ratio u_*/U_o can vary as a function of stability, where z = 10 m, z_o = 0.25 m, and $1/L$ is varied from –0.1 to +0.1 to account for a wide range of stability. Similarly, figure 3 shows that u_*/U_o converges to

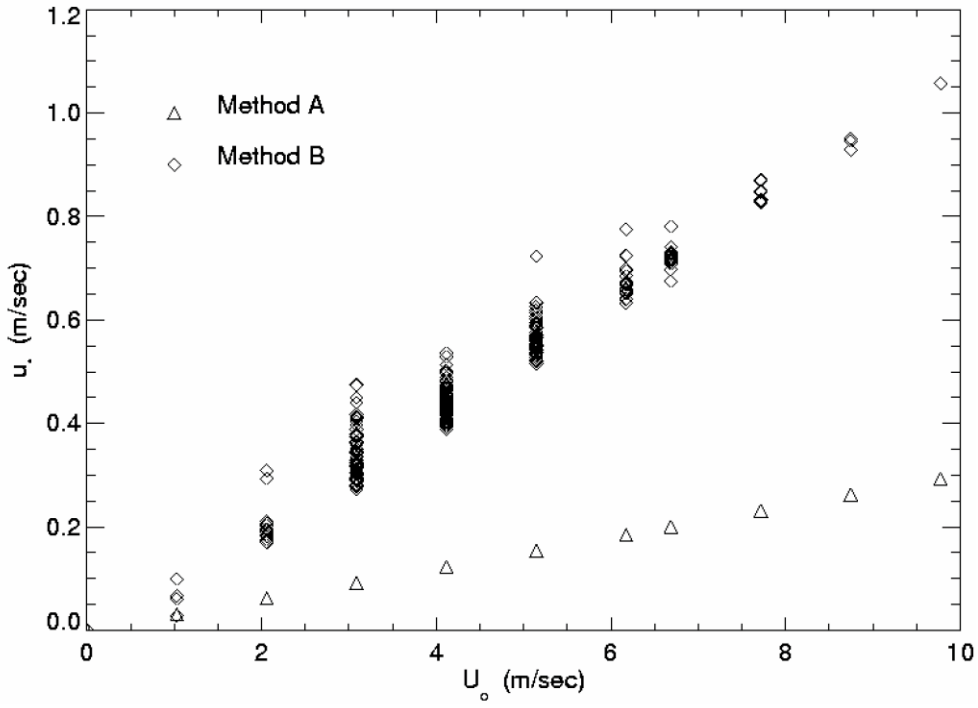

Figure F-1. Computed friction velocities (u_*) as a function of the lowest sounding level wind speed (U_o) for methods A and B.

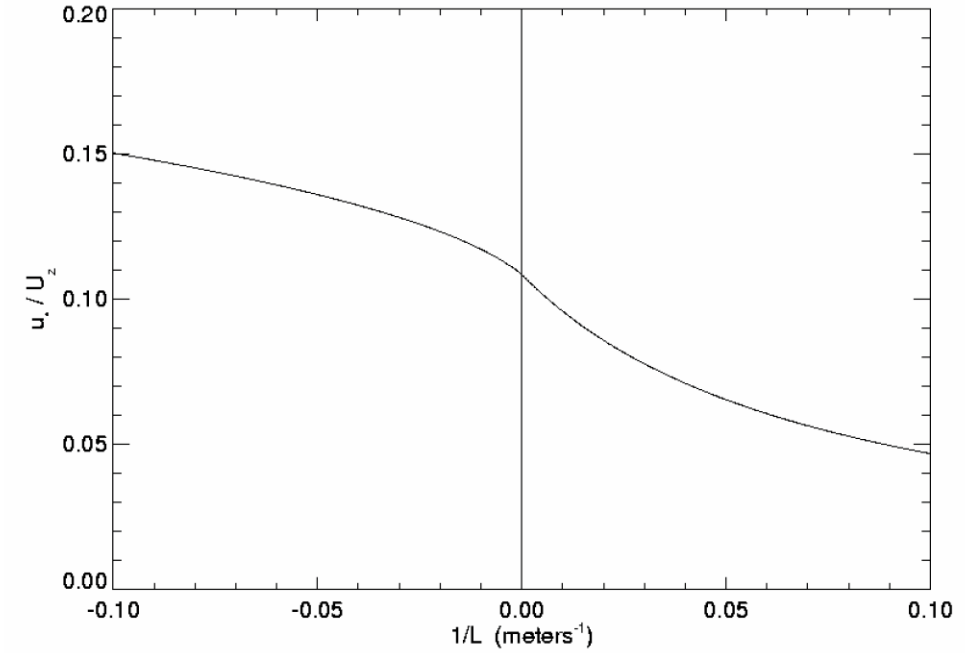

Figure F-2. The ratio of friction velocity to wind speed as a function of the inverse of the Monin-Obukhov length. Negative values of $1/L$ indicate negative stability and positive values indicate positive stability. Neutral conditions are centered around the value of $1/L = 0$.

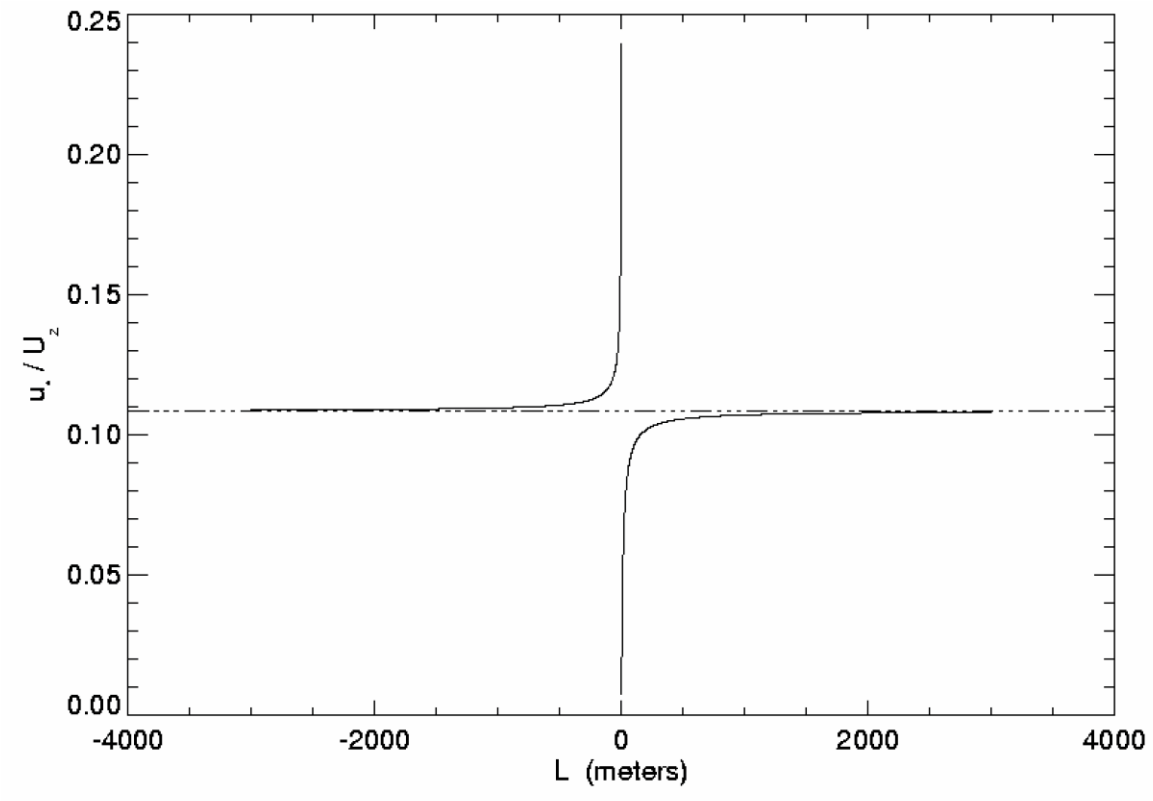

Figure F-3. The ratio of friction velocity to wind speed as a function of the Monin-Obukhuv length. u_*/U_z converges to a value of approximately 0.11 for neutral cases.

a value of approximately 0.11 for neutral cases (L = -∞, ∞) and that values of L between –200 and +200 meters have the most influence on u_*/U_o.

From the 299 soundings analyzed, u_*/U_z was calculated for each using method B (equation B5). The distribution of these ratios is depicted in figure 4 and gives a mean and standard deviation of 0.107 and 0.012, respectively. A separate analysis was performed to determine the feasibility of using a linear relationship between u_* and U_o, namely:

$$u_* = 0.107U_o \tag{B16}$$

Figure 5 shows how this relationship compares to equation B5, with the line representing B16. Percent differences were then determined by taking the difference between u_* computed with B5 and values computed with B16. This distribution is presented in figure 6 and shows that the differences are centered on 0% with a general spread between –20 and +20%. However, caution must be used when considering the use of B16 as a

substitute to B5. Figure 7 shows that the error in the estimation increases with decreasing wind speed.

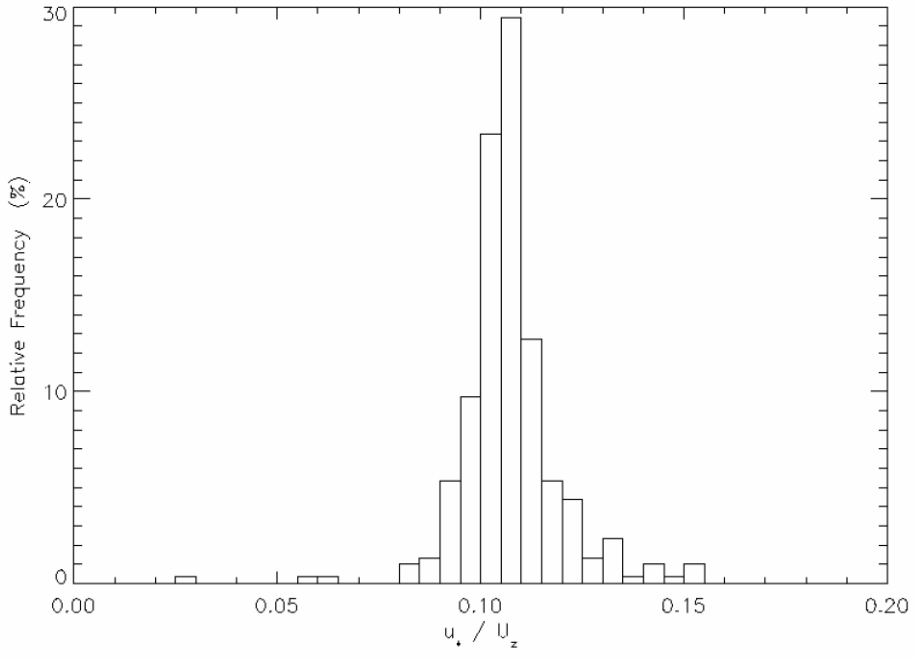

Figure F-4. Distribution of the ratio of friction velocity to wind speed determined from method B. The distribution gives a mean of 0.107 and a standard deviation of 0.012.

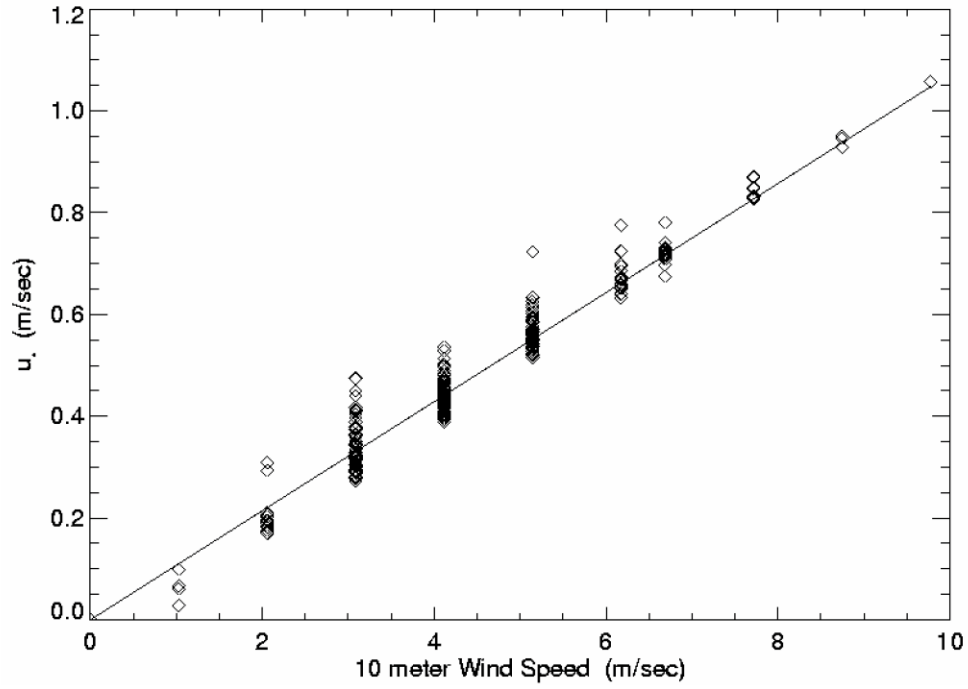

Figure F-5. Comparison of equation B16 with u_* calculated from 299 soundings using equation B5. The straight line represents u_* = 0.107 U_o (B16).

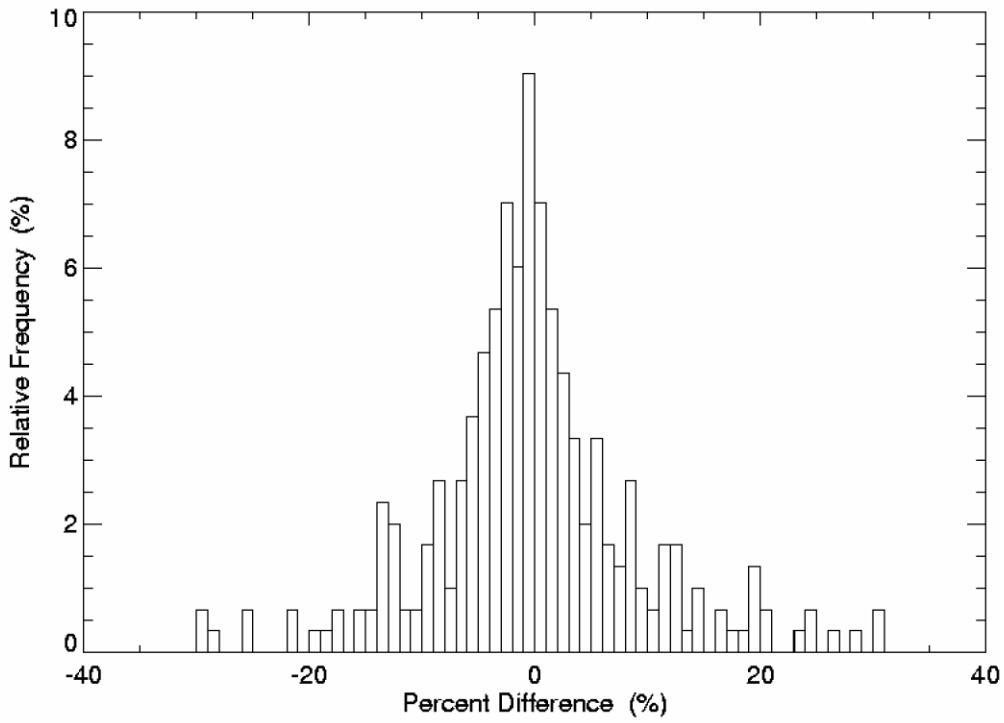

Figure F-6. Distribution of percent differences between friction velocities determined from data using equation B5, compared to equation B16.

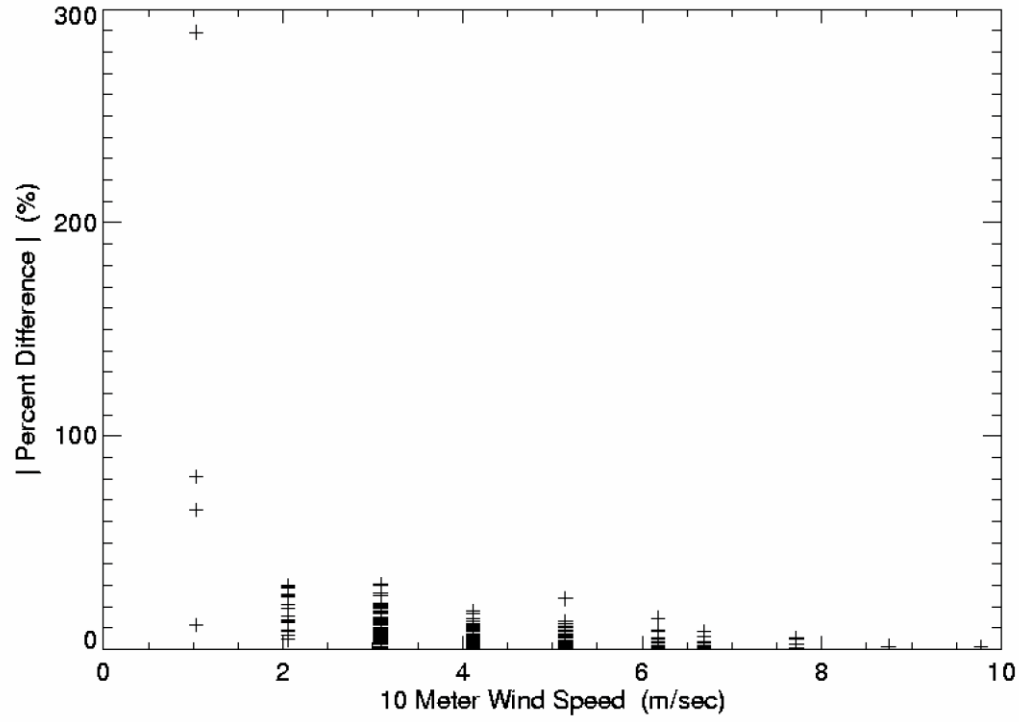

Figure F-7. The absolute value of the percent difference as a function of wind speed when comparing equations B5 and B16.

Figures 8 and 9 show the upward heat flux as a function of stability ($\Delta\theta$) for both methods. Examination of the two plots reveals that heat flux changes very little with a wide range of stability in method A, while the flux is greatly influenced by negative stability in method B. The effect this has on calculation of the Monin-Obukhov length is seen in figure 10. It is observed that method A routinely over-estimates L compared to method B.

Determination of Mixing Height

Method A

The mixing height was determined to be at the level in which the temperature gradient with height changed from negative to positive and where the difference between the dry bulb temperature and dew point temperature exceeded 15 degrees C.

Method B

Estimation of mixing heights from rawinsonde releases is performed using a technique suggested by Marsik (1995). In this method, potential temperature profiles are computed for each sounding. The profiles are analyzed for the existence of a "critical inversion," which is assumed to mark the top of the mixed layer. In this scheme, a critical inversion is defined as the lowest inversion that meets the following two criteria:

$$1)\ \Delta\theta / \Delta Z \geq 0.005\ \mathrm{K\ m^{-1}}$$
$$2)\ \theta_{\mathrm{top}} - \theta_{base} \geq 2\ \mathrm{K}$$

where $\Delta\theta/\Delta Z$ is the potential temperature lapse rate in the inversion layer and θ_{top} and θ_{base} refer to the potential temperatures at the top and bottom of the critical inversion layer. The height of the mixed layer is that point in the inversion layer at which the temperature is 2 K above the temperature at the inversion base. This method recognizes the likelihood of mixing (caused by buoyant thermals) to overshoot the base of the critical inversion. This scheme does not directly address the possible vertical extension of the mixed layer caused by wind shear effects within the critical inversion, one source of possible error. Another possible source of error that can arise is the overestimation of the depth of mixing within a surface-based inversion. Under such conditions, the only source of turbulent kinetic energy to cause mixing near the surface would have to come from mechanical effects, such as surface wind shear. The use of 2 K above the inversion base as the mixing height may result in unrealistically high values.

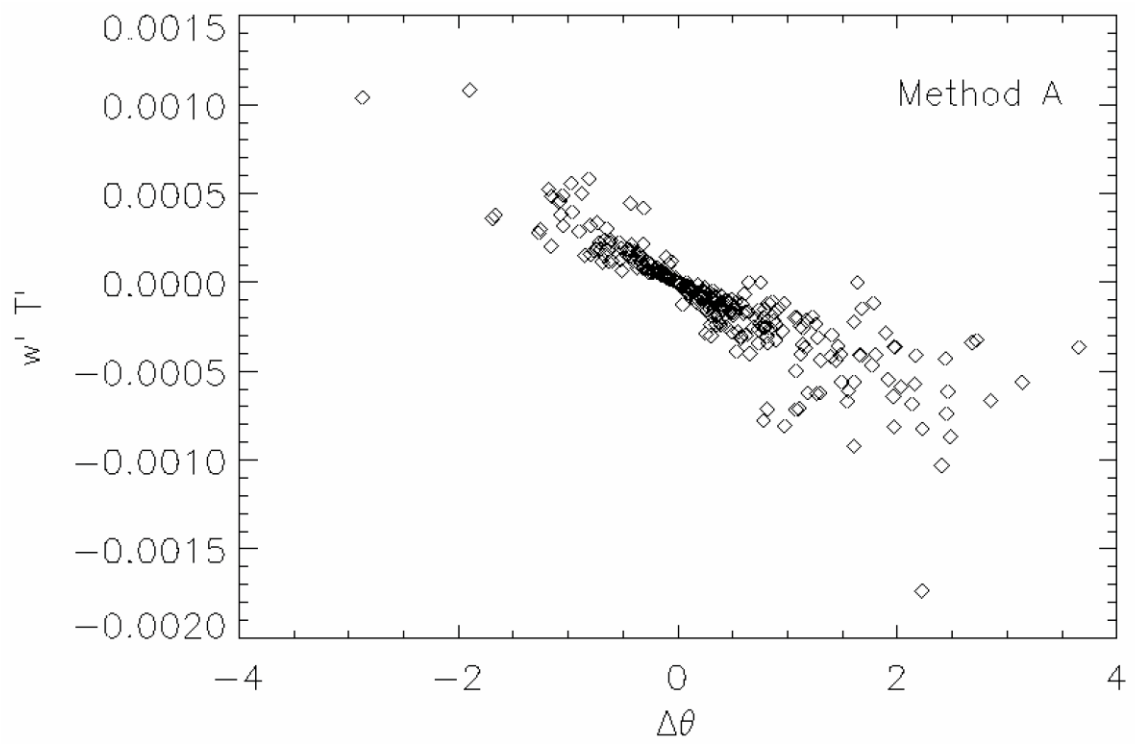

Figure F-8. Upward heat flux as a function of stability for method A.

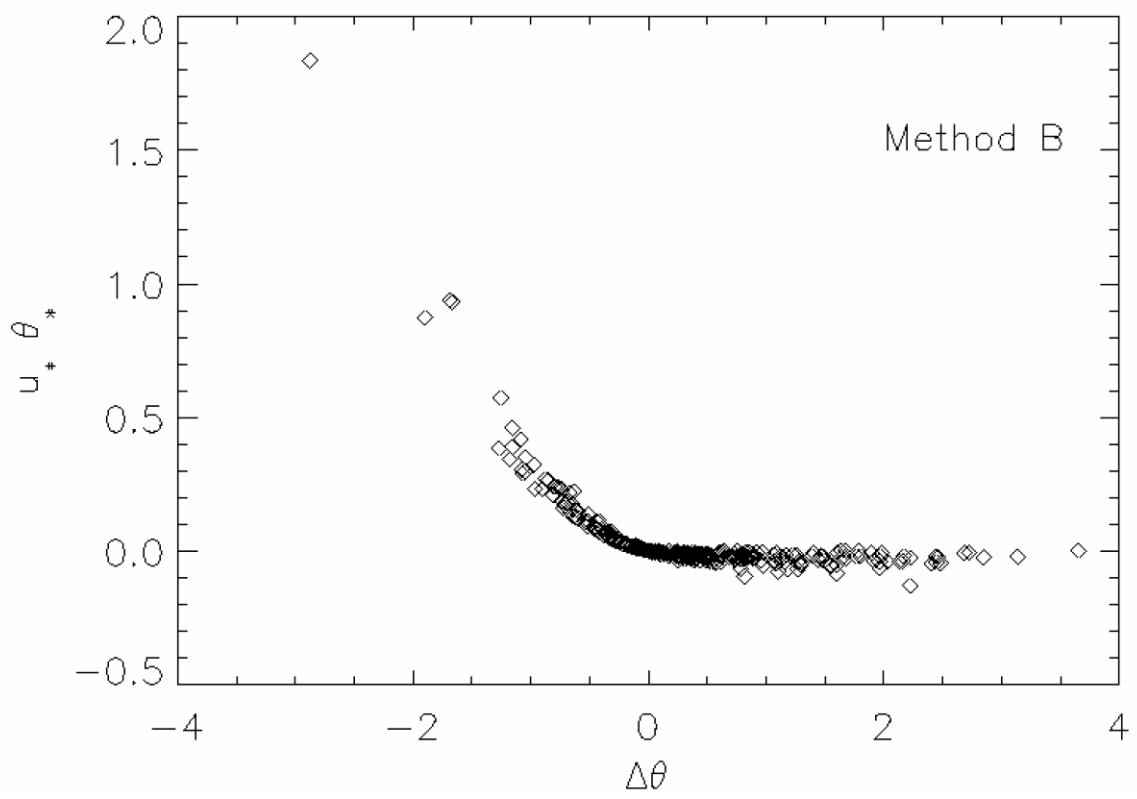

Figure F-9. Upward heat flux as a function of stability for method B.

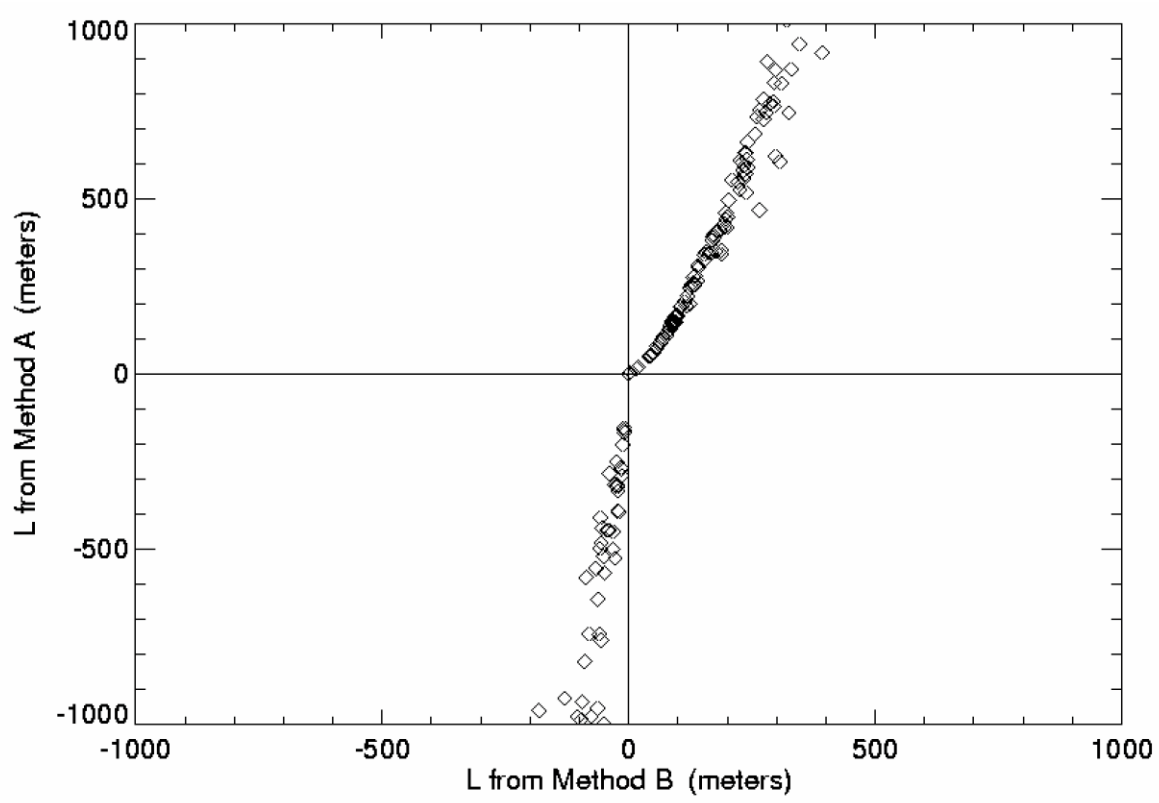

Figure F-10. Comparison of Monin-Obukhov length (*L*) computed by methods A and B.

REFERENCES

1. Adelfang, S. I.: Memorandum to B.J. Anderson, "Coefficient of Variation." May 10, 1999.

2. Dyer, A. J.: "A review of flux-profile relationships." *Bound.-Layer Meteor.,* 7, pp. 363-372, 1974.

3. Fichtl, G. H. and G. E. McVehil: "Longitudinal and lateral spectra of turbulence in the atmospheric boundary layer at the Kennedy Space Center." *J. Appl. Meteor.,* **9**, pp. 51-63, 1970.

4. Holtslag, A. A. M. and A. P. Van Ulden: "A simple scheme for daytime estimates of surface fluxes from routine weather data." *J. Clim. And Appl. Meteor.,* **22**, pp. 515–529, 1983.

5. Marsik, F. J., K. W. Fischer, T. D. McDonald, and P. J. Samson: "Comparison of methods for estimating mixing height used during the 1992 Atlanta Field Intensive." *J. Appl. Meteor.,* **34**, pp.1802-1814, 1995.

6. Panofsky, H. A. and J. A. Dutton: *Atmospheric Turbulence,* John Wiley & Sons, Toronto, Canada, 1984.

7. Pielke, R. A.: *Mesoscale Meteorological Modeling,* Academic Press, Orlando, Florida, 1984.

8. Tennekes, H. and J. L. Lumley: *A First Course in Turbulence,* The MIT Press, Cambridge, Massachusetts, 1972.

Review of Meteorological Input Parameter Recommendations For CALPUFF

TO:	Mark Bennett/CH2M HILL/MGM
FROM:	Kirk Stopenhagen/CH2M HILL/SEA
DATE:	July 7, 2000

This memorandum summarizes CH2M HILL's review of the recommendations made by Mr. Frank Leahy in his technical discussion dated May 23, 2000.

It is clear from the intercomparison of the methods that the Method A calculations present an extremely conservative approach. They do not serve the purpose of accurately estimating u*, L and mixing height from sounding data. In conversations with Kent Norville, who devised Method A, this method was drafted as a cursory tool at a time when EPA was still debating new tools such as CALMET and CALPUFF. NASA's intent is to define a concise and accurate method. For these reasons, Method A should not be considered.

Review of Method B

The Method B calculations presented by Mr. Leahy based on actual data (299 soundings) have been reviewed. The approach is well thought out and consistent with methods for calculating u*, L and mixing height in several EPA-approved/proposed meteorological data preprocessor programs such as PCRAMMET, MPRM and CALMET. For example, Equation B5 is identical to Equation 2-49 from the CALMET User's Guide.

The interative process defined based on Equations B4 through B13 is similar to standard EPA methods. Our only concern is that the process differs somewhat from the published EPA methodology. For example, the unstable terms (L<0) in Equations B11 and B12 can be found in PCRAMMET. It is unclear though how the stable (L>0) terms were derived. Similarly, step 3) under Methodology on Page 4 of the May 23 document does not explain the basis for ending the iterations when L does not change by more than 5%.

The basis for each assumption should be clearly defined and referenced so a critical reviewer can accept the approach.

The analysis that leads to the relationship presented in Equation B16 is also valuable. Using the results of the interative calculations from 299 soundings is statistically significant. As shown in Figures 5 through 7, Equation B16 overpredicts u* at low wind speeds. Although we did not review the implications of this with respect to outputs from CALPUFF, the u* values are not realistic. This proves that a simple linear relationship (like that proposed in Method A and Equation B16) should not be used to calculate these stability parameters. This goes to show that the methodology that is selected should be clear and defensible.

Recommendations

CH2M HILL recommends following the calculations for u* and L as defined in the CALMET User's Guide. This will serve several purposes. First, a proposed EPA methodology will be used. Second, the CALMET approach differs from Method B in that different calculations are used for describing overland and overwater boundary conditions. Parameters such as surface roughness, albedo, surface heat flux, diurnal patterns and surface temperature vary significantly between land and water surfaces. Since the CALPUFF model grid will cover both land and water receptors, the CALMET preprocessing approach should be used to best estimate these differences. It should be noted that the overwater Monin-Obukhov length calculation (Equation 2-68 in CALMET User's Guide) requires sounding data over land and water to determine virtual potential temperatures. We do not know if overwater soundings are available.

Lastly, this regulatory approved preprocessing approach will stand up under an external critical review process. Although we are confident that the Method B approach could be strongly defended, the CALMET approach provides even more margin of acceptance.

REFERENCES

1. Final Environmental Impact Statement Space Shuttle Program, NASA, Washington, DC, 1978.

2. Advanced Solid Rocket Motor Final Environmental Impact Statement, NASA Marshall Space Flight Center, Huntsville, AL, 1989.

3. Memorandum of Agreement 15E–2–2 Between 45th SW and NASA/KSC for Missile/Space Vehicle Safety, NASA/USAF, July 26, 2000.

4. Memorandum of Agreement 15E–2–16, 3000, Among 45th SW, NASA/KSC, and Brevard County Office of Emergency Management for the Formation of a Joint Hazard Control Team, July 26, 2000.

5. Linn, R.R.; Bossert, J.E.; Reisner, J.M.; et al.: Preliminary Assessment of HCl Dispersion from a Worst-Case Shuttle Abort Scenario at the Kennedy Space Center, FL, 2001.

6. Safety Requirements, EWR 127–1, USAF Eastern Western Range, 1997.

7. Guided Missiles—Joint Long Range Proving Ground, Public Law (PL) 81–60, U.S. Congress, 1949.

8. Executive Order 13148, April 21, 2000.

9. Emergency Planning and Community Right-to-Know Act of 1986, 42 U.S.C. 11,001–11,050, U.S. Congress, 1986.

10. Provisions for Chemical Accident Prevention, 40 CFR 68, U.S. Congress, 1994.

11. Risk Management Programs for Chemical Accidental Release Prevention, 40 CFR 68: 54192–54213, U.S. Congress, 1995.

12. Common Risk Criteria for National Test Ranges Inert Debris, Range Commanders Council, Range Safety Group, Risk and Lethality Commonality Team, Published by the Secretariat, Range Commanders Council, U.S. Army White Sands Missile Range, NM, 1997.

13. Common Risk Criteria for National Test Ranges, Standard 321–00, published by the Secretariat, Range Commanders Council, Range Safety Group, Risk and Lethality Commonality Team, U.S. Army White Sands Missile Range, NM, 2000.

14. Assessment of Exposure—Response Functions for Rocket Emissions Toxicants, National Research Council, Committee on Toxicology, National Academy Press, Washington, DC, 1998.

15. NASA Report of the Presidential Commission on the Space Shuttle *Challenger* Accident, Vol. III, 1986.

16. Isakowitz, S.J.K.; Hopkins, Jr., J.P., and Hopkins, J.B.: *International Reference Guide to Space Launch Systems*, Third Edition, American Institute of Aeronautics and Astronautics, 1999.

17. Final Environmental Impact Statement for the Space Shuttle Solid Rocket Motor DDT&E Program at Thiokol/Wasatch Division, Promontory, UT, NASA Marshall Space Flight Center, Huntsville, AL, 1979.

18. Dawbarn, R.M.; M. Kinslow; and D.J. Watson, "Analysis of the Measured Effects of the Principal Exhaust Effluents from Solid Rocket Motors," NASA Contractor Report 3136, Contract PO H–19386B, Arnold Engineering Development Center, TN, 1980.

19. Anderson B.J.; and Keller, V.W.: "Space Shuttle Exhaust Cloud Properties," *NASA Technical Paper 2258*, Marshall Space Flight Center, AL, 1983.

20. Radke, L.F.; Hobbs P.V.; and Eltgroth, M.W.: Airborne Measurements in the Column Cloud From a Titan III Rocket/Contract 61–9806, Final Report for Naval Weapons Center, China Lake, CA, by the Atmospheric Sciences Department, University of Washington, Seattle WA, 1979.

21. Radke, L.F.: Hobbs, P.V.: and Hegg, D.A.: "Aerosols and Trace Gases in the Effluents Produced by the Launch of Large Lquid- and Solid-Fueled Rockets, *J. Applied Meteorology*, Vol. 21, p. 1332, September 1982.

22. Guideline on Air Quality Models, 61 FR 41840, Bureau of National Affairs, Inc., Appendix W to Part 51, 1996.

REPORT DOCUMENTATION PAGE

Form Approved
OMB No. 0704-0188

1. AGENCY USE ONLY *(Leave Blank)*	2. REPORT DATE	3. REPORT TYPE AND DATES COVERED
	June 2004	Technical Publication

4. TITLE AND SUBTITLE

Toxic Gas Exposure Risks Associated With Potential Shuttle Catastrophic Failures

5. FUNDING NUMBERS

6. AUTHORS

B. Jeffrey Anderson and Rebecca C. McCaleb

7. PERFORMING ORGANIZATION NAMES(S) AND ADDRESS(ES)

George C. Marshall Space Flight Center
Marshall Space Flight Center, AL 35812

8. PERFORMING ORGANIZATION REPORT NUMBER

M–1116

9. SPONSORING/MONITORING AGENCY NAME(S) AND ADDRESS(ES)

National Aeronautics and Space Administration
Washington, DC 20546–0001

10. SPONSORING/MONITORING AGENCY REPORT NUMBER

NASA/TP—2004–213284

11. SUPPLEMENTARY NOTES

Prepared by the Engineering Systems Department, Engineering Directorate

12a. DISTRIBUTION/AVAILABILITY STATEMENT

Unclassified-Unlimited
Subject Category 45
Availability: NASA CASI (301) 621–0390

12b. DISTRIBUTION CODE

13. ABSTRACT *(Maximum 200 words)*

From early in the Shuttle program, the National Aeronautics and Space Administration has modeled hydrogen chloride (HCl) release by burning solid propellant in the solid rocket boosters. In 1998, the United States Air Force 45th Space Wing instituted more stringent launch commit criteria (LCC) for the Titan and Delta vehicles and proposed that the same LCC be applied to the Shuttle to enhance safety of onsite visitors and offsite public. Two types of health and safety standards were applicable: (1) Expected casualties and risk and (2) air quality emergency response.

This study addresses the issues using the U.S. Environmental Protection Agency-recommended model, CALPUFF. Results were compared to those produced by the USAF model, REEDM, developed for projecting air quality from nominal launches. Model performance was also evaluated against results of a Kennedy Space Center-sponsored study at the Los Alamos National Laboratory (LANL) using a computer-intensive, wild-fire model.

CALPUFF and the LANL model are capable of multipuff modeling of multiple sources. REEDM is a single-source, single-puff model. This study revealed significant deficiencies in REEDM when applied to the catastrophic failure problem. CALPUFF results indicate that, if a Shuttle abort were to occur over land, serious levels of HCl exposure could occur out to distances of at least 10 km, sufficient range to include major onsite visitor viewing areas. A preliminary survey of mitigation alternatives indicates cost-effective measures could be implemented that are sufficiently protective. Recent safety initiatives in response to the *Columbia* Accident Investigation Board report are not reflected here.

14. SUBJECT TERMS

Space Shuttle failure, toxic cloud, hydrogen chloride, range safety

15. NUMBER OF PAGES

104

16. PRICE CODE

17. SECURITY CLASSIFICATION OF REPORT	18. SECURITY CLASSIFICATION OF THIS PAGE	19. SECURITY CLASSIFICATION OF ABSTRACT	20. LIMITATION OF ABSTRACT
Unclassified	Unclassified	Unclassified	Unlimited